

REGULATION OF THE YEAST *PAH1*-ENCODED PHOSPHATIDATE
PHOSPHATASE BY PHOSPHORYLATION

by

WEN-MIN SU

A Dissertation submitted to the
Graduate School-New Brunswick
Rutgers, The State University of New Jersey

in partial fulfillment of the requirements

for the degree of

Doctor of Philosophy

Graduate Program in Food Science

Written under the direction of

Dr. George M. Carman

and approved by

New Brunswick, New Jersey

May, 2013

ABSTRACT OF THE DISSERTATION

Regulation of the Yeast *PAH1*-encoded Phosphatidate Phosphatase by Phosphorylation

by WEN-MIN SU

Dissertation Director:

Dr. George M. Carman

Pah1p, which functions as phosphatidate phosphatase (PAP) in the yeast *Saccharomyces cerevisiae*, plays a crucial role in lipid homeostasis by controlling the relative proportions of its substrate phosphatidate and its product diacylglycerol. The diacylglycerol produced by PAP is used for the synthesis of triacylglycerol as well as for the synthesis of phospholipids via the Kennedy pathway. Pah1p is a highly phosphorylated protein *in vivo*, and has been previously shown to be phosphorylated by the protein kinases Pho85p-Pho80p and Cdc28p-cyclin B. In this work, we showed that Pah1p was a *bona fide* substrate for protein kinase A (PKA) and protein kinase C (PKC). PKA phosphorylated Pah1p on Ser-10, Ser-677, Ser-773, Ser-774, and Ser-788, whereas Ser-677 and Ser-788 are also the PKC target sites in addition to Ser-769. PKA-mediated phosphorylation of Pah1p inhibited its PAP activity by decreasing catalytic efficiency, and the inhibitory effect was primarily conferred by phosphorylation at Ser-10. On the other hand, the phosphorylation of Pah1p by PKC caused a slight increase in PAP activity. The pre-phosphorylation of Pah1p with PKA caused a reduction on the phosphorylation by PKC and *vice versa*. The phosphorylation of Pho85p-Pho80p

suppressed the subsequent phosphorylation by PKC but did not affect PKA. The analysis of the S10A and S10D mutations (mimicking dephosphorylation and phosphorylation, respectively), alone or in combination with the seven alanine (7A) mutations of the sites phosphorylated by Pho85p-Pho80p and Cdc28p-cyclin B, indicated that phosphorylation at Ser-10 stabilized Pah1p abundance and inhibited its association with membranes, PAP activity, and triacylglycerol synthesis. The S10A mutation enhanced the physiological effects imparted by the 7A mutations, whereas the S10D mutations attenuated the effects of the 7A mutations. The analyses of PKC target site mutations revealed that neither 3A nor 3D Pah1p mutant affected the protein abundance, localization of pah1p and TAG synthesis. Collectively, these data indicated that the protein kinase A-mediated phosphorylation of Ser-10 functions in conjunction with the phosphorylations mediated by Pho85p-Pho80p and Cdc28p-cyclin B, and that phospho-Ser-10 should be dephosphorylated for proper PAP function.

ACKNOWLEDGMENTS

I would like to express my sincere gratitude to Dr. George M. Carman for supporting me throughout these years. I have been very fortunate to have him as my mentor. He is always available whenever I need help, advice, and inspiration. His guidance and encouragement have been invaluable and his enthusiasm for research and perfection is infectious.

I would like to acknowledge my thesis committee members: Drs. Gil-Soo Han, Judith Storch, Loredana Quadro, and Mikhail Chikindas for their thought-provoking questions and valuable comments. Special thanks go to Gil-Soo for all his assistance, insightful suggestions and helpful criticism.

I would like to thank the current members of Carman lab: Florencia Pascual, Stylianos Fakas, Yeon Hee Park, Yixuan Qiu, Lu-Sheng Hsieh and Caroline Davis for helping me in many ways to make my PhD life easier and enjoyable. I am also grateful to former lab members: Hyeon-Son Choi, Anibal Soto-Cardalda, Minjung Chae, Jeanelle Morgan, Jessica Casciano, and Zhi Xu for their help during the early stages of my graduate studies. Thank you all to members of the Rutgers Center for Lipid Research, and the staff in the Food Science department.

Finally, special thanks to my family and friends for their endless love, understanding and support during my doctoral journey.

TABLE OF CONTENTS

	<u>Page</u>
ABSTRACT OF THE DISSERTATION.....	ii
ACKNOWLEDGMENTS.....	iv
TABLE OF CONTENTS.....	v
LIST OF TABLES.....	viii
LIST OF ILLUSTRATIONS.....	ix
LIST OF ABBREVIATIONS.....	xi
INTRODUCTION.....	1
Synthesis of Phospholipids.....	2
Synthesis of TAG.....	5
<i>PAH1</i> -encoded PAP.....	8
Physiological Roles of Pah1p PAP.....	12
Other PAPs in Yeast.....	14
Pah1p is the Mammalian Lipin Ortholog.....	15
Regulation of Pah1p/Lipin PAP.....	17
SPECIFIC AIMS.....	24
EXPERIMENTAL PROCEDURES.....	25
Materials.....	25
Strains and Growth Conditions.....	26
DNA Manipulations.....	28
Construction of Plasmids.....	28
Purification of Pah1p and Pho85p-Pho80p.....	32

Preparation of Yeast Cell Extracts and Subcellular Fractionation.....	33
SDS-PAGE and Western Blot Analysis.....	33
Phosphorylation and Dephosphorylation Reactions.....	34
Preparation of Liposomes.....	35
Phosphoamino Acid and Phosphopeptide Mapping Analyses.....	35
Mass Spectrometry Analysis of Pah1p Phosphorylation Sites.....	36
Preparation of ³² P-labeled PA and Measurement of PAP Activity.....	36
<i>In Vivo</i> Labeling of Pah1p.....	37
Labeling and Analysis of Lipids.....	37
Analyses of Data.....	38
RESULTS.....	39
Pah1p is Phosphorylated by Multiple Protein Kinases.....	39
Phosphorylation Decreases the Interaction of Pah1p with PC-PA Liposomes.....	42
PKA Phosphorylates Pah1p and Attenuates its PAP activity.....	45
Ser-10, Ser-677, Ser-773, Ser-774, and Ser-788 in Pah1p are Phosphorylated by PKA.....	53
The Phosphorylation State of Ser-10 Alone and in Combination with the 7A Mutations Affects Cell Growth.....	56
The Phosphorylation State of Ser-10 in Combination with the 7A Mutations Affects the Abundance and the Localization of Pah1p.....	67
The Phosphorylation State of Ser-10 in Combination with the 7A Mutations Affects TAG Content.....	70
Phosphorylation of Pah1p by PKC.....	76

Ser-677, Ser-779, and Ser-788 Are Major PKC Phosphorylation Sites.....	76
PKC Phosphorylation-deficient 3A Mutations Affect the Pah1p Phosphorylation <i>in vivo</i> and <i>in vitro</i>	83
Effect of Pah1p Phosphorylation by PKC on PAP Activity.....	87
Effects of the PKC Phosphorylation Site Mutations on Temperature Sensitivity, Pah1p Abundance and Localization, and Lipid Composition.....	90
The Interrelations of Pah1p Phosphorylation by PKA, PKC and Pho85p-Pho80p	93
DISCUSSION.....	101
CONCLUSIONS AND FUTURE DIRECTIONS.....	111
REFERENCES.....	114
CURRICULUM VITAE.....	132

LIST OF TABLES

	<u>Page</u>
I. Strains used in this study.....	27
II. Plasmids used in this study.....	29
III. Oligonucleotides used in this study.....	31

LIST OF ILLUSTRATIONS

	<u>Page</u>
1. Phospholipids and TAG synthesis pathways.....	3
2. Roles of PAP in the synthesis of TAG and membrane phospholipids.....	6
3. Domain structures of Pah1p, App1p, Dpp1p, Lpp1p and lipin-1.....	10
4. Phosphorylation sites in Pah1p and model for the regulation by phosphorylation/dephosphorylation.....	21
5. Phosphorylation of Pah1p by protein kinases.....	40
6. Effect of phosphorylation on the interaction of Pah1p with PC-PA liposomes	43
7. PKA phosphorylates Pah1p on a serine residue <i>in vitro</i> and <i>in vivo</i>	46
8. Pah1p is a <i>bona fide</i> substrate of PKA.....	49
9. Phosphorylation of Pah1p by PKA attenuates PAP activity.....	51
10. Phosphopeptide mapping analysis of Pah1p mutants phosphorylated by PKA	54
11. Effects of PKA phosphorylation site mutations on the phosphorylation of Pah1p and on the inhibitory effects of PKA on PAP activity.....	57
12. Effects of PKA phosphorylation site mutations on the complementation of the <i>pah1Δ</i> temperature sensitive phenotype.....	60
13. Effects of S10A mutation in combination with the 7A mutations on the complementation of the <i>pah1Δ</i> temperature sensitive phenotype.....	63
14. The S10A mutation in combination with the 7A mutations reduces growth in medium lacking inositol and choline.....	65

15. The phosphorylation state of Ser-10 in combination with the 7A mutations affects the abundance of Pah1p.....	68
16. The phosphorylation state of Ser-10 in combination with the 7A mutations affects the localization of Pah1p.....	71
17. The phosphorylation state of Ser-10 in combination with the 7A mutations affects lipid content.....	74
18. Characterization of Pah1p phosphorylation by PKC.....	77
19. PKC phosphorylates Pah1p on a serine residue.....	79
20. Phosphopeptide mapping analysis of Pah1p mutations phosphorylated by PKC	81
21. Effects of the 3A mutations on <i>in vivo</i> phosphorylation and the time-dependent phosphorylation of Pah1p.....	85
22. Effect of PKC phosphorylation site mutations on PAP activity.....	88
23. Effect of PKC phosphorylation site mutations on the complementation of temperature sensitivity of <i>pah1Δ NEM1</i> and <i>pah1Δ nem1Δ</i> mutant cells.....	91
24. Effect of PKC phosphorylation site mutations on protein abundance	94
25. Effect of PKC phosphorylation sites mutations on the content of TAG and phospholipids.....	96
26. The interrelations of Pah1p phosphorylation by PKA, PKC, and Pho85p-Pho80p	99
27. Summary of Pah1p phosphorylation by PKA, PKC, Pho85p-Pho80p, and Cdc28p-cyclin B.....	103

LIST OF ABBREVIATIONS

3A	phosphorylation-deficient mutant for protein kinase C
5A	phosphorylation-deficient mutant for protein kinase A
7A	phosphorylation-deficient mutant for Pho85p-Pho80p
ATP	adenosine triphosphate
cAMP	cyclic adenosine monophosphate
CDP	cytidine diphosphate
CDP-DAG	cytidine diphosphate diacylglycerol
Cho	choline
CKII	casein kinase II
CL	cardiolipin
CMP	cytidine monophosphate
Cpm	counts per minute
CTP	cytidine triphosphate
DAG	diacylglycerol
DGK	diacylglycerol kinase
DGPP	diacylglycerol pyrophosphate
DHAP	dihydroxyacetone phosphate
EDTA	ethylenediamine tetraacetic acid
EGTA	ethylene glycol bis-(aminoethyl ether) N,N,N',N'-tetraacetic acid
ER	endoplasmic reticulum
Etn	ethanolamine

Glc-6-P	glucose-6-phosphate
Gro-3-P	glycerol-3-phosphate
HAD	haloacid dehalogenase
Ins	inositol
kDa	kilo Daltons
LB	Luria-Bertani
LPA	lysophosphatidic acid
Ni ²⁺ -NTA	nickel-nitrilotriacetic acid
PA	phosphatidic acid
PAP	phosphatidate phosphatase
PC	phosphatidylcholine
P-Cho	phosphocholine
PDE	phosphatidyl dimethylethanolamine
PE	phosphatidylethanolamine
P-Etn	phosphoethanolamine
PI	phosphatidylinositol
Pi	inorganic phosphate
PL	phospholipid
PKA	protein kinase A
PKC	protein kinase C
PME	phosphatidylmonomethylethanolamine;
PS	phosphatidylserine
PVDF	polyvinylidene difluoride

SC	synthetic complete
SDS	sodium dodecyl sulfate
TAG	triacylglycerol
TLC	thin layer chromatography
UAS _{INO}	an inositol-responsive upstream activating sequence
UAS _{ZRE}	an zinc-responsive upstream activating sequence

INTRODUCTION

Lipids, a diverse group of compounds characterized by their water insolubility, play a variety of cellular roles. Phospholipids and sterols are major structural elements of cell membranes (1). TAG is a principal form of stored energy in many organisms (1). In addition, some lipids that are usually present in lower cellular amounts function as signaling molecules, enzyme cofactors, surfactants, and hormones (1). Abnormal lipid metabolism results in various diseases. For instance, obesity, characterized by the excessive accumulation of TAG in adipose tissue and other organs, is associated with type II diabetes, coronary heart disease, hypertension, and certain types of cancers (2). Thus, a well-controlled lipid metabolism is critical for normal cellular physiology and development.

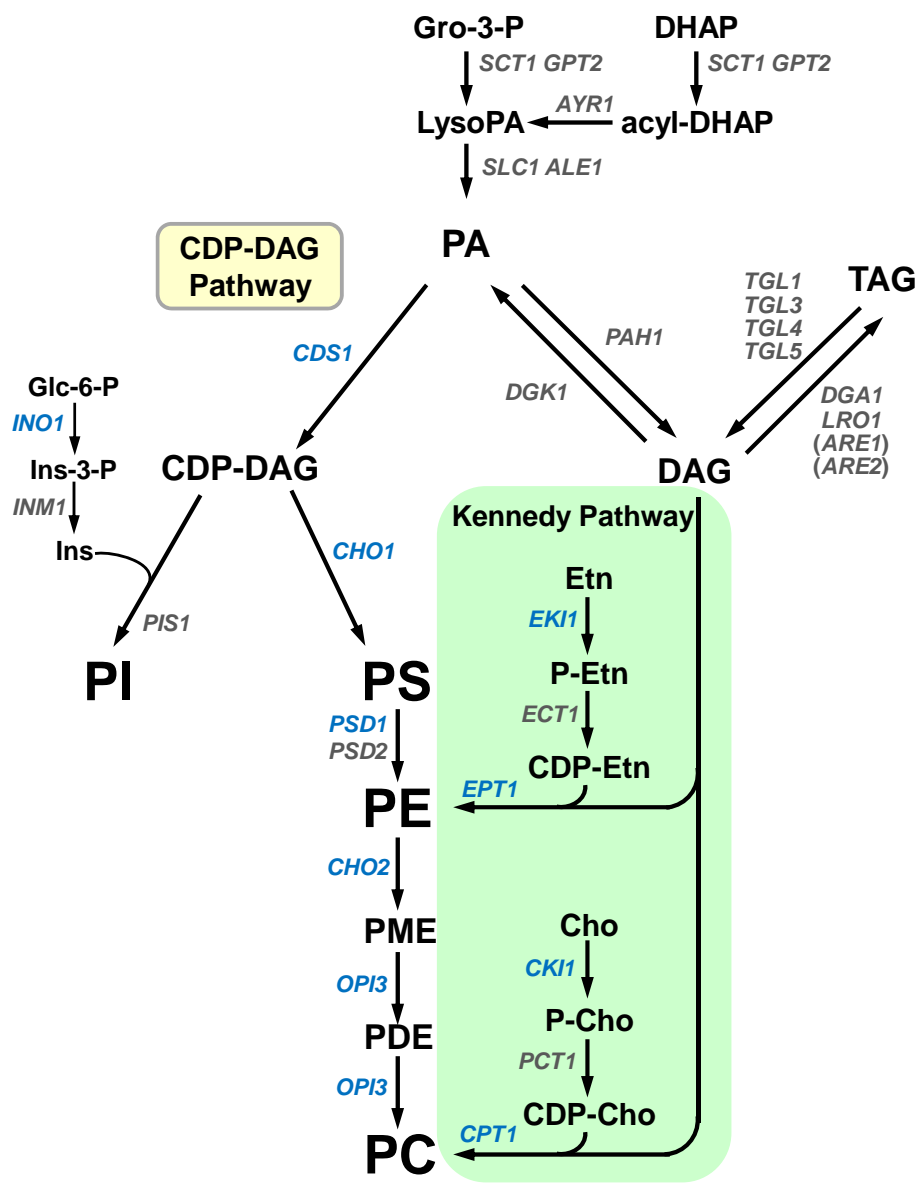
Saccharomyces cerevisiae has been extensively used as a model eukaryote to study lipid metabolism. The budding yeast synthesizes membrane phospholipids and TAG by the pathways that are generally common to those in higher eukaryotes (3-6). Because of its short generation time, yeast can be easily grown to large quantities for biochemical studies and enzyme purification. Moreover, the availability of *S. cerevisiae* genome database facilitates the genetic and biochemical studies. Almost all of the structural genes responsible for the synthesis of phospholipids and TAG have been identified, and mutations in these genes have been characterized (3, 5-7). Therefore, *S. cerevisiae* is an ideal organism for studying the regulation of lipid metabolism.

Synthesis of Phospholipids

Phospholipids are amphipathic lipids composed of a glycerol backbone, two hydrophobic fatty acyl chains, and a hydrophilic head group. They are major building blocks of cellular membranes; in addition, phospholipids function as lipid signaling molecules, molecular chaperones, and anchors for proteins to associate with cell membranes (1, 3, 8).

In yeast as well as in higher eukaryotic cells, all phospholipids are derived from PA, the simplest membrane phospholipid (Fig. 1). PA is synthesized from the glycolysis product, glycerol-3-phosphate or dihydroxyacetone phosphate, after two acylation reactions catalyzed by glycerol-3-phosphate acyltransferase (encoded by *SCT1* and *GPT2* genes) and lysophospholipid acyltransferase (encoded by *SLC1* and *ALE1* genes) (9-14). The major phospholipids PC, PE, PI and PS are synthesized from PA primarily via the CDP-DAG pathway (Fig. 1). PA is converted to the energy-rich intermediate CDP-DAG by the *CDS1*-encoded CDP-DAG synthase (15, 16). The CMP moiety of CDP-DAG can then be displaced by inositol to form PI by the *PIS1*-encoded PI synthase (17, 18). Inositol used in this reaction can be obtained exogenously or it can be derived from glucose-6-phosphate via reactions catalyzed by the *INO1*-encoded inositol-3-phosphate synthase and by the *INM1*-encoded inositol-3-phosphate phosphatase (19-21). The CMP moiety of CDP-DAG can also be replaced with serine by the *CHO1*-encoded PS synthase to form PS (22-24). After decarboxylation catalyzed by the *PSD1*- and *PSD2*-encoded PS decarboxylase, PS is converted to PE (25-27), which then undergoes three-step AdoMet-dependent methylation reactions on its amine group to form PC (28). The first

FIGURE 1. Phospholipids and TAG synthesis pathways. The pathways for the synthesis of phospholipids and TAG are shown. Italics indicate genes that are known to encode enzymes catalyzing individual steps in the lipid synthesis pathway. UAS_{INO}-containing genes are highlighted in blue. Modified from Carman and Han 2011 (29).



methylation is catalyzed by the *CHO2*-encoded PE methyltransferase (30, 31) and the last two methylation reactions are carried out by the *OPI3*-encoded phospholipid methyltransferase (30, 32).

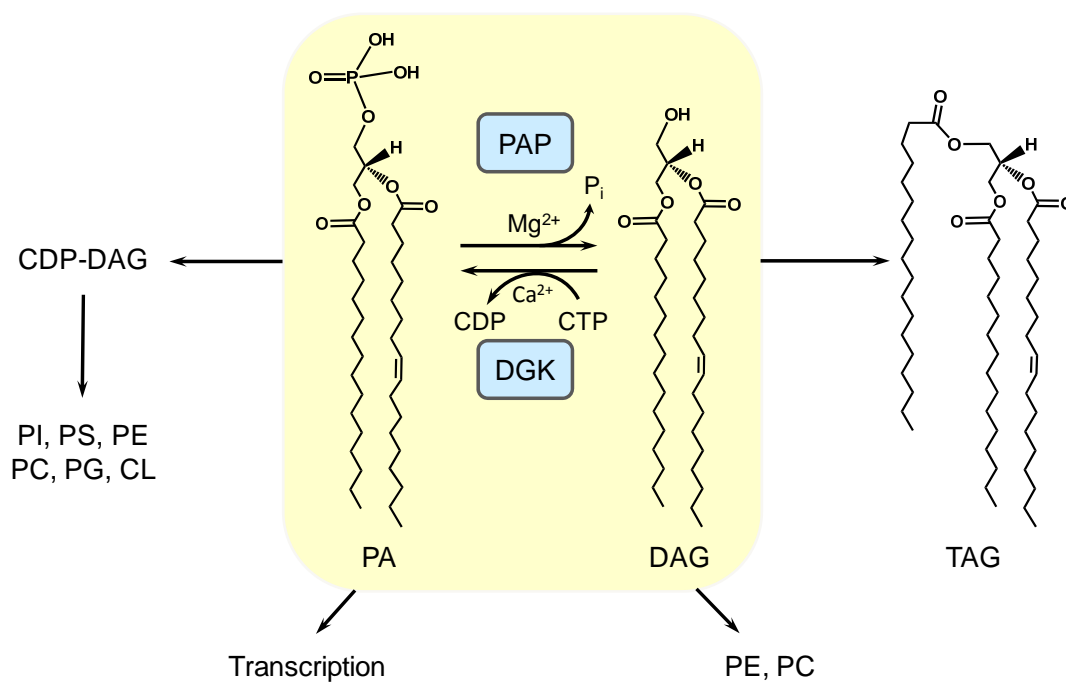
Yeast cells can also synthesize PE and PC via the Kennedy pathway, the major route for phospholipid synthesis in mammals. Ethanolamine and choline are phosphorylated by the *EKII*-encoded ethanolamine kinase and by the *CKII*-encoded choline kinase to form phosphoethanolamine and phosphocholine, respectively (33, 34). These intermediates are then activated by CTP to form CDP-ethanolamine and CDP-choline by the *ECTI*-encoded phosphoethanolamine cytidylyltransferase and by the *PCTI*-encoded phosphocholine cytidylyltransferase (35, 36). Finally, CDP-ethanolamine and CDP-choline react with DAG to generate PE and PC by the *EPTI*-encoded ethanolamine phosphotransferase and by the *CPTI*-encoded choline phosphotransferase enzymes, respectively (37-40).

Synthesis of TAG

TAG, composed of a glycerol backbone with three esterified fatty acids, is an energy-dense molecule normally accumulated in lipid droplets. Cells store excess energy as TAG that can be hydrolyzed upon the nutrient-deficient condition and the resulting fatty acids can be oxidized for the generation of energy (41). The turnover products of TAG can also serve as the building blocks for the synthesis of phospholipids and thus are crucial for yeast cells to resume growth from the stationary phase (41-43). In addition, the synthesis of TAG is an important mechanism to protect cells from fatty acid-induced

FIGURE 2. Roles of PAP in the synthesis of TAG and membrane phospholipids

The reactions catalyzed by the *PAH1*-encoded PAP and the *DGKI*-encoded DAG kinase are shown. The activity of PAP plays a major role in governing the relative amounts of DAG and PA, which in turn controls whether cells favor the synthesis of TAG or membrane phospholipids. In addition, PA regulates the expression of UAS_{INO}-containing phospholipid synthesis genes.



lipotoxicity. Cells deficient in TAG synthesis cannot survive with excess fatty acid supplementation (44-46).

PA is also a precursor for TAG (Fig. 1 and 2). After dephosphorylation catalyzed by the *PAHI*-encoded PAP (47, 48), PA is converted to DAG, which is then acylated to generate TAG by acyltransferase enzymes encoded by *DGAI* and *LROI* genes (49-52) (Fig. 2). In addition, this acylation reaction can be catalyzed by the *ARE1*- and *ARE2*-encoded acyltransferase enzymes, which are mainly responsible for the synthesis of ergosterol esters (52). During growth resumption or energy depleted conditions, the stored TAG can be hydrolyzed back to DAG and free fatty acid by TAG lipases encoded by *TGL1*, *TGL3*, *TGL4*, and *TGL5* genes (52-55). DAG is then converted to PA by the *DGKI*-encoded DAG kinase (56).

***PAHI*-encoded PAP**

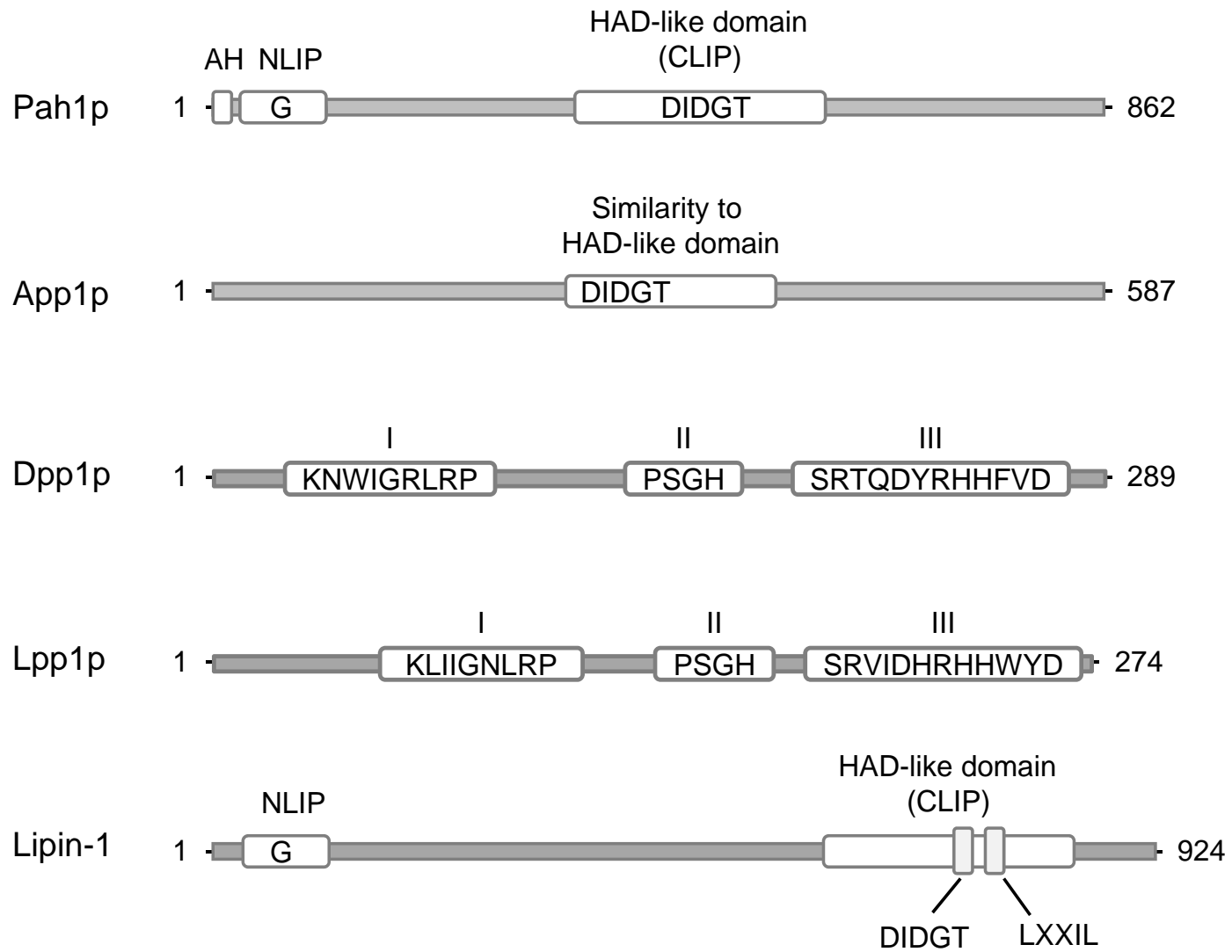
PAP catalyzes the dephosphorylation of PA, yielding DAG and inorganic phosphate (57) (Fig. 2). As described above, its reaction product DAG can be acylated to form TAG and it can be utilized for the synthesis of PE or PC via the Kennedy pathway (58-60). The reaction substrate PA is also used for the synthesis of phospholipids via the liponucleotide intermediate CDP-DAG (58, 59). Thus, PAP being positioned at the PA branch point plays an important role in lipid synthesis (58-60).

The PAP enzyme reaction was first demonstrated in animal tissues by Kennedy and colleagues in 1957 (57). The discovery of this enzyme provided a link between the phospholipid and TAG synthesis pathways (57). Subsequent studies revealed the importance of PAP in lipid metabolism (58, 61, 62). However, the attempts to isolate this

enzyme from animal tissues were unsuccessful, and the genetic and molecular information of PAP remained elusive for more than five decades. In 1989, PAP was successfully purified to near-homogeneity from *S. cerevisiae* (63). Nevertheless, it was not until 2006 that *PAHI* (phosphatidic acid phosphohydrolase) was identified as the gene encoding PAP (47).

The *PAHI* gene encodes a protein with 862 amino acids and a predicted molecular mass of 95 kDa (47). However, the Pah1p expressed in *S. cerevisiae* and *E. coli* migrates upon SDS-PAGE at 124 and 114 kDa, respectively (47). The difference between the predicted and observed protein molecular mass is due to, but not solely, the posttranslational phosphorylation (47). The enzyme contains an N-terminal amphipathic helix, a conserved NLIP domain, and a DXDXT catalytic motif within the HAD-like domain (previously known as CLIP domain) (Fig. 3). The purified recombinant Pah1p exhibits identical enzymatic properties of the enzyme purified from yeast (47, 63). Pah1p PAP activity is specific for PA and is dependent on Mg^{2+} (47, 63). Mutations of the aspartate residues of its DXDXT catalytic motif within the HAD-like domain (Fig. 3) abolish the PAP function *in vivo* (48). In addition, a glycine residue in the NLIP domain is also essential for its PAP activity (48). Although its reaction substrate PA resides in the membrane, in contrast to most other lipid synthesis enzymes, Pah1p PAP does not contain any transmembrane spanning domains. Pah1p is found in both the cytosol and membrane fractions while the majority of this enzyme is located in the cytosol (64, 65). Pah1p translocates from the cytosol onto a nuclear membrane sub-domain when the level of PA is elevated by overexpressing Dgk1p DAG kinase, indicating the recruitment of Pah1p onto the membrane is regulated by its substrate PA (66). In addition, the N-

FIGURE 3. Domain structures of Pah1p, App1p, Dpp1p, Lpp1p and lipin-1. The basic characteristics of Pah1p, App1p, Dpp1p, Lpp1p, and lipin-1 are indicated in the figure. *AH*, amphipathic helix; *HAD*, haloacid dehalogenase. The diagrams of each protein are not drawn on scale.



terminal amphipathic domain is essential for Pah1p to anchor onto the nuclear/ER membrane (66).

Physiological Roles of Pah1p PAP

The importance of Pah1p PAP in lipid metabolism has been revealed in cells defective in this enzyme activity (46-48). Along with the lack of PAP activity, *pah1Δ* mutant cells have increased levels of PA and decreased levels of DAG and its derivative TAG (47, 48). The effect of *pah1Δ* mutation on TAG (more than 90% decrease) is more evident in the stationary phase (46, 47) where the synthesis of TAG and PAP activity are elevated (67). Additionally, phospholipids, free fatty acids, and sterol ester amounts are increased, and the molecular species of phospholipids are varied in *pah1Δ* mutant cells (46, 47). The increased contents of phospholipids and fatty acids are attributed to the derepression of UAS_{INO}-containing lipid synthesis genes, whose expression are regulated by PA content (48, 68-72). The expression of UAS_{INO}-containing genes is activated by the association of Ino2p-Ino4p with the core sequence (5'CANNTG3') in their promoter (73-75), and is repressed by the binding to Opi1p to the Ino2p (76). In the *pah1Δ* mutant, the elevated PA, along with Scs2p, tethers Opi1p at nuclear/ER membrane preventing its translocation into the nucleus (76), which in turn results in the derepression of UAS_{INO}-containing lipid synthesis genes (77, 78). PA also regulates the expression of phospholipid synthesis genes in a manner that is independent of Opi1p (79). The increase of free fatty acids may also be due to the decreased ability to utilize fatty acids for TAG synthesis; likewise, the sterol ester content is elevated in the *pah1Δ* mutant cells (47). Abnormal lipid metabolism caused by the lack of Pah1p PAP activity reflects

several *pah1*Δ mutant phenotypes that include temperature sensitivity (47, 68), aberrant expansion of nuclear/ER membrane (48, 68), respiratory deficiency (47, 48), defects in the lipid droplet formation and morphology (46, 80, 81), defects in vacuole homeostasis and fusion (82), fatty acid-induced lipotoxicity (46), and elevated apoptosis in stationary phase (46).

The aberrant nuclear/ER membrane expansion in *pah1*Δ mutant has been attributed to the increased expression of UAS_{INO}-containing lipid synthesis genes (68). However, derepression of phospholipid synthesis genes by themselves is not sufficient for nuclear/ER membrane expansion (79), indicating that another factor must be involved with this abnormality. Data indicate that the elevated PA level in *pah1*Δ mutant cells is a responsible factor. Indeed, the introduction of *dgk1*Δ mutation into *pah1*Δ mutant cells causes a decrease in PA level and restores normal nuclear/ER membrane structure (83). In addition, the overexpression of Dgk1p DAG kinase activity results in an increase in PA levels and the aberrant nuclear/ER membrane proliferation (83).

Lipid droplets consist of a neutral lipid core, mainly TAG and sterol ester, surrounded by a monolayer of phospholipids. The reduction of lipid droplet formation in *pah1*Δ mutant cells correlates with the decreased levels of TAG (47, 48). The reduced DAG contributes to this phenotype not only by being a direct precursor for TAG but also by a mechanism that is independent of the generation of neutral lipids (80). In addition to DAG, PA is also involved in lipid droplet formation. The introduction of *dgk1*Δ mutation into *pah1*Δ mutant cells restores the lipid droplet formation (46, 80), and the *dgk1*Δ mutation alone causes slightly more lipid droplets (80). A supersized lipid droplet has been found in the *pah1*Δ cells as well as other mutants which share a common feature

of high PA levels (81). Thus, Pah1p PAP affects the lipid droplet formation and morphology via controlling the levels of PA and DAG.

Because of the reduced ability to incorporate fatty acids into TAG, *pah1Δ* mutant cells are susceptible to fatty acid-induced lipotoxicity (46). This phenotype cannot be rescued by the introduction of *dgk1Δ* mutation (46), although, as described above, it complements the defect in lipid droplet formation (46, 80), suggesting the elevated PA is not the basis for the fatty acid-induced lipotoxicity phenotype. In addition, the elevated apoptosis of the stationary phase *pah1Δ* mutant cells (46) appears to be due to the accumulated fatty acids that could cause a chronic lipotoxicity and may be also related to the changes in the phospholipid molecular species (46).

Other PAPs in Yeast

Besides Pah1p, three additional proteins, App1p, Dpp1p, and Lpp1p also exhibit PAP activity in yeast. App1p (66 kDa) is a cytosolic enzyme whose PAP activity requires Mg^{2+} while Mn^{2+} can partially compensate this requirement (84). In addition to PA, App1p can also dephosphorylate DGPP and LPA (85). Like Pah1p, App1p lacks a transmembrane domain and its PAP activity is governed by the DXDXT motif whereas this motif is not located within the HAD-like domain (Fig. 3) (84). App1p PAP activity does not affect lipid metabolism, while its association with cortical actin patches suggests this enzyme may be involved with endocytosis/vesicle movement (84).

Dpp1p and Lpp1p are lipid phosphate phosphatase enzymes that dephosphorylate various lipid phosphate molecules (e.g., PA, LPA, DGPP, sphingoid base phosphate and isoprenoid phosphate) by a catalytic mechanism that does not require Mg^{2+} as cofactor

(86, 87). In contrast to Pah1p, Dpp1p (33.5 kDa) and Lpp1p (31.5 kDa) are relatively smaller proteins containing six transmembrane domains and are located in the vacuole and Golgi, respectively (86, 87). Their activities are governed by a three-domain lipid phosphatase motif, KX_6RP (I), $PSGH$ (II), and SRX_5HX_3D (III) (Fig. 3) (88, 89). The conserved arginine in domain I and histidine in domain II and III are essential for their catalytic activity (89). Although Dpp1p and Lpp1p contribute to the majority of PAP activity (90), they are not involved in lipid synthesis (47); instead, their broad substrate specificity suggests these enzymes play a role in lipid signaling (91, 92).

Pah1p is the Mammalian Lipin Ortholog

Pah1p PAP is evolutionarily conserved from yeast to mammals (93). The lipin family proteins, encoded by *Lpin1*, *Lpin2* and *Lpin3* genes (94), are the mammalian orthologs of Pah1p (47). *Lpin1* was first identified by positional cloning as the mutated gene responsible for the phenotypes observed in the fatty liver dystrophy (*fld*) mouse (94); *Lpin2* and *Lpin3* were discovered based on their sequence similarity to *Lpin1* (94). At that time, lipin-1 functions were linked to lipid metabolism because lacking functions of lipin-1 in mice results in lipodystrophy, neonatal fatty liver, insulin resistance, and peripheral neuropathy, and its overexpression cause obesity and insulin sensitivity (94, 95). However, the molecular function of lipin proteins as PAP enzymes was not known until the identification of yeast *PAH1* as the gene encoding PAP. The sequence analysis of Pah1p revealed that this enzyme shares homology with lipin proteins at the NLIP and CLIP domains (47) (Fig. 3). Like yeast Pah1p, all lipin proteins (lipin-1 α , β , and γ , lipin-2 and lipin-3) contain a DXDXT catalytic motif within the HAD-like domain (48) and

their activities are Mg^{2+} dependent and specific to PA (47, 96, 97). The finding that lipin-1 is a PAP enzyme provides a molecular explanation for the lipodystrophy phenotype observed in *fld* mouse as well as the obesity phenotype when overexpressing lipin-1 (47, 94, 95). In addition, the subsequent studies found that neuropathy in *fld* mouse is attributed to the elevated PA level, which activates the mitogen-activated protein kinase/extracellular signal-regulated kinase kinase (MEK)-extracellular signal-regulated kinase (ERK) signaling pathway and in turn results in the degradation of myelin and Schwann cell dedifferentiation and proliferation (98).

In addition to PAP activity, lipin-1 also functions as a transcriptional coregulator modulating the expression of genes involved in lipid metabolism and inflammation (99-101). Lipin-1 co-activates a transcriptional complex containing peroxisome proliferator-activated receptor α (PPAR α) and PPAR γ coactivator-1 α (PGC-1 α) to regulate fatty acid metabolism in liver (99). On the other hand, lipin-1 also serves as a transcriptional repressor inhibiting the activity of nuclear factor of activated T-cell c4 (NFATc4), and consecutively suppresses the secretion of inflammatory factors (101). Lipin-1 regulates gene expressions through a direct interaction with transcription factors via a LXXIL motif located in the CLIP domain (99, 100) (Fig. 3). The DXDXT catalytic motif is not required for its activity as a transcriptional coactivator (99); however, a mutation on the first aspartate in this motif abolishes the interaction between lipin-1 and NFATc4 (100).

In human, mutations in *Lpin1* cause recurrent acute myoglobinuria in children; however, patients do not exhibit lipodystrophy as observed in the *fld* mouse (102). This may be due to a different tissue expression pattern of lipin genes between human and mouse (102). Human lipin-1 and lipin-2 are similarly expressed in adipose tissue while

mouse lipin-1 is the dominant PAP in this tissue (96, 102). In addition, the variations in the *Lpin1* gene have been shown to associate with insulin resistance and metabolic syndrome (103, 104). Mutations of *Lpin2* that eliminate its PAP activity result in the Majeed syndrome, an autoinflammatory disorder characterized by recurrent osteomyelitis, anemia, and dermatosis (105, 106).

Regulation of Pah1p/Lipin PAP

The functions of PAP are regulated by multiple factors including growth stage (67, 84), nutrient status (107-109), zinc (110), phosphate (65), oxygen (111), nucleotides (112) and lipids (46, 62, 113, 114). These regulations occur at the genetic and/or biochemical levels to modulate PAP enzyme catalytic activity and/or its subcellular localization.

Genetic Regulation of Pah1p PAP

Zinc, an essential mineral in eukaryotes, serves as a cofactor for various enzymes and is essential for structural integrity of many proteins (115). The intracellular levels of zinc are tightly controlled by regulating the zinc transporters at the transcriptional level (116-118). In zinc limiting conditions, the transcription factor Zap1p is induced, binds to the zinc responsive element (UAS_{ZRE}) in the promoter of genes and stimulates their expression (116-118). This mechanism is also involved in the regulation of many phospholipid synthesis genes including *PAHI* (110, 119-122). The *PAHI* gene contains a UAS_{ZRE} in the promoter and its expression is up-regulated in response to zinc depletion through the interaction of Zap1p with the UAS_{ZRE} (110). This induction results in elevated PAP activity and TAG levels (110). In addition, several genome-wide studies have showed that the expression of *PAHI* gene is affected by various conditions such as

carbon source (123), diauxic shift (124), and sporulation (125). Additional studies are required to understand the mechanism involved in these regulations.

In mammals, the regulations of *Lpin1* gene expression have been extensively studied and many transcriptional factors were found to be involved in these regulations (2, 126, 127). For instance, glucocorticoid is known to activate the transcription of *Lpin1* through a mechanism mediated by a glucocorticoid receptor response element located in *Lpin1* promoter (128, 129). This regulatory mechanism contributes to the induction of *Lpin1* expression by fasting, obesity, and during adipocyte differentiation (128, 129). In contrast, the expression of *Lpin2* gene is repressed during adipogenesis (93), and is not activated by glucocorticoid (129). In addition, the alternative *Lpin1* mRNA splicing results in three lipin-1 isoforms having different enzymatic properties and localization that may play distinct roles in adipogenesis (97, 130).

Biochemical regulation of Pah1p PAP by lipids and nucleotides

The activity of Pah1p PAP is activated by several membrane phospholipids synthesized through the CDP-DAG pathway including CDP-DAG, PI and CL (114). These phospholipids stimulate PAP activity by decreasing the K_m value of Pah1p for PA (114). Activation of PAP would channel PA toward DAG for the synthesis of TAG or phospholipids via the Kennedy pathway. Simultaneously, the stimulated PAP activity would cause a reduction in PA levels and thus result in the repression of UAS_{INO}-containing genes such as CDP-DAG synthase-encoding gene *CDS1* and inositol-3-phosphate synthase-encoding gene *INO1* (131). Nevertheless, the activation of PAP by PI and CL is antagonized by sphinganine that causes an increase in the activation constant for PI and an increase in the cooperativity of CL activation (131). Additionally,

sphinganine as well as other sphingoid bases sphingosine and phytosphingosine have shown to inhibit PAP activity in a parabolic competitive manner, indicating more than one sphingoid bases contribute to the exclusion of PA from Pah1p (113).

The activity of PAP is also inhibited by the nucleotides ATP and CTP, which affect both V_{max} and K_m of enzyme activity with respect to PA and act as the competitive inhibitors with respect to Mg^{2+} (112). The inhibitory effect of ATP on PAP activity correlates with the finding that high cellular ATP favors elevated PA content and phospholipid synthesis, while low cellular ATP favors reduced PA and increased TAG synthesis (112). In addition, high levels of CTP favor increased PA content and derepression of UAS_{INO}-containing genes (132)

Biochemical regulation of Pah1p PAP by phosphorylation/dephosphorylation

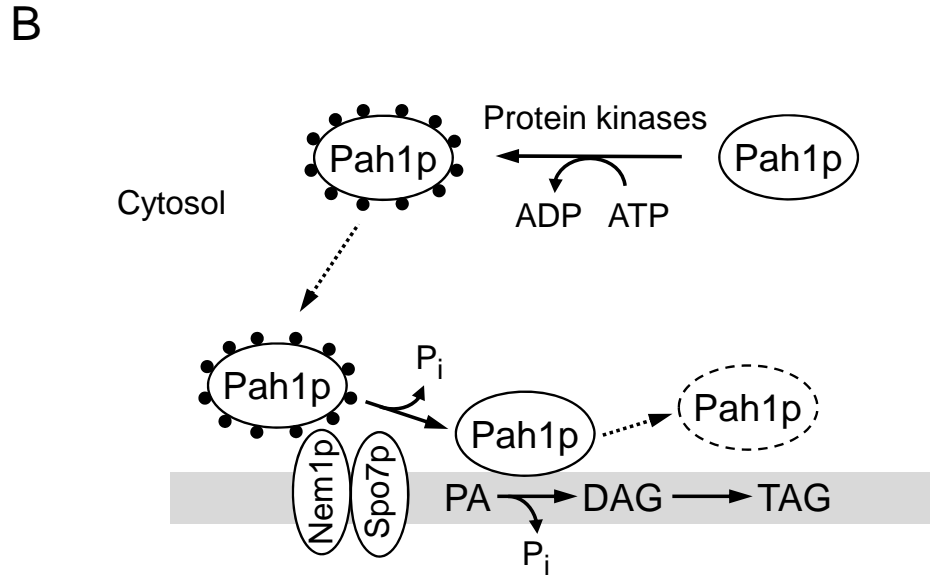
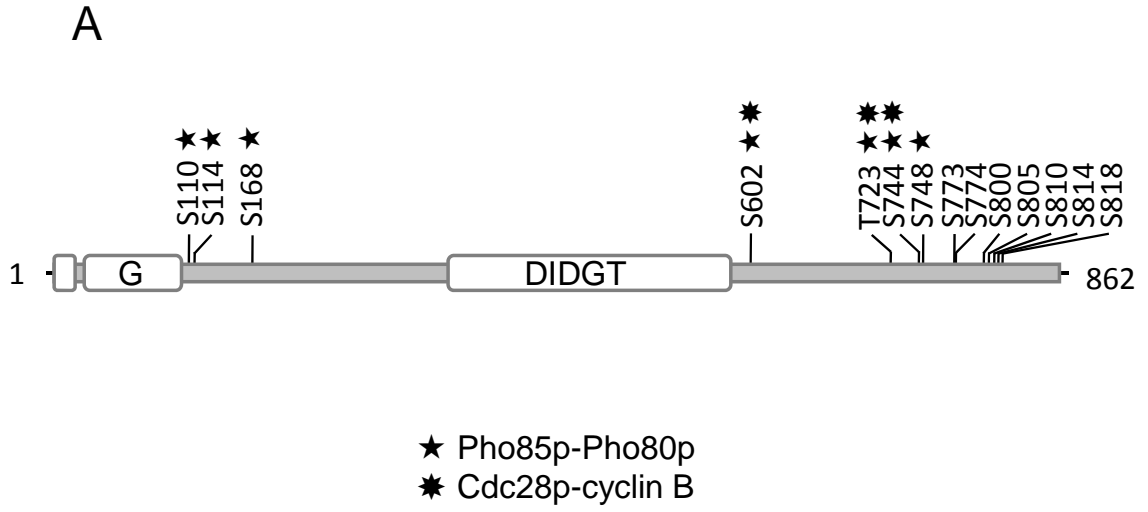
It was known even before *PAH1* (previously known as *SMP2*) was identified as the gene encoding PAP that the phosphorylation/dephosphorylation status of Pah1p affects its functions in phospholipid biosynthesis and nuclear membrane growth (68). At that time, Pah1p was found to be phosphorylated in a cell cycle-dependent manner and is dephosphorylated by Nem1p-Spo7p, a protein phosphatase complex located on the nuclear/ER membrane (68, 133). Cells lacking Nem1p-Spo7p complex accumulate the phosphorylated-form of Pah1p and exhibit similar phenotypes shown in the *pah1Δ* mutant cells including nuclear/ER membrane expansion and derepression of UAS_{INO}-containing genes (68, 133).

Consistent with early observations, more recent studies have shown that the *nem1Δ* mutant cells contain low levels of TAG and high levels of phospholipids and exhibit a temperature sensitive phenotype as the *pah1Δ* mutant cells (65, 134),

confirming the Nem1p-Spo7p complex is essential for Pah1p functions. Moreover, the phosphorylated-form of Pah1p favors the cytosolic location where it is physiologically inactive, while its dephosphorylated-form (phosphorylation-deficient mutant 7A, discussed in later section) favors the membrane location where its substrate PA resides and thus it is physiologically active (64, 65). Therefore, the phosphorylated Pah1p in cytosol is recruited to the nuclear/ER membrane where it is dephosphorylated by Nem1p-Spo7p protein phosphatase (64, 65, 68) (Fig. 4). This dephosphorylation allows Pah1p to directly associate with the membrane via a short N-terminal amphipathic helix for interaction with its substrate PA and enzyme catalysis (64, 65). As described above, Pah1p lacks a transmembrane domain although its reaction ought to occur on nuclear/ER membrane; thus, this phosphorylation/dephosphorylation-mediated translocation mechanism is critical for the regulation of Pah1p physiological functions.

Mass spectrometry and immunoblot analyses have identified multiple sites of phosphorylation in Pah1p (79, 135, 136) (Fig. 4). Proteome-wide phosphorylation studies have shown that Pah1p PAP can be phosphorylated by various protein kinases including Pho85p and Cdc28p (137-140). Pho85p and Cdc28p are cyclin-dependent kinases that phosphorylate protein on Ser/Thr-Pro residue(s) (141). Cdc28p is essential for the cell cycle progression, while the non-essential Pho85p works in support of Cdc28p and plays a vital role in regulating cellular response to low cellular phosphate levels (141-144). Pho85p-Pho80p phosphorylates Pah1p on seven sites (Ser-110, Ser-114, Ser-168, Ser-602, Thr-723, Ser-744, and Ser-748) and this phosphorylation inhibits Pah1p PAP activity by causing a 6-fold reduction in the enzyme specificity constant (V_{max}/K_m) (65). Three (Ser-602, Thr-723, and Ser-744) of the Pho85p-Pho80p

FIGURE 4. Phosphorylation sites in Pah1p and model for the regulation by phosphorylation/dephosphorylation. *A*, the diagram shows the serine (*S*) or threonine (*T*) phosphorylation sites identified from the purified yeast Pah1p (79). The protein kinases responsible for the phosphorylation are indicated (64, 65). *B*, Pah1p in the cytosol is phosphorylated on sites (*black circles* decorating Pah1p) by multiple protein kinases. The phosphorylated enzyme is translocated to the nuclear/ER membrane (*dotted arrow*) for its dephosphorylation by the Nem1p-Spo7p phosphatase complex. The dephosphorylated membrane-associated form of Pah1p catalyzes the dephosphorylation of PA to generate DAG for the synthesis of TAG. The *dotted line ellipse* signifies the loss of Pah1p after catalysis.



phosphorylated sites are also phosphorylated by the Cdc28p-cyclin B complex; however, this phosphorylation does not affect PAP activity (64). The simultaneous mutations of the seven Pho85p-Pho80p phosphorylation sites (7A) results in a 1.8-fold increase in PAP activity (79), and increased interaction with the membrane fraction, while at the same time causing a dramatic reduction in Pah1p abundance (65). In addition, the 7A mutant complements the *pah1Δ nem1Δ* phenotypes including temperature sensitivity, nuclear/ER membrane expansion, derepression of *INO1* gene and decreased TAG level, indicating the 7A mutant Pah1p can circumvent the requirement of Nem1p-Spo7p dephosphorylation (64, 65). However, the simultaneous mutation of the three Cdc28p-cyclin B phosphorylation sites (3A) only partially mimics the physiological effects of the 7A mutations (64). Collectively, the phosphorylations of the seven Ser/Thr-Pro sites play a major role in controlling the enzyme's function in lipid metabolism. (64, 65, 79).

The mammalian lipin-1 and lipin-2 enzymes are also subject to phosphorylation modification (93, 145, 146). Lipin-1 is phosphorylated in response to insulin (145, 146). In 3T3-L1 adipocyte, this insulin mediated-phosphorylation is dependent on the mammalian target of rapamycin (mTOR) signaling pathway and results in a subcellular translocation of lipin-1 from membrane fraction to cytosolic fraction (146). In HeLa cells, the lipin-1 and lipin-2 are phosphorylated on the Pro-directed Ser/Thr sites during mitotic phase and this phosphorylation causes a decrease in PAP activity (93). Recent studies showed that lipin-1 can be dephosphorylated by the mammalian ortholog of Nem1p-Spo7p (147), suggesting that the regulatory mechanism of PAP via phosphorylation/dephosphorylation is evolutionary conserved.

SPECIFIC AIMS

The phosphorylation/dephosphorylation is a major regulatory mechanism by which the functions of *PAH1*-encoded PAP are controlled (65, 68, 79, 148). Bioinformatics analyses suggested that Pah1p contains more than 90 putative phosphorylation sites. Mass spectrometry analyses of Pah1p identified multiple phosphorylation sites that are located within several protein kinase consensus motifs, including PKA and PKC (79). PKA is the principal mediator of signals transmitted through the *RAS/cAMP* pathway in *S. cerevisiae*, and plays a role in controlling cell metabolism including phospholipid synthesis (29, 149, 150). PKC is important in the cell wall integrity pathway, microtubule functions, and cell cycle (151, 152). In this dissertation, we examined the hypothesis that Pah1p is regulated by phosphorylation via PKA and PKC. Indeed, Pah1p was shown to be a substrate for these protein kinases, and we determined the major sites of phosphorylation. By using phosphorylation-deficient or phosphorylation-mimic mutants, we examined the effect of Pah1p phosphorylation on its activity, protein abundance and localization, temperature sensitivity, cell growth under different nutrient, and lipid composition. In addition, we examined the hypothesis that the phosphorylations of Pah1p are interrelated.

EXPERIMENTAL PROCEDURES

Materials

All chemicals were reagent grade or better. Growth medium supplies were obtained from Difco Laboratories. Qiagen was the supplier of the DNA gel extraction kit, plasmid DNA purification kit, and nickel-nitrilotriacetic acid agarose (Ni-NTA) resin. The QuikChange site-directed mutagenesis kit was from Stratagene and carrier DNA for yeast transformation was from Clontech. New England Biolabs was the source of enzyme reagents for DNA manipulations, nucleotides, and CKII (human glioblastoma). PCR primers were prepared by Genosys Biotechnologies. DNA size ladders, molecular mass protein standards, and reagents for electrophoresis, Western blotting, and protein assay reagent were purchased from Bio-Rad. PKA catalytic subunit (bovine heart) and conventional mammalian PKC (rat brain) were from Promega. Q-Sepharose, IgG-Sepharose, PVDF paper, mouse anti-His₆ antibody, and the enhanced chemifluorescence Western blotting detection kit were from GE Healthcare. Lipids and thin layer chromatography plates (cellulose and silica gel 60) were from Avanti Polar Lipids and EM science, respectively. Radiochemicals were from Perkin-Elmer Life Sciences, and scintillation counting supplies and acrylamide solutions were from National Diagnostics. Alkaline phosphatase-conjugated goat anti-rabbit IgG antibodies, alkaline phosphatase-conjugated goat anti-mouse IgG antibodies, mouse anti-phosphoglycerate kinase antibodies, and rabbit anti-(phosphoserine/phosphothreonine) PKA substrate antibodies were from Thermo Scientific, Pierce, Invitrogen, and Cell Signaling Technology, respectively. β -mercaptoethanol, bovine serum albumin, phosphoamino acid standards, isopropyl- β -D-1-thiogalactoside, L-1-tosylamido-2-phenylethyl chloromethyl ketone-

trypsin, protease inhibitors, phosphatase inhibitor cocktail I and II, antifoam A emulsion, and Triton X-100 were purchased from Sigma-Aldrich.

Strains and Growth Conditions

Table I lists the *Escherichia coli* and *S. cerevisiae* strains used in this work. *E. coli* strains DH5 α was used for the propagation of plasmids. BL21(DE3)pLysS and BL21(DE3) were used for the expression of yeast His₆-tagged Pah1p and His₆-tagged Pho85p, respectively. The bacterial cells were grown at 37 °C in LB medium (1% tryptone, 0.5% yeast extract, 1% NaCl, pH 7). Antibiotics, such as ampicillin (100 μ g/ml), carbenicillin (100 μ g/ml) and chloramphenicol (34 μ g/ml) were added to medium to select strains that carry specific plasmids. The expression of Pah1p in BL21(DE3)pLysS cells bearing *PAHI* derivatives of plasmid pET-15b was induced with 1 mM isopropyl- β -D-1-thiogalactoside for two hours at room temperature when cells were grown to $A_{600} = 0.5$ (47).

S. cerevisiae strains SS1026, SS1132, and GHY58 are *pah1* Δ , *pah1* Δ *nem1* Δ , and *pah1* Δ *dpp1* Δ *lpp1* Δ mutants, respectively, and were used for the expression of wild type and phosphorylation mutant Pah1p. Yeast cells were grown in standard synthetic complete medium containing 2% glucose, and appropriate amino acids were omitted from the growth medium to select for cells carrying specific plasmids (153). Synthetic complete growth medium lacking inositol and choline was prepared as described by Culbertson and Henry (154). Growth of cultures (200 μ l, $A_{600nm} = 0.1$) in 96-well plates was monitored with a Thermomax plate reader. The modified Gompertz equation (155)

TABLE I. Strains used in this study

Strain	Genotype or relevant characteristics	Reference/Source
<i>E. coli</i>		
DH5 α	F ⁻ ϕ 80dlacZ Δ M15 Δ (lacZYA-argF)U169 <i>deoR recA1 endA1 hsdR17(r_k⁻ m_k⁺)</i>	(156)
BL21(DE3)pLysS	<i>phoA supE44 λ⁻ thi-1 gyrA96 relA1</i> F- <i>ompT hsdSB (r_B-m_B-) gal dcm</i> (DE3) pLysS	Novagen
BL21(DE3)	F ⁻ <i>ompT hsdS_B (r_B⁻m_B⁻) gal dcm</i> (DE3)	Invitrogen
<i>S. cerevisiae</i>		
RS453	<i>MATa ade2-1 his3-11,15 leu2-3,112 trp1-1 ura3-52</i>	(157)
SS1026	<i>pah1Δ::TRP1</i> derivative of RS453	(68)
SS1132	<i>pah1Δ::TRP1 nem1Δ::HIS3</i> derivative of RS453	(64)
W303-1A	<i>MATa ade2-1 can1-100 his3-11,15 leu2-3,112 trp1-1 ura3-1</i>	(158)
GHY58	<i>dpp1Δ::TRP1/Kan^r lpp1Δ::HIS3/ Kan^r pah1Δ::URA3</i> derivative of W303-1A	(47)

was used to calculate growth parameters. Cell numbers in liquid cultures were determined spectrophotometrically at an absorbance of 600 nm. The liquid growth medium was supplemented with agar (2% for yeast or 1.5% for *E. coli*) for growth on solid medium.

DNA Manipulations

Isolation of genomic and plasmid DNA, digestion and ligation of DNA, and PCR amplification of DNA were performed by standard protocols (156, 159). Site-specific mutations were constructed by QuikChange site-directed mutagenesis using appropriate templates and primers. All mutations were confirmed by DNA sequencing. Plasmid transformations of *E. coli* (156) and yeast (160) were performed as described previously.

Construction of Plasmids

All plasmids and primers used in this study are listed in Table II and Table III, respectively. Plasmid pGH313 directs the isopropyl- β -D-1-thiogalactopyranoside-induced expression of His₆-tagged Pah1p in *E. coli* (47), whereas plasmid pGH315 directs low copy expression of Pah1p in *S. cerevisiae* (64). Truncated PAH1-1-752, 1-646, and 18-862 derivatives of pGH313 were constructed by Gil-Soo Han. pGH313-1-752 and pGH313-1-646 were made by generating a nonsense mutation at codon 753 and codon 647, respectively, of pGH313. pGH313-18-862 was constructed from pGH313 by replacing codons 1-17 with a start codon, and pGH313-235-752 was produced from pGH313-235-862 by replacing codons 753-862 with a stop codon. The derivatives of

TABLE II. Plasmids used in this study

Plasmid	Genotype or relevant characteristics	Reference/Source
pET-15b	<i>E. coli</i> expression vector with N-terminal His6-tag fusion	Novagen
pGH313	<i>PAH1</i> gene inserted into pET-15b	(47)
pGH313-1-752	<i>PAH1</i> (1-752 truncation) derivative of pGH313	This work
pGH313-1-646	<i>PAH1</i> (1-646 truncation) derivative of pGH313	This work
pGH313-235-752	<i>PAH1</i> (235-752 truncation) derivative of pGH313	This work
pGH313-18-862	<i>PAH1</i> (18-862 truncation) derivative of pGH313	This work
pGH313-S10A	<i>PAH1</i> S10A mutation derivative of pGH313	This work
pGH313-S12A	<i>PAH1</i> S12A mutation derivative of pGH313	This work
pGH313-S16A	<i>PAH1</i> S16A mutation derivative of pGH313	This work
pGH313-S17A	<i>PAH1</i> S17A mutation derivative of pGH313	This work
pGH313-S677A	<i>PAH1</i> S677A mutation derivative of pGH313	This work
pGH313-S694A	<i>PAH1</i> S694A mutation derivative of pGH313	This work
pGH313-S769A	<i>PAH1</i> S769A mutation derivative of pGH313	This work
pGH313-S773A	<i>PAH1</i> S773A mutation derivative of pGH313	This work
pGH313-S774A	<i>PAH1</i> S775A mutation derivative of pGH313	This work
pGH313-S788A	<i>PAH1</i> S788A mutation derivative of pGH313	This work
pGH313-S677/S788A	<i>PAH1</i> S677A/ S788A mutation derivative of pGH313	This work
pGH313-S773/S774A	<i>PAH1</i> S773A/S774A mutation derivative of pGH313	This work
pGH313-3A	<i>PAH1</i> S677A/S769A/S788A mutation derivative of pGH313	This work
pGH313-4A	<i>PAH1</i> S677A/S773A/774A/S788A mutation derivative of pGH313	This work
pGH313-5A	<i>PAH1</i> S10A/S677A/S773A/S774A/S788A mutation derivative of pGH313	This work
pGH313-7A	<i>PAH1</i> S110A/S114A/S168A/S602A/T723A/S774A/S748A mutation derivative of pGH313	(64)
pRS415	Low copy <i>E. coli</i> /yeast shuttle vector with <i>LEU2</i>	(161)
pGH315	<i>PAH1</i> gene inserted into pRS415	(64)
pGH315-S10A	<i>PAH1</i> S10A mutation derivative of pGH315	This work
pGH315-S10D	<i>PAH1</i> S10D mutation derivative of pGH315	This work

TABLE II. Plasmids used in this study

Plasmid	Genotype or relevant characteristics	Reference/Source
pGH315-S677A	<i>PAH1</i> S677A mutation derivative of pGH315	This work
pGH315-S677D	<i>PAH1</i> S677D mutation derivative of pGH315	This work
pGH315-S769A	<i>PAH1</i> S769A mutation derivative of pGH315	This work
pGH315-S769D	<i>PAH1</i> S769D mutation derivative of pGH315	This work
pGH315-S773A	<i>PAH1</i> S773A mutation derivative of pGH315	This work
pGH313-S773D	<i>PAH1</i> S773D mutation derivative of pGH315	This work
pGH315-S774A	<i>PAH1</i> S774A mutation derivative of pGH315	This work
pGH315-S774D	<i>PAH1</i> S774D mutation derivative of pGH315	This work
pGH315-S788A	<i>PAH1</i> S788A mutation derivative of pGH315	This work
pGH315-S788D	<i>PAH1</i> S788D mutation derivative of pGH315	This work
pGH315-3A	<i>PAH1</i> S677A/S769A/S788A mutation derivative of pGH315	This work
pGH315-3D	<i>PAH1</i> S677D/S769D/S788D mutation derivative of pGH315	This work
pGH315-4A	<i>PAH1</i> S677A/S773A/S774A/S788A mutation derivative of pGH315	This work
pGH315-4A	<i>PAH1</i> S677D/S773D/S774D/S788D mutation derivative of pGH315	This work
pGH315-5A	<i>PAH1</i> S10A/S677A/S773A/S774A/S788A mutation derivative of pGH315	This work
pGH315-5D	<i>PAH1</i> S10D/S677D/S773D/S774D/S788D mutation derivative of pGH315	This work
pGH315-7A	<i>PAH1</i> S110A/S114A/S168A/S602A/T723A/S774A/S748A mutation derivative of pGH315	(64)
pGH315-S10A-7A	<i>PAH1</i> S10A/S110A/S114A/S168A/S602A/T723A/S774A/S748A mutation derivative of pGH315	This work
pGH315- S10D-7A	<i>PAH1</i> S10D/S110A/S114A/S168A/S602A/T723A/S774A/S748A mutation derivative of pGH315	This work
EB1164	<i>PHO85</i> -His ₆ derivative of pQE-60	(162)
EB1076	<i>PHO80</i> derivative of pSBETA	(162)

TABLE III. Oligonucleotides used in this study

Oligonucleotides	Sequence
S10A-F	5'-GAGCTCTTGGGGCTGTGTCTAAAAC-3'
S10A-R	5'-GTTTTAGACACAGCCCCAAGAGCTC-3'
S10D-F	5'-GAGCTCTTGGGGATGTGTCTAAAAC-3'
S10D-R	5'-GTTTTAGACACATCCCCAAGAGCTC-3'
S12A-F	5'-TTGGGTCTGTGGCTAAAACATGGTC-3'
S12A-R	5'-GACCATGTTTTAGCCACAGACCCAA-3'
S16A-F	5'-AAACATGGTCTGCTATCAATCCGGC-3'
S16A-R	5'-GCCGGATTGATAGCAGACCATGTTT-3'
S17A-F	5'-AAACATGGTCTGCTATCAATCCGGC-3'
S17A-R	5'-GCCGGATTGATAGCAGACCATGTTT-3'
S677A-F	5'-ATAGGGCAAATGCAGTCAAACC-3'
S677A-R	5'-GCGGTTTTGACTGCATTTGCCCTAT-3'
S677D-F	5'-ATAGGGCAAATGATGTCAAACC-3'
S677D-R	5'-GCGGTTTTGACATCATTTGCCCTAT-3'
S694A-F	5'-ATGTGAGCGGCCCAATAACAA-3'
S694A-R	5'-TTGTTATTTGTGGCGCCGCTCACAT-3'
S769A-F	5'-ATAGA ACTAAAGCAAGGAGAGCATC-3'
S769A-R	5'-GATGCTCTCCTTGCTTTAGTTCTAT-3'
S769D-F	5'-ATAGA ACTAAAGATAGGAGAGCATC-3'
S769D-R	5'-GATGCTCTCCTATCTTTAGTTCTAT-3'
S773A-F	5'-CAAGGAGAGCAGCTTCTGCAGCCGC-3'
S773A-R	5'-GCGGCTGCAGAAGCTGCTCTCCTTG-3'
S773D-F	5'-CAAGGAGAGCAGATTCTGCAGCCGC-3'
S773D-R	5'-GCGGCTGCAGAATCTGCTCTCCTTG-3'
S774A-F	5'-GGAGAGCATCTGCTGCAGCCGCCAC-3'
S774A-R	5'-GTCGCGGCTGCAGCAGATGCTCTCC-3'
S774D-F	5'-GGAGAGCATCTGATGCAGCCGCCAC-3'
S774D-R	5'-GTCGCGGCTGCATCAGATGCTCTCC-3'
S773A/S774A-F	5'-GGAGAGCAGCTGCTGCAGCCGCCAC-3'
S773A/S774A-R	5'-GTCGCGGCTGCAGCAGCTGCTCTCC-3'
S773D/S774D-F	5'-GGAGAGCAGATGATGCAGCCGCCAC-3'
S773D/S774D-R	5'-GTGGCGGCTGCATCATCTGCTCTCC-3'
S788A-F	5'-TCAAAAAGCTCGCTGTGTCAAAGGC-3'
S788A-R	5'-GCCTTTGACACAGCGAGCTTTTTGA-3'
S788D-F	5'-TCAAAAAGCTCGATGTGTCAAAGGC-3'
S788D-R	5'-GCCTTTGACACATCGAGCTTTTTGA-3'

pGH313 and pGH315 that contain serine-to-alanine/aspartate mutations were constructed by QuikChange site-directed mutagenesis using appropriate templates and primers. Plasmids containing multiple missense mutations were constructed by the general strategies described previously (64). Plasmids EB1164 and EB1076 were used for the overexpression of His₆-tagged Pho85p and untagged Pho80p, respectively, in *E. coli* (162).

Purification of Pah1p and Pho85p-Pho80p

All steps were performed at 4 °C. The BL21(DE3)pLysS cells expressing His₆-tagged wild type and mutant Pah1p were disrupted by French press in breaking buffer containing 20 mM Tris-HCl (pH 7.9), 0.5 M NaCl, 5 mM imidazole, 1 mM phenylmethylsulfonyl fluoride, and protease inhibitor tablets. Cell lysates were centrifuged at 12,000 × *g* for 30 min, and the supernatant was applied to a Ni-NTA affinity column. To remove unbound proteins, the column was washed with 10 column volumes of buffer A (20 mM Tris-HCl (pH 7.9), 0.5 M NaCl, 10% glycerol, and 7 mM β-mercaptoethanol) containing 45 mM imidazole. The bound His₆-tagged Pah1p was eluted with buffer A containing 250 mM imidazole (47, 163). The fractions containing Pah1p were diluted with 5 sample volumes of buffer B (50 mM Tris-HCl (pH 7.5), 0.2 M NaCl, 10% glycerol, and 7 mM β-mercaptoethanol) and then applied to a Q-Sepharose column previously equilibrated with the same solution. The Q-Sepharose column was then washed with 10 column volumes of buffer B and Pah1p was eluted by increasing the NaCl concentration in buffer B to 0.3 M. Protein A-tagged wild type and 7A mutant forms of Pah1p expressed in *S. cerevisiae* were purified by affinity chromatography using

IgG-Sepharose as described previously (79). His₆-tagged Pho85p-Pho80p complex was purified from *E. coli* BL21(DE3) expressing plasmids EB1164 and EB1076 (162). Protein concentration was estimated by the method of Bradford (164) using bovine serum albumin as the standard.

Preparation of Yeast Cell Extracts and Subcellular Fractionation

All steps were performed at 4 °C. Yeast cells were disrupted with glass beads (0.5 mm diameter) using a BioSpec Products Mini-BeadBeater-16 (165). The cell disruption buffer contained 50 mM Tris-HCl (pH 7.5), 0.3 M sucrose, 0.15 M NaCl, 10 mM β -mercaptoethanol, 0.5 mM phenylmethanesulfonyl fluoride, 1 mM benzamidine, 5 μ g/ml aprotinin, 5 μ g/ml leupeptin, 5 μ g/ml pepstatin, and phosphatase inhibitor cocktail I and II (47). The cell lysate was centrifuged at 1500 \times g for 10 min, and the supernatant was referred to as the cell extract. The cytosol (supernatant) and total membrane (pellet) fractions were separated by centrifugation at 100,000 \times g for 1 h (165). The pellets were resuspended in the cell disruption buffer to the same volume of the cytosol fraction.

SDS-PAGE and Western Blot Analysis

SDS-PAGE (166) using 8% (for phosphorylation experiments) or 10% (for localization experiments) slab gels and Western blotting (167, 168) with PVDF membrane were performed by standard protocols. For detection of His₆-tagged wild type and truncated Pah1p, mouse anti-His₆ antibodies were used at a dilution of 1:3000 as primary antibody. Rabbit anti-Pah1p antibodies (64), rabbit anti-phosphatidylserine synthase antibodies (169), and mouse anti-phosphoglycerate kinase antibodies were used

at a concentration of 2 $\mu\text{g/ml}$. Rabbit anti-(phosphoserine/phosphothreonine) PKA substrate antibodies were used at a dilution of 1:1000. Alkaline phosphatase-conjugated goat anti-rabbit IgG antibodies and goat anti-mouse IgG antibodies were used at a dilution of 1:5,000. Immune complexes were detected using the enhanced chemifluorescence Western blotting detection kit. Fluorimaging was used to acquire images from Western blots, and the relative densities of the images were analyzed using ImageQuant software. Signals were in the linear range of detectability.

Phosphorylation and Dephosphorylation Reactions

The phosphorylation reactions of Pah1p were performed in triplicate at 30 °C. The phosphorylation reaction mixture for PKA contained 50 mM Tris HCl (pH 7.5), 10 mM MgCl_2 , 100 μM dithiothreitol, 100 μM $[\gamma\text{-}^{32}\text{P}]$ ATP (3000 cpm/pmol), 50 $\mu\text{g/ml}$ Pah1p, and the indicated amounts of PKA (170). The PKC reaction mixture contained 50 mM Tris HCl (pH 7.5), 10 mM MgCl_2 , 10 mM β -mercaptoethanol, 1.7 mM CaCl_2 , 500 μM PS, 156 μM DAG, 100 μM $[\gamma\text{-}^{32}\text{P}]$ ATP (3000 cpm/pmol), 50 $\mu\text{g/ml}$ Pah1p, and the indicated amounts of PKC (170). The reaction mixture for Pho85p-Pho80p contained 25 mM Tris HCl (pH 7.5), 10 mM MgCl_2 , 100 μM dithiothreitol, 100 μM $[\gamma\text{-}^{32}\text{P}]$ ATP (3000 cpm/pmol), 50 $\mu\text{g/ml}$ Pah1p, and 40 $\mu\text{g/ml}$ purified recombinant Pho85p-Pho80p (65). The CKII reaction mixture contained 50 mM Tris-HCl (pH 7.5), 10 mM MgCl_2 , 10 mM dithiothreitol, 50 μM $[\gamma\text{-}^{32}\text{P}]$ ATP (2000 cpm/pmol), 50 $\mu\text{g/ml}$ Pah1p and CKII (20 unit). One unit of PKA, PKC or CKII activity was defined as the amount of enzyme required to transfer 1 pmole of phosphate per minute. After kinase reactions, samples were treated with 4x Laemmli sample buffer (166) and were subjected to SDS-PAGE for the

separation of Pah1p and radioactive ATP. The incorporation of the radioactive γ -phosphate from ATP to Pah1p was detected by phosphorimaging analysis and the level of phosphorylation was quantified by ImageQuant analysis software using [γ - ^{32}P]ATP as the standard. Pah1p isolated from yeast was dephosphorylated with 50 units of lambda protein phosphatase in 50 mM Tris-HCl (pH 7.5), 2 mM MnCl_2 , 2 mM dithiothreitol, 0.01% Brij 35, 0.1 mM EGTA, 100 mM NaCl.

Preparation of Liposomes

Liposomes (unilamellar phospholipid vesicles) were prepared by the lipid extrusion method of MacDonald *et al.* (171). In brief, chloroform was evaporated from the indicated phospholipids under nitrogen to form a thin film. The phospholipids were then resuspended in 20 mM Tris-HCl (pH 7.5), 150 mM NaCl, and 1 mM EDTA. After five cycles of freezing and thawing, the phospholipid suspensions were extruded 11 times through a polycarbonate filter (100 nm diameter).

Phosphoamino Acid and Phosphopeptide Mapping Analyses

^{32}P -labeled Pah1p from radioactive phosphorylation reaction was resolved by SDS-PAGE and was transferred to PVDF membrane. For phosphoamino acid analysis, ^{32}P -labeled Pah1p on PVDF membrane was treated with 6 N HCl at 110 °C to obtain free amino acids. The hydrolytes containing amino acids were mixed with standard phosphoamino acids (phosphoserine, phosphothreonine and phosphotyrosine) and subjected to two-dimensional electrophoresis on cellulose thin layer chromatography (172, 173). ^{32}P -labeled phosphoamino acids were detected by phosphorimaging analysis

and the standard phosphoamino acids were visualized with 0.25% ninhydrin stain (173). For phosphopeptide mapping analysis, ^{32}P -labeled Pah1p on PVDF membrane was proteolytically digested with L-1-tosylamido-2-phenylethyl chloromethyl ketone-trypsin. The resulting hydrolytes were subjected to electrophoresis followed with TLC analysis using cellulose thin layer chromatography (174). Phosphorimaging analysis was used to detect ^{32}P -labeled phosphopeptides.

Mass Spectrometry Analysis of Pah1p Phosphorylation Sites

Mass spectrometry analysis of phosphorylated Pah1p was performed at the Center for Advanced Proteomics Research of the University of Medicine and Dentistry of New Jersey, Newark. After trypsin digestion of phosphorylated Pah1p in SDS-polyacrylamide gel slices, peptides were analyzed by matrix-assisted laser desorption ionization tandem time-of-flight mass spectrometry to identify phosphopeptide candidates. Based on the phosphopeptide ion inclusion list, quadrupole time-of-flight and Orbitrap liquid chromatography-mass spectrometry/mass spectrometry were performed to identify phosphorylation sites (64).

Preparation of ^{32}P -labeled PA and Measurement of PAP Activity

^{32}P -labeled PA was synthesized enzymatically from DAG and $[\gamma\text{-}^{32}\text{P}]\text{ATP}$ with *E. coli* DAG kinase, and the radioactive product was purified by thin-layer chromatography (165). PAP activity was determined by measuring the release of water-soluble $^{32}\text{P}_i$ from chloroform-soluble $[\text{}^{32}\text{P}]\text{PA}$ (10,000 cpm/nmol) (165). The reaction mixture contained 50 mM Tris-HCl buffer (pH 7.5), 1 mM MgCl_2 , 0.2 mM PA, 2 mM Triton X-100, and

enzyme protein in a total volume of 0.1 ml. All enzyme assays were conducted in triplicate at 30 °C. The average standard deviation of the assays was \pm 5%. The reactions were linear with time and protein concentration. A unit of PAP activity was defined as the amount of enzyme that catalyzed the formation of 1 nmol of product per minute.

***In Vivo* Labeling of Pah1p**

The *S. cerevisiae* *pah1* Δ *dpp1* Δ *lpp1* Δ cells expressing wild type or mutant Pah1p were grown in the medium containing ^{32}P i (15 $\mu\text{Ci/ml}$) to the exponential phase. The ^{32}P -labeled cells were harvested, resuspended in cell disruption buffer with 2 $\mu\text{l/ml}$ antifoam A emulsion and then disrupted with glass beads using a vortex mixer (169). Cell lysates were centrifuged at 1500 g for 10 min to obtain cell extracts. The ^{32}P -labeled Pah1p was immunoprecipitated from the cell extract (1 mg of total protein) with 5 μg anti-Pah1p antibody. Pah1p was dissociated from protein-antibody complexes, subjected to SDS-PAGE and transferred to PVDF membrane. The radioactive signal of ^{32}P -labeled Pah1p was quantified using ImageQuant software after phosphorimaging and the amount of protein was determined by immunoblot analysis.

Labeling and Analysis of Lipids

Steady-state labeling of lipids with [2- ^{14}C]acetate was performed as described previously (175), and lipids were extracted from labeled cells by the method of Bligh and Dyer (176). Lipids were analyzed by one-dimensional TLC on silica gel plates (177). The identity of radiolabeled TAG and total phospholipids on TLC plates was confirmed

by comparison of its migration with that of standards after exposure to iodine vapor. Radiolabeled lipids were visualized by phosphorimaging analysis, and were quantified using ImageQuant software.

Analyses of Data

Statistical analyses were performed with SigmaPlot software. The p values < 0.05 were taken as a significant difference. The Enzyme Kinetics module of SigmaPlot software was used to analyze kinetic data according to the Michaelis-Menten and Hill equations.

RESULTS

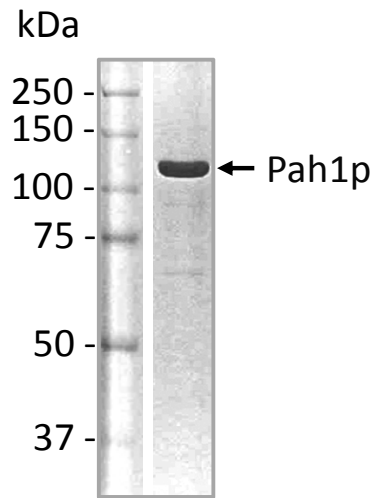
Pah1p is Phosphorylated by Multiple Protein Kinases

Yeast Pah1p was shown to be highly phosphorylated on the serine and threonine residues which are putative target sites of several protein kinases including cyclin-dependent kinases, PKA, PKC, CKI, CKII and Dbf2-Mob1 kinase complex (79). To identify the protein kinases that are responsible for the phosphorylation of Pah1p, we conducted protein kinase assays using the recombinant Pah1p that was free from endogenous phosphorylations (79). The *E. coli*-expressed His₆-Pah1p was purified by Ni-NTA affinity chromatography followed by Q-Sepharose anion-exchange chromatography. The SDS-PAGE analysis of the purified recombinant Pah1p showed it was nearly homogenous and migrated as a 114-kDa protein (Fig. 5A).

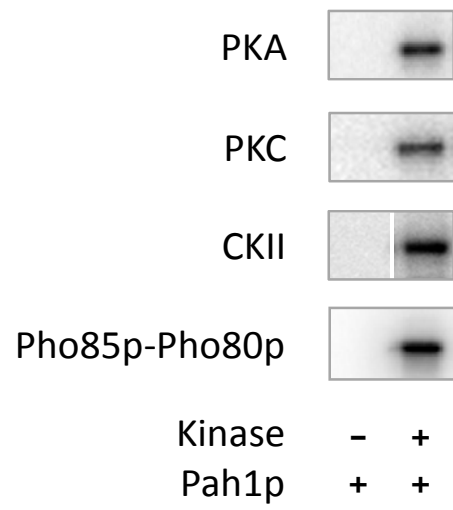
The phosphorylation of Pah1p was examined by incubating it with [γ -³²P]ATP and protein kinases that are predicted to phosphorylate Pah1p including PKA, PKC, CKII, and Pho85p-Pho80p protein kinase complex (138, 139). In this study, mammalian orthologs of PKA, PKC, and CKII were used. These mammalian orthologs are structurally and functionally similar to their yeast counterparts (178-180), and thus have been used to study the phosphorylation of several phospholipid synthesis proteins from yeast (169, 181-184). Pho85p-Pho80p complex was purified from *E. coli* cells that were co-transformed with yeast *PHO85* and *PHO80* genes (162). After the kinase reactions, the phosphorylation of Pah1p was monitored by following the incorporation of the radioactive γ phosphate from [γ -³²P]ATP into the enzyme (Fig. 5B). Phosphorimaging analysis of kinase reaction products resolved by SDS-PAGE indicated the recombinant

FIGURE 5. Phosphorylation of Pah1p by protein kinases. The His₆-tagged Pah1p was expressed in *E. coli* and purified by Ni-NTA affinity chromatography followed with Q-Sepharose anion-exchange chromatography. *A*, purified Pah1p was subjected to SDS-PAGE and stained with Coomassie blue. The positions of the protein molecular mass standards and Pah1p (~114 kDa) are indicated in the figure. *B*, purified recombinant Pah1p (1 μg) was incubated with the indicated protein kinases and [γ -³²P]ATP for 10 min. Following the reaction, Pah1p was separated from ATP and the protein kinases by SDS-PAGE. The SDS-polyacrylamide gel was dried and subjected to phosphorimaging analysis. The figures are the partial image of polyacrylamide gels that were analyzed for Pah1p phosphorylation by phosphorimaging.

A



B



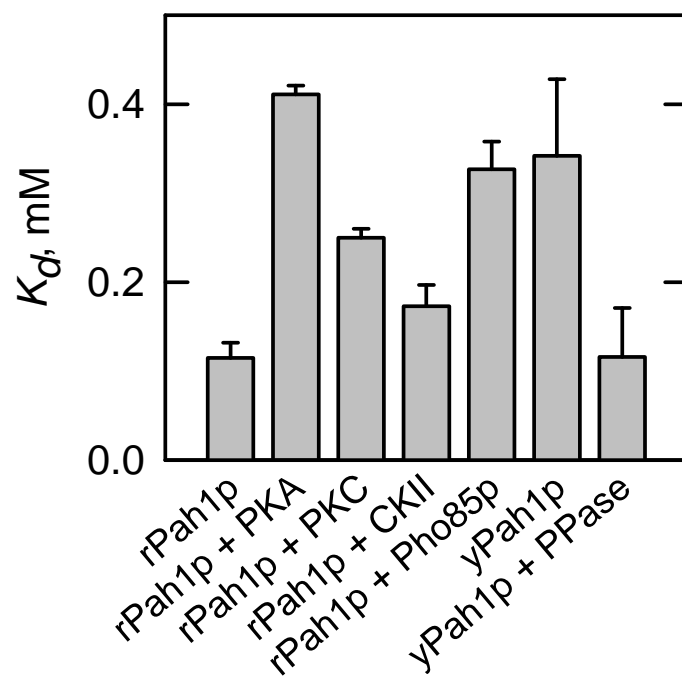
Pah1p served as a substrate for PKA, PKC, CKII, and the Pho85p-Pho80p protein kinase complex.

Phosphorylation Decreases the Interaction of Pah1p with PC-PA Liposomes

Studies with yeast expressing a phosphorylation-deficient mutant (7A) Pah1p indicated that phosphorylation form of Pah1p favors a cytosolic location whereas dephosphorylation favors a membrane association (64, 66). Using the fluorescence assay, we examined the effects of phosphorylation on the interaction of Pah1p with phospholipid liposomes. The phosphorylations with PKA, PKC, CKII and Pho85p-Pho80p caused a decrease in the interaction of Pah1p with the PC-PA liposomes with increased K_d values of 3.8-fold, 2.3-fold, 1.5-fold, and 2.8-fold, respectively, when compared with the unphosphorylated enzyme (Fig. 6). Moreover, the K_d value of yeast-derived PAP that is endogenously phosphorylated was 3.2-fold greater than the K_d value of the unphosphorylated enzyme isolated from *E. coli* (Fig. 6). The dephosphorylation of the yeast-derived PAP resulted in an increase in liposome interaction as indicated by a 3.15-fold decrease in the K_d value for the enzyme (Fig. 6).

These results indicate that PKA, PKC, CKII and Pho85p-Pho80p complex may participate in the phosphorylation and regulation of Pah1p in yeast cells. In the following studies, the regulation of Pah1p by PKA and PKC was examined in further detail. The phosphorylation of Pah1p by Pho85p-Pho80p and CKII are the subject of studies conducted by other members in the Carman laboratory.

FIGURE 6. Effect of phosphorylation on the interaction of Pah1p with PC-PA liposomes. Purified recombinant Pah1p (*rPah1p*) was phosphorylated with the indicated protein kinases. Pah1p isolated from yeast (*yPah1p*) was dephosphorylated with lambda protein phosphatase (PPase). The various Pah1p preparations were incubated with PC-PA liposomes at concentrations ranging from 0.01 to 0.8 mM. Following 10-min incubation, the increase in Pah1p fluorescence was measured. The dissociation constants (K_d) were determined from data where relative fluorescence was plotted with respect to total phospholipid concentration in the liposomes.



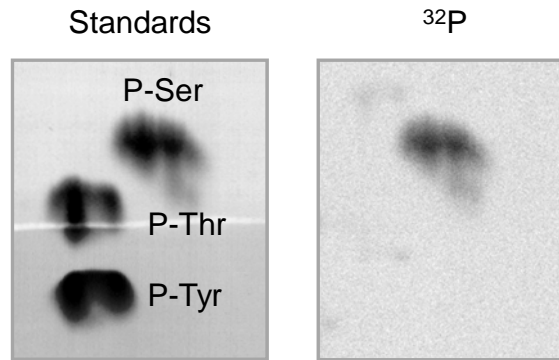
PKA Phosphorylates Pah1p and Attenuates its PAP activity

PKA is a serine/threonine-specific protein kinase (185). To identify the target amino acid residue of PKA, ^{32}P -labeled Pah1p was prepared by phosphorylating it with PKA and $[\gamma\text{-}^{32}\text{P}]\text{ATP}$ and then was subjected to the phosphoamino acid analysis. The result indicated that the protein kinase A phosphorylates Pah1p only on a serine residue (Fig. 7A).

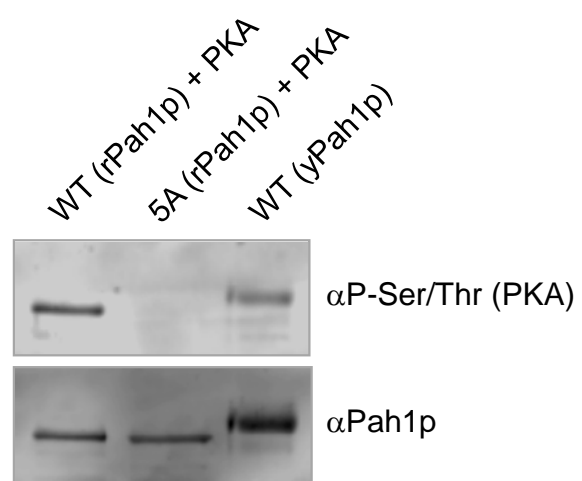
Previous studies have shown that Pah1p isolated from *S. cerevisiae* is a phosphoprotein (79). We sought evidence that some of this phosphorylation was mediated by PKA. To address this question, we made use of antibodies that are generated against a peptide containing phosphoserine/phosphothreonine within the PKA consensus motif. Indeed, these antibodies recognized Pah1p isolated from yeast (Fig. 7B), which had been known to be phosphorylated *in vivo* on Ser-773 and Ser-774 (79). These are two of the five sites that were found here to be targets of PKA *in vitro* (see below). To confirm that these antibodies recognized Pah1p phosphorylated by PKA, a Western blot was performed on purified recombinant wild type and 5A mutant (see below) enzymes that were incubated with PKA and ATP. The antibodies recognized wild type Pah1p phosphorylated with PKA, but did not recognize the PKA-treated 5A mutant enzyme (Fig. 7B). The electrophoretic mobility of the Pah1p isolated from yeast was slower than the enzyme isolated from *E. coli* (Fig. 7B). This was due to the fact that in yeast Pah1p is phosphorylated by Pho85p-Pho80p and Cdc28p-cyclin B at Thr-723, an event that also causes a decrease in the electrophoretic mobility of the purified recombinant enzyme (65).

FIGURE 7. PKA phosphorylates Pah1p on a serine residue *in vitro* and *in vivo*. *A*, purified recombinant Pah1p (1 μ g) was phosphorylated with PKA (2 unit) and [γ - 32 P]ATP (1 nmol) for 10 min. Following the reaction, Pah1p was subjected to SDS-PAGE and was transferred to PVDF membrane. The portion of PVDF membrane containing 32 P-labeled Pah1p was incubated with 6 N HCl for 90 min at 110 $^{\circ}$ C, and the hydrolysates were separated by 2-dimensional electrophoresis. The positions of the standard phosphoamino acids phosphoserine (*P-Ser*), phosphothreonine (*P-Thr*), and phosphotyrosine (*P-Tyr*) are indicated. *B*, samples (1 μ g) of wild type Pah1p purified from *S. cerevisiae* (*yPah1p*) and purified recombinant (*rPah1p*) wild type and 5A mutant enzymes that were incubated with PKA (20 unit) and ATP (1 nmol) for 20 min were subjected to SDS-PAGE and Western blot analysis using anti-(phosphoserine/phosphothreonine) PKA substrate antibodies (α *P-Ser/Thr* (PKA)). The membranes were stripped and then reprobed with anti-Pah1p antibodies (α *Pah1p*). The data shown are representative of three experiments.

A



B

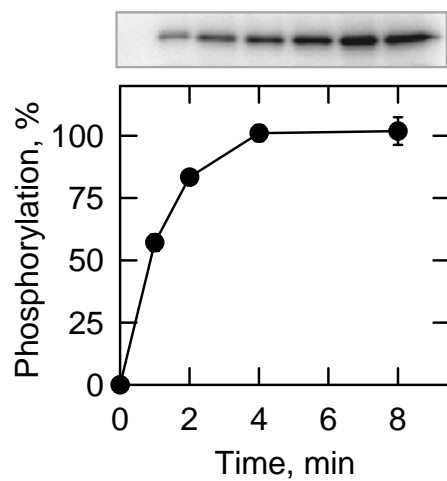


PKA activity was further characterized to confirm that Pah1p was a *bona fide* substrate. The phosphorylation was dependent on the time of the reaction (Fig. 8A) and the amount of PKA used in the reaction (Fig. 8B). In addition, the dependencies of PKA activity on ATP and Pah1p followed saturation kinetics (Fig. 8C) and positive cooperative kinetics (Fig. 8D), respectively. The analysis of the kinetic data indicated that K_m values for ATP and Pah1p were 4.4 μM and 0.44 μM , respectively, and a Hill number for Pah1p was 1.9. At the point of maximum phosphorylation (Fig. 8), PKA catalyzed the incorporation of 1 mol of phosphate/mol of Pah1p.

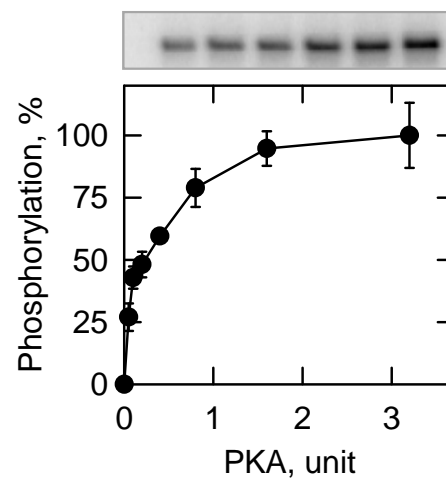
To examine the effect of PKA phosphorylation on PAP activity, the phosphorylated and unphosphorylated forms of Pah1p were assayed for enzyme dependence on the surface concentration of PA. The surface concentration of PA, as opposed to its molar concentration, was varied because PAP activity follows surface dilution kinetics (47, 186, 187). Under the conditions of these experiments, PAP activity was independent of the molar concentration of PA (187). As described previously (47), the unphosphorylated enzyme showed positive cooperative (Hill number of 2.4) kinetics with respect to PA (Fig. 9A). The PKA phosphorylation of Pah1p caused a decrease in PAP activity (Fig. 9A) with a reduction in V_{max} and an increase in K_m (Fig. 9B). Consequently, the phosphorylation of Pah1p by PKA caused a 1.8-fold decrease in its catalytic efficiency (Fig. 9B). The phosphorylation, however, did not affect the cooperative behavior of PAP activity.

FIGURE 8. Pah1p is a *bona fide* substrate of PKA. Phosphorylation of Pah1p by PKA was measured by following the incorporation of the radiolabeled phosphate from [γ - ^{32}P]ATP into purified recombinant Pah1p under standard reaction conditions by varying time (*A*), the amount of PKA (*B*), the ATP concentration (*C*), and the Pah1p concentration (*D*). Following the phosphorylation reactions, the samples were subjected to SDS-PAGE; the polyacrylamide gels were dried and then subjected to phosphorimaging analysis. The relative amounts of phosphate incorporated into Pah1p were quantified using ImageQuant software. The data shown in *A-D* are the averages of three experiments \pm S.D. (*error bars*).

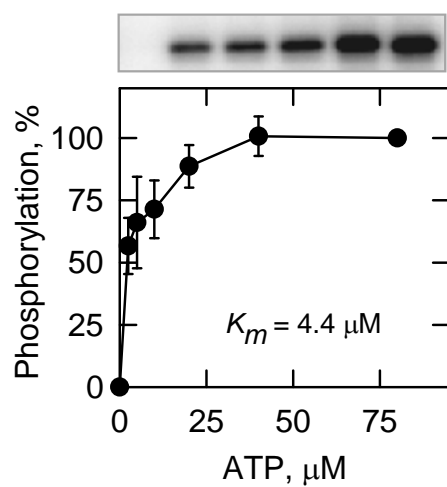
A



B



C



D

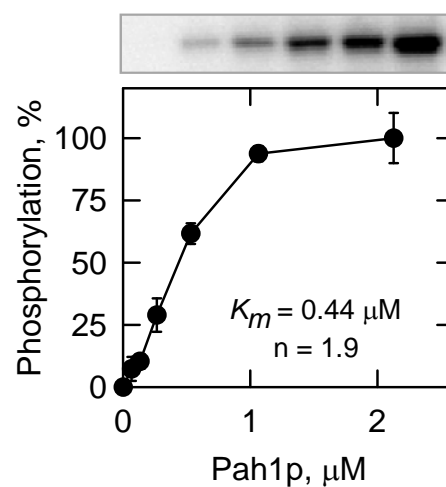
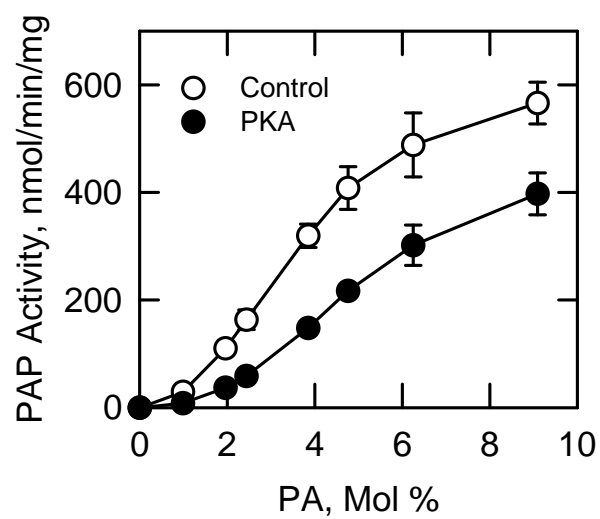


FIGURE 9. Phosphorylation of Pah1p by PKA attenuates PAP activity. *A*, purified recombinant Pah1p (0.5 μ g) was incubated with and without PKA (*PKA*, 20 unit) and ATP (2 nmol) for 5 min. The PAP activity of the phosphorylated and unphosphorylated forms of the enzyme was measured as a function of the surface concentration (mol %) of PA. The molar concentration of PA was held constant at 0.2 mM, and the molar concentration of Triton X-100 was varied to obtain the indicated surface concentrations. The values indicated are the average of three experiments \pm S.D. (*error bars*). *B*, The V_{\max} , K_m , and Hill values were determined from the data in *A* using the Enzyme Kinetics module of SigmaPlot software.

A



B

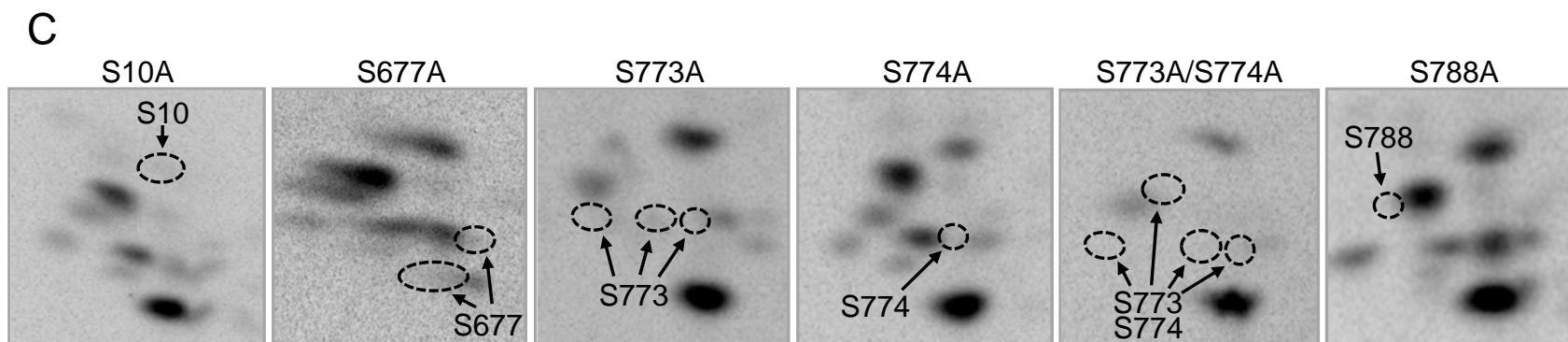
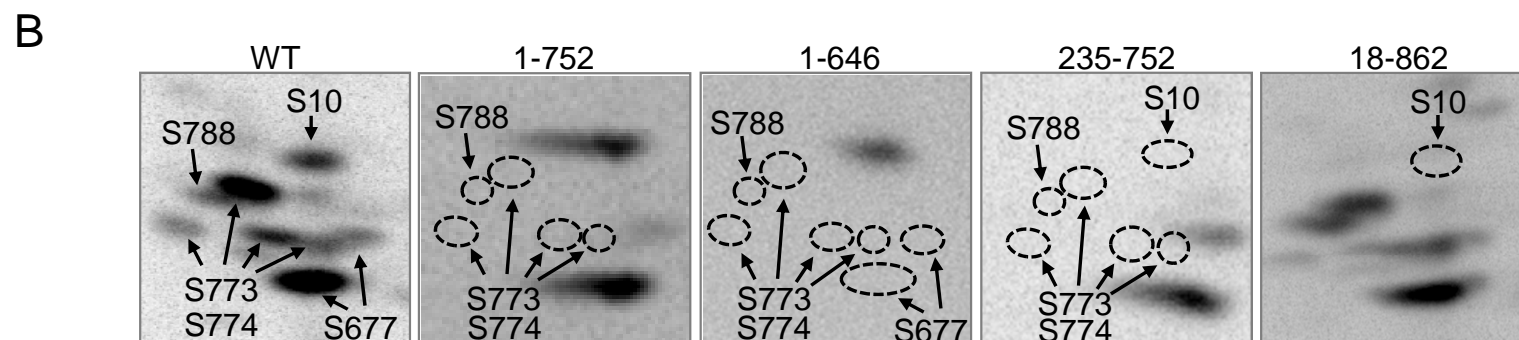
Pah1p	V_{\max}	K_m	V_{\max}/K_m	Hill
	<i>nmol/min/mg</i>	<i>mol %</i>		<i>n</i>
Control	638 ± 10	3.8 ± 0.1	168	2.4
PKA	494 ± 10	5.3 ± 0.1	93	2.6

Ser-10, Ser-677, Ser-773, Ser-774, and Ser-788 in Pah1p are Phosphorylated by PKA

A combination of mass spectrometry and mutagenesis was used to identify PKA phosphorylation sites in Pah1p. In an initial approach, full-length and truncated forms of recombinant Pah1p were phosphorylated with PKA and [γ - 32 P]ATP, and were subjected to phosphopeptide mapping analysis. The phosphopeptide map of full length Pah1p showed multiple signals, indicating that PKA phosphorylated Pah1p at several sites (Fig. 10B, *WT*). Analyses of the phosphopeptide maps derived from truncations at the N- and C-terminal ends of Pah1p indicated that one site is between amino acid residues 1-18 and the remaining sites are between amino acid residues 646 and 862 (Fig. 10B).

The mass spectrometry analysis of peptides from the phosphorylated full length protein identified Ser-773, Ser-774, and Ser-788 as phosphorylation sites. To confirm these sites, Pah1p with alanine mutations were expressed in *E. coli*, purified, phosphorylated with PKA, and subjected to phosphopeptide mapping analysis. Each of the three mutations (e.g., S773A, S774A, and S788A) affected the phosphopeptide map of Pah1p, and by comparing the maps of the wild type and mutant proteins, we could assign which sites were contained within the phosphopeptides present in the map of wild type Pah1p (Fig. 10C). Four phosphopeptides could be attributed to Ser-773 and Ser-774, and the S773A/S774A double mutation eliminated the four phosphopeptides from the map. The maps of the individual mutations indicated that Ser-773 was the more heavily phosphorylated when compared with Ser-774. That multiple spots in the phosphopeptide map contained the same phosphorylation sites indicated incomplete proteolytic digestions.

FIGURE 10. Phosphopeptide mapping analysis of Pah1p mutants phosphorylated by PKA. *A*, the diagrams show the full length and truncated versions of *E. coli*-expressed recombinant Pah1p that were used for phosphorylation and phosphopeptide mapping analysis. The positions of the Pah1p phosphorylation sites are indicated in the full length protein. Purified recombinant wild type and the indicated truncation (*B*) and phosphorylation site (*C*) Pah1p mutants (1 μ g) were phosphorylated with PKA (20 units) and [γ - 32 P]ATP (2 nmol) for 20 min. After phosphorylation, the samples were subjected to SDS-PAGE and transferred to PVDF membrane. The 32 P-labeled proteins were digested with L-1-tosylamido-2-phenylethyl chloromethyl ketone-trypsin. The resulting peptides were separated on cellulose thin layer plates by electrophoresis (from *left* to *right*) in the first dimension and by chromatography (from *bottom* to *top*) in the second dimension. The identity of the phosphorylation sites in the radioactive phosphopeptides of the wild type enzyme was determined from the maps of the Pah1p mutant enzymes. The positions of the phosphopeptides that were absent in the mutant enzymes (indicated by the *dotted line ellipse*) but were present in the wild type enzyme are indicated in the figure. The data shown are representative of three independent experiments.



Analysis of the full length, N- and C- terminal truncations, and the S773A, S774A, and S788A mutants revealed there were additional sites that had not been identified by mass spectrometry. The unidentified sites were located between amino acid 1-18 and 646-752 (Fig. 10B). There are four serine residues (e.g., Ser-10, Ser-12, Ser-16, and Ser-17) between amino acids 1-18, none of which is contained within a PKA consensus sequence, while the 646-752 region contains three putative PKA sites (Ser-677, Ser-692 and Ser-694). Alanine mutations of the seven residues were constructed, expressed in *E. coli*, and subjected to phosphopeptide mapping after phosphorylation with PKA. The only mutations that affected the phosphorylation of Pah1p were S10A and S677A. The phosphopeptides that contained Ser-10 and Ser-677 (Fig. 10B, *WT*) were missing in the phosphopeptide maps of the S10A and S677A mutant enzymes (Fig. 10).

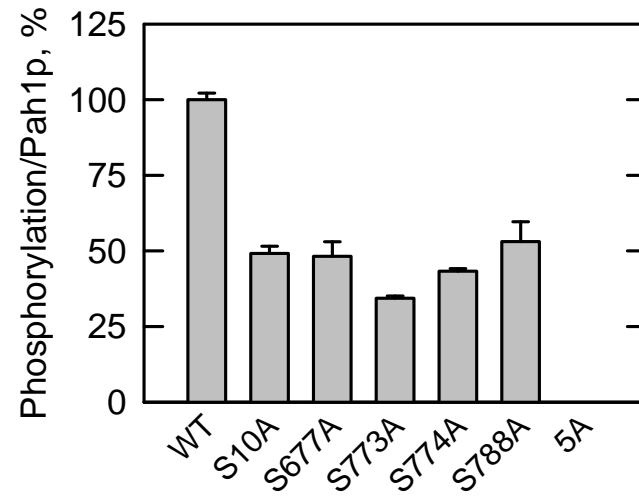
The effects of each of the PKA phosphorylation site mutations on Pah1p phosphorylation and activity are shown in Fig. 11. Each of the five single mutations caused a reduction in phosphorylation by 50-66 %, whereas the quintuple mutation (e.g., 5A mutation) abolished the phosphorylations by PKA (Fig. 11A). The 5A mutation also eliminated the inhibitory effect that PKA had on PAP activity, and this effect was primarily attributed to the S10A mutation (Fig. 11B).

The Phosphorylation State of Ser-10 Alone and in Combination with the 7A Mutations Affects Cell Growth

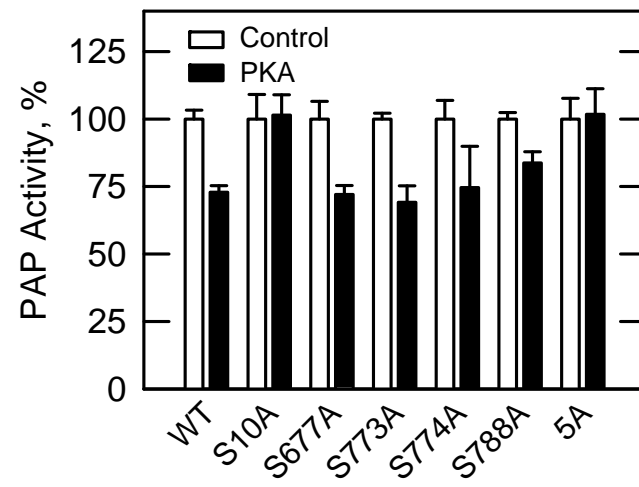
Serine- to alanine/aspartate mutations were constructed for the five PKA phosphorylation sites to examine the physiological effects of phosphorylation deficiency/mimicry of Pah1p. The mutant proteins were expressed in both *pah1Δ NEM1*

FIGURE 11. Effects of PKA phosphorylation site mutations on the phosphorylation of Pah1p and on the inhibitory effects of PKA on PAP activity. Wild type and the indicated phosphorylation site mutant Pah1p enzymes were expressed and purified from *E. coli*. *A*, the recombinant Pah1p (1 μ g) was phosphorylated with PKA (20 unit) and [γ - 32 P]ATP (1 nmol) for 20 min. Following the reaction, Pah1p was separated from ATP and PKA by SDS-PAGE. The polyacrylamide gel was dried and subjected to phosphorimaging and ImageQuant analysis. Afterward, the dried gel was swollen with water, stained with Coomassie blue, and subjected to image analysis. The relative phosphorylation/Pah1p of the mutant enzymes was compared with the wild type enzyme that was set at 100%. The data reported are the average of three independent experiments \pm S.D. (*error bars*). *B*, the recombinant wild type and mutant Pah1p enzymes (0.5 μ g) were phosphorylated with PKA (20 unit) and then assayed for PAP activity under standard assay conditions. The controls for the mutant enzymes were the unphosphorylated mutant forms of the enzyme. The values reported were the average of three experiments \pm S.D. (*error bars*).

A



B



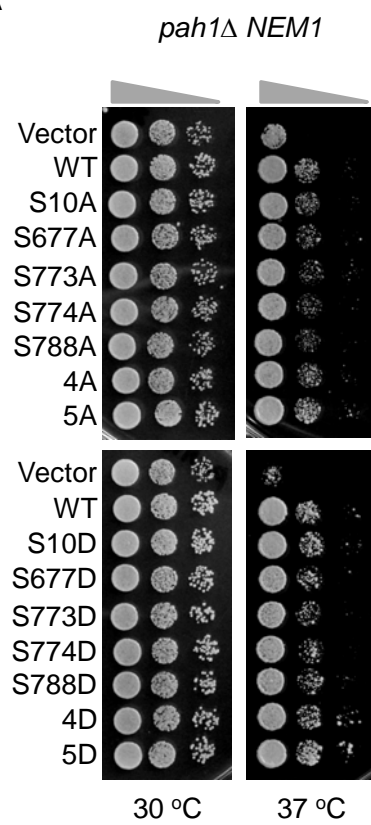
and *pah1Δ nem1Δ* mutant cells. In this way, we could examine the dependence of Pah1p function on Nem1p-Spo7p protein phosphatase activity. In addition, the expression of the phosphorylation site mutants in *nem1Δ* affords examination of the mutations in a genetic background that favors phosphorylation of other non-mutated phosphorylation sites in Pah1p.

The *pah1Δ* mutant exhibits a temperature-sensitive phenotype (e.g., loss of growth at 37 °C) that reflects an important role of PAP activity in lipid metabolism (47, 48, 188). The expression of wild type *PAHI* in the *pah1Δ* mutant allowed some growth on agar plates at 37 °C, but the growth was more limited in the *nem1Δ* mutant background (64) (Fig. 12). This emphasized the importance of Nem1p-Spo7p phosphatase activity for normal PAP function *in vivo* (64). The expression of *PAHI* with the five alanine mutations alone and in combination did not have a major effect on the complementation of the *pah1Δ* temperature-sensitive phenotype regardless of whether or not *NEMI* was present (Fig. 12). The five aspartate mutations did not affect the complementation of temperature sensitivity when *NEMI* was present (Fig. 12A). However, in the *nem1Δ* mutant background, the S10D and 5D mutations did not permit growth on agar plates at 37 °C (Fig. 12B). The other four aspartate mutations alone and in combination were not distinguished from wild type *PAHI* with respect to the complementation of growth at 37 °C (Fig. 12B). Thus, the lack of growth caused by the 5D mutations was attributed to the S10D mutation.

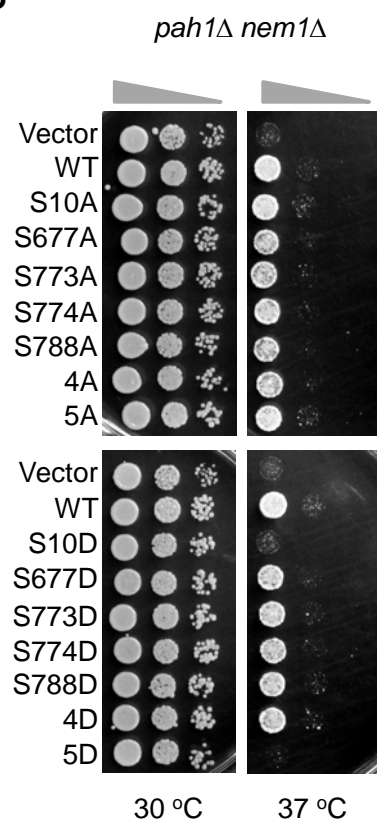
These results suggested that Nem1p-Spo7p dephosphorylates other sites to compensate for the loss of Pah1p function caused by the S10D mutation. Previous studies have shown that phosphorylation of Pah1p by Pho85p-Pho80p and Cdc28p-cyclin

FIGURE 12. Effects of PKA phosphorylation site mutations on the complementation of the *pah1*Δ temperature sensitive phenotype. The indicated wild type and phosphorylation site mutant forms of *PAH1* were expressed in *pah1*Δ *NEM1* (A) and *pah1*Δ *nem1*Δ (B) cells. Serial dilutions (10-fold) of the cells were then spotted onto agar plates, and were incubated at 30 and 37 °C for 3-4 days. The data are representative of three independent experiments.

A



B



B on seven Ser/Thr-Pro sites is a major regulator of PAP function (65, 148). Moreover, the expression of *PAHI* with alanine mutations of the seven sites (7A) allowed for growth of *pah1Δ nem1Δ* mutant cells on agar plates at 37 °C (Fig. 13B), indicating that the 7A mutations can bypass the requirement of Nem1p-Spo7p for Pah1p PAP function (64, 66). Thus we decided to investigate the effects of mutations in Ser-10 in combination with the 7A mutations. When S10A + 7A mutations were expressed in *pah1Δ* and *pah1Δ nem1Δ* cells, the growth on agar plates at 37 °C was attenuated when compared with the growth of cells expressing the 7A mutations alone (Fig. 13). In fact, the growth of cells carrying these mutations appeared less at the permissive temperature of 30 °C (Fig. 14). Accordingly, growth was examined in more detail in liquid medium at 30 °C (Fig. 14). In the presence and absence of *NEMI*, the growth of cells expressing the S10A + 7A mutations was reduced when compared with cells expressing wild type *PAHI* and *PAHI* with the S10A, S10D, S10D + 7A, and 7A mutations. The S10A + 7A mutations caused increases in both the lag time (*pah1Δ NEMI*: from 5.9 ± 0.1 to 9.9 ± 0.1 h; *pah1Δ nem1Δ*: from 6.6 ± 0.1 to 9.5 ± 0.1 h) and the generation time (*pah1Δ NEMI*: from 4.8 ± 0.2 to 6.0 ± 0.1 h; *pah1Δ nem1Δ*: from 4.4 ± 0.2 to 5.4 ± 0.1 h) when compared with wild type *PAHI*. However, by the time cells reached the stationary phase, the cell density of cells expressing the S10A + 7A mutations was not significantly different from the wild type control (Fig. 14). This result indicated that the mutations affected Pah1p function during the exponential phase of growth.

We questioned if the growth defects caused by the S10A + 7A mutations at 30 °C could be overcome by supplementations with inositol and choline. We reasoned that if these mutations gave rise to a more active PAP enzyme, then PA would be channeled into

FIGURE 13. Effects of S10A mutation in combination with the 7A mutations on the complementation of the *pah1*Δ temperature sensitive phenotype. The indicated wild type and phosphorylation site mutant forms of *PAH1* were expressed in *pah1*Δ *NEM1* (A) and *pah1*Δ *nem1*Δ (B) cells. Serial dilutions (10-fold) of the cells were then spotted onto agar plates, and were incubated at 30 and 37 °C for 3-4 days. The data are representative of three independent experiments.

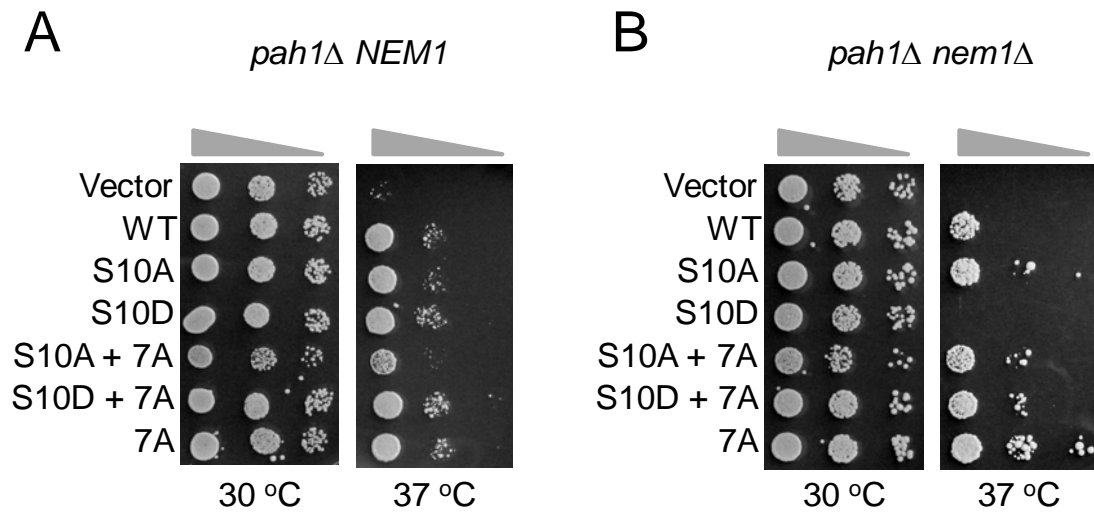
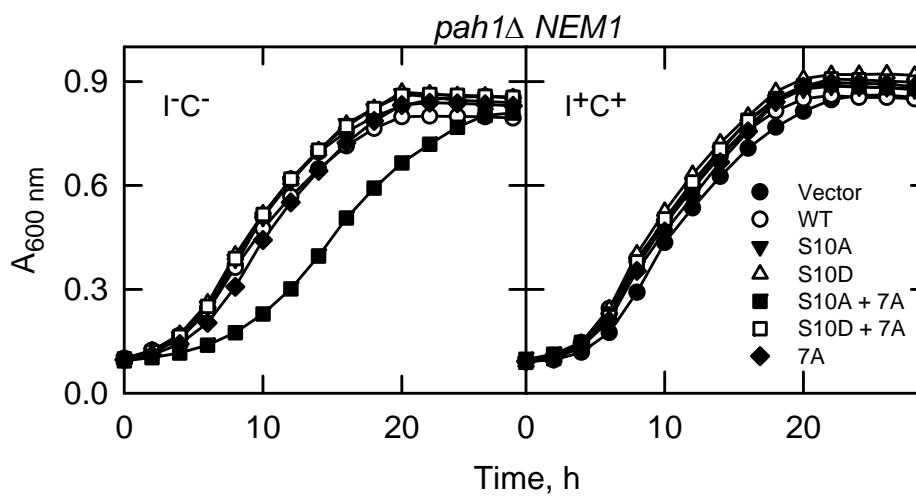
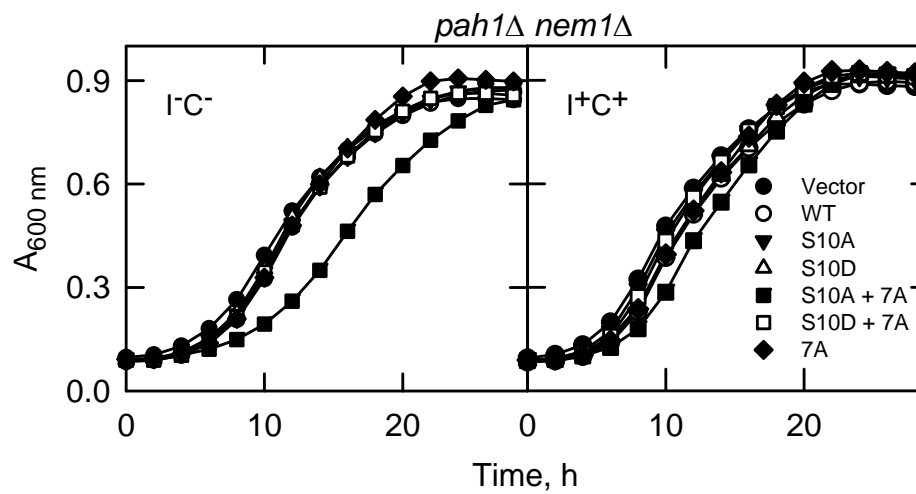


FIGURE 14. The S10A mutation in combination with the 7A mutations reduces growth in medium lacking inositol and choline. The indicated wild type and phosphorylation site mutant forms of *PAHI* were expressed in *pah1Δ NEM1* (A) and *pah1Δ nem1Δ* (B) cells. Cells were grown in synthetic medium without (I⁻C⁻) and with inositol and choline (I⁺C⁺). Growth was monitored at $A_{600\text{ nm}}$. Each data point represents the average of three independent cultures, and the average S.D. for each data point was $\pm 3\%$.

A



B

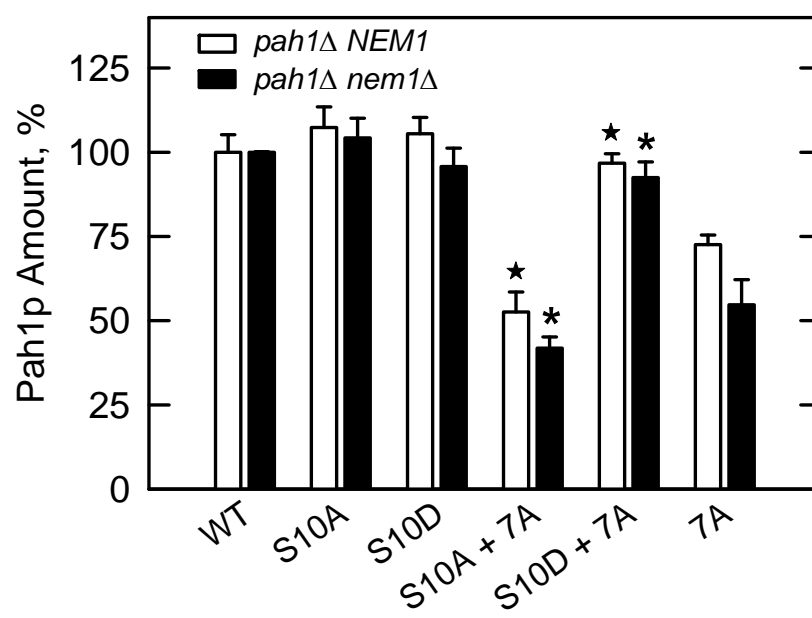


DAG and TAG at the expense of phospholipid synthesis via the CDP-DAG pathway (6, 131). At the same time, a reduction in PA levels would cause the translocation of the repressor Opi1p into the nucleus where it would inhibit the expression of *INO1* (a key gene encoding an enzyme for inositol synthesis) and other UAS_{INO}-containing phospholipid synthesis genes (6, 131). Thus, the combination of inositol and choline would bypass the repression of *INO1* and stimulate the synthesis of phosphatidylinositol and PC (via the Kennedy pathway) (6, 29). In fact, the addition of inositol and choline did correct the slower growth caused by the S10A + 7A mutations (Fig. 14).

The Phosphorylation State of Ser-10 in Combination with the 7A Mutations Affects the Abundance and the Localization of Pah1p

The Pah1p levels of the phosphorylation site mutant enzymes expressed in *pah1Δ NEM1* and in *pah1Δ nem1Δ* cells were examined by Western blot analysis using anti-Pah1p antibodies. This analysis indicated that none of the serine- to alanine/aspartate mutations had a major effect on the abundance of Pah1p (data not shown). As described previously (65, 148), the 7A mutations caused a decrease (30 % in *pah1Δ NEM1* and 45 % in *pah1Δ nem1Δ*) in Pah1p abundance (Fig. 15). The S10A mutation in combination with 7A caused a further reduction (28 % and 25 %, respectively) in Pah1p abundance. On the other hand, Pah1p abundance in *pah1Δ NEM1* and *pah1Δ nem1Δ* cells expressing the S10D + 7A mutations was similar to that observed for wild type Pah1p expressed in these cells (Fig. 15). These data indicated that the S10D mutation had a stabilizing effect on the loss of abundance caused by the 7A mutations, whereas the S10A mutation enhanced the destabilizing effect of the 7A mutations.

FIGURE 15. The phosphorylation state of Ser-10 in combination with the 7A mutations affects the abundance of Pah1p. The indicated wild type and phosphorylation site mutant forms of *PAH1* were expressed in *pah1Δ NEM1* and *pah1Δ nem1Δ* cells. Cell extracts prepared from exponential phase cells were subjected to Western blot analysis using anti-Pah1p and anti-phosphoglycerate kinase antibodies. The relative amounts of Pah1p from the cells were determined by ImageQuant analysis of the data. Each data point represents the average of four experiments \pm S.D. (*error bars*). ★, $p < 0.05$ versus 7A in *pah1Δ NEM1*; ★, $p < 0.05$ versus 7A in *pah1Δ nem1Δ*



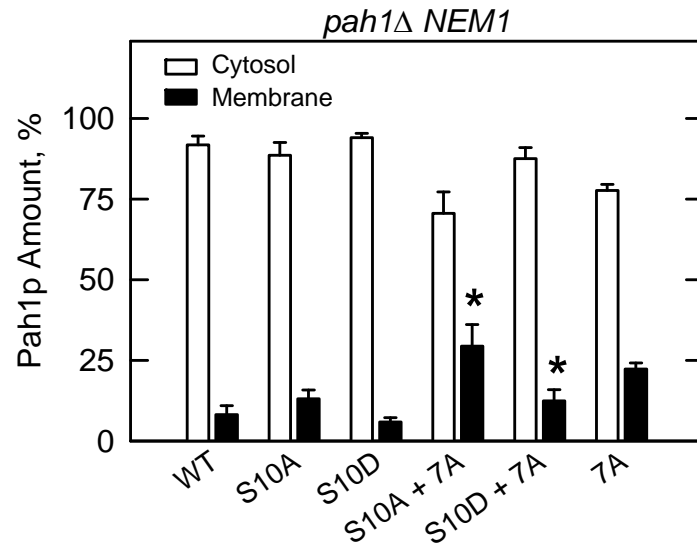
The effects of the PKA phosphorylation site mutations on the localization of Pah1p were examined. In *pah1Δ NEM1* and *pah1Δ nem1Δ* cells, greater than 90 % of wild type Pah1p was associated with the cytosolic fraction (Fig. 16). This amount is slightly greater than that shown in previous work (64, 65). This may be explained by the fact that in the current study we included 0.15 M NaCl in the buffers to prevent non-specific associations of Pah1p with membranes. None of the single mutations had a significant effect on the localization of Pah1p whether they were expressed in *pah1Δ NEM1* or *pah1Δ nem1Δ* cells. Consistent with previous work (64, 65), the 7A mutations caused an increase (175 % in *pah1Δ NEM1* and 411 % in *pah1Δ nem1Δ*) in the association of Pah1p with membranes (Fig. 16). In combination with the 7A mutations, S10A caused a further increase (32% in *pah1Δ NEM1* and 37 % in *pah1Δ nem1Δ*) in membrane association. On the other hand, the amounts of Pah1p associated with membranes of *pah1Δ NEM1* and *pah1Δ nem1Δ* cells expressing the S10D + 7A mutations were 45 % and 33 % less, respectively, when compared with the cells expressing the 7A mutations (Fig. 16).

The Phosphorylation State of Ser-10 in Combination with the 7A Mutations Affects TAG Content

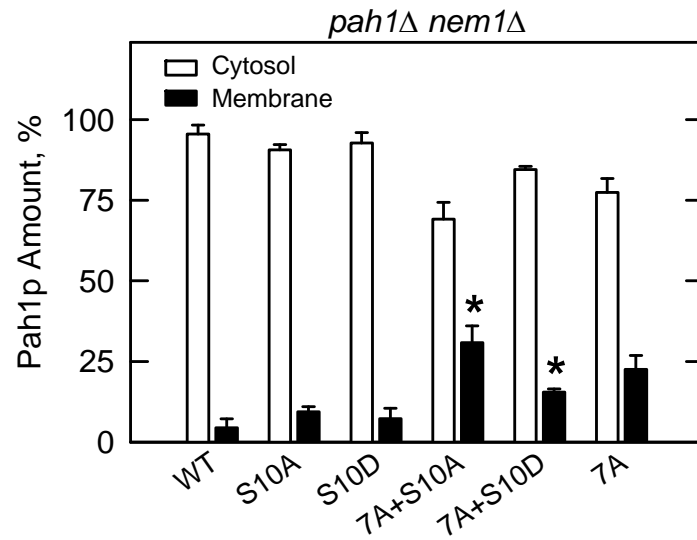
The effects of the PKA phosphorylation site mutations on the amounts of TAG were examined. Our analysis was performed at the stationary phase because this is the phase of growth where the effect of PAP on TAG content is most pronounced (46-48). As described previously (64), the TAG content of *pah1Δ nem1Δ* cells expressing wild type *PAH1* was reduced by 5.8-fold when compared with *pah1Δ NEM1* cells expressing

FIGURE 16. The phosphorylation state of Ser-10 in combination with the 7A mutations affects the localization of Pah1p. The indicated wild type and phosphorylation site mutant forms of *PAH1* were expressed in *pah1Δ NEM1* (A) and *pah1Δ nem1Δ* (B) cells. Cell extracts prepared from exponential phase cells were fractionated into the cytosol and membrane fractions by centrifugation. The membrane fraction was resuspended in the same volume as the cytosol fraction and equal volumes of the fractions were subjected to Western blot analysis using anti-Pah1p, anti-phosphoglycerate kinase (cytosol marker), and anti-phosphatidylserine synthase (ER marker) antibodies. The Western blot analysis for the marker proteins indicated highly enriched cytosol and membrane fractions as described previously (148). The relative amounts of cytosol and membrane-associated Pah1p were determined for the wild and phosphorylation site mutant forms of the enzyme by ImageQuant analysis of the data. Each data point represents the average of four experiments \pm S.D. (*error bars*). \star , $p < 0.05$ versus 7A membrane.

A



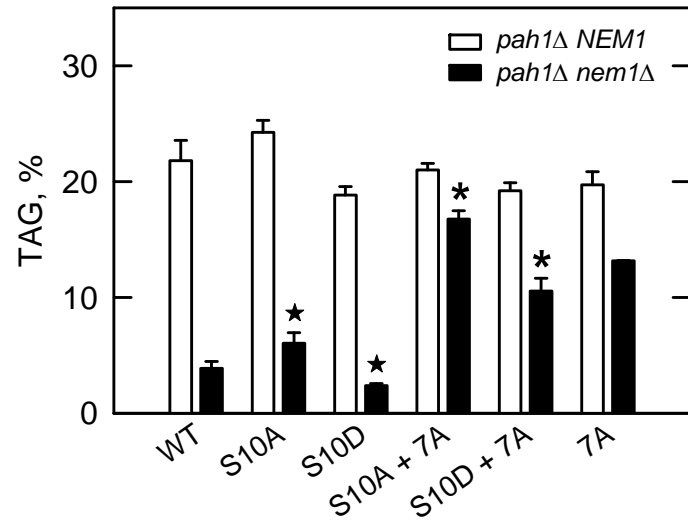
B



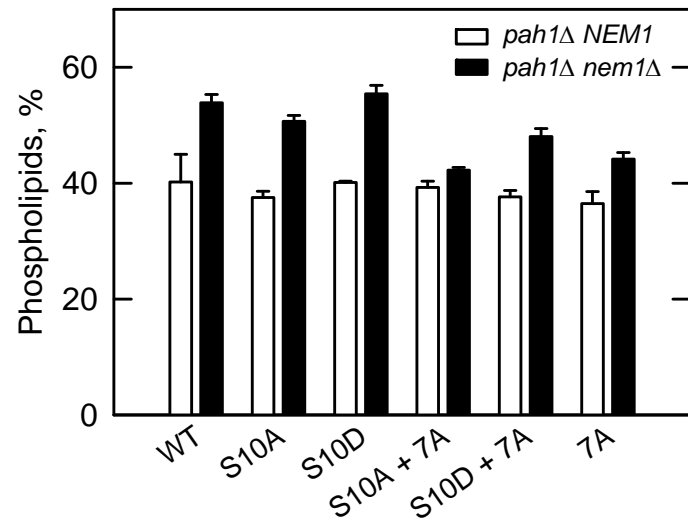
the wild type gene (Fig. 17A). The reduction of TAG content in *pah1Δ nem1Δ* cells expressing wild type *PAH1* was accompanied by a 35% increase in phospholipids (64) (Fig. 17B). These observations further emphasized the importance of Nem1p-Spo7p-mediated dephosphorylation of Pah1p for PAP function *in vivo* (64). In *pah1Δ NEM1* cells, the expression of the PKA phosphorylation site alanine/aspartate mutant alleles had relatively minor effects on the amount of TAG (Fig. 17A). However, the phosphorylation site mutations had more dramatic effects on TAG content when they were expressed in *pah1Δ nem1Δ* cells (Fig. 17A). The S10A mutation caused a 57% increase in TAG content whereas the S10D mutation caused a 37% decrease in TAG, and the difference in TAG between the S10A and S10D mutations was 2.5-fold. The effects of the 5A and 5D mutations on TAG content mirrored the effects of the S10A and S10D mutations, respectively, and the 4A and 4D mutations were not distinguished from the wild type control (data not shown). Thus, of the five PKA sites, the phosphorylation state of Ser-10 played the major role in regulating PAP function. In combination with the 7A mutations, S10A caused a 347% increase in TAG content when compared with the wild type control (Fig. 17A). As described previously (64, 65), the 7A mutations caused a 244% increase in TAG content, and the S10D mutation attenuated this effect by 20 % (Fig. 17A). The difference in the amount of TAG between the S10A + 7A and S10D + 7A mutations was 1.6-fold. Although the effects of the phosphorylation site mutations on the total phospholipid content were not great, there were correlations between the relative amounts of TAG and phospholipids of *pah1Δ nem1Δ* cells expressing the S10A and S10D mutations (Fig. 17B).

FIGURE 17. The phosphorylation state of Ser-10 in combination with the 7A mutations affects lipid content. The indicated wild type and phosphorylation site mutant forms of *PAHI* were expressed in *pah1Δ NEM1* and *pah1Δ nem1Δ* cells. Cultures were grown to the stationary phase in synthetic medium containing [2-¹⁴C]acetate (1 μCi/ml). Lipids were extracted, separated by one-dimensional TLC, and the phosphorimages were subjected to ImageQuant analysis. The percentages shown for TAG (*A*) and phospholipids (*B*) were normalized to the total ¹⁴C-labeled chloroform-soluble fraction. Each data point represents the average of three experiments ± S.D. (*error bars*). ★, *p* < 0.05 versus WT in *pah1Δ nem1Δ*; ✱, *p* < 0.05 versus 7A in *pah1Δ nem1Δ*

A



B



Phosphorylation of Pah1p by PKC

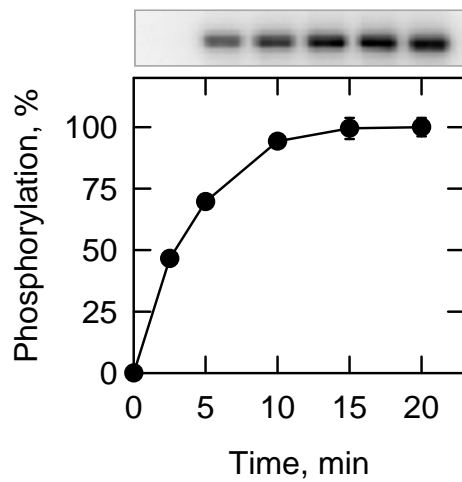
As discussed above (Fig. 5B), the purified recombinant Pah1p was phosphorylated by PKC. The phosphorylation reaction was further characterized with respect to the reaction time, the amount of PKC, and the concentrations of ATP and Pah1p (Fig. 18). The phosphorylation of Pah1p was dependent on the reaction time (Fig. 18A) and the amount of PKC (Fig. 18B). The dependencies of PKC activity on ATP and Pah1p followed saturation kinetics. The analysis of the kinetic data according to the Michaelis-Menten equation yielded K_m values for ATP and Pah1p of 4.5 and 0.75 μM , respectively. The stoichiometry of the phosphorylation was determined by allowing the reaction to reach completion. At the point of maximum phosphorylation, PKC catalyzed the incorporation of 0.8 mol of phosphate/mol Pah1p.

Ser-677, Ser-779, and Ser-788 Are Major PKC Phosphorylation Sites

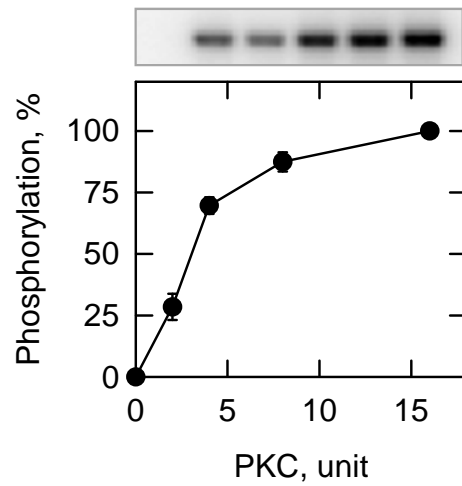
The analysis of the Pah1p sequence with the NetPhosK 2.0 server indicated that multiple serine and threonine residues are putative target sites for PKC. While phosphopeptide mapping analysis of Pah1p phosphorylated with PKC showed multiple phosphopeptide signals (Fig. 20C, *WT*), only phosphoserine was detected upon phosphoamino acid analysis (Fig. 19). This indicated that threonine is not a major PKC target site in Pah1p. To narrow down the region(s) that contains the PKC target sites, we analyzed the phosphorylation of N- and C-terminal truncations of Pah1p. The phosphorylation of the N-terminal truncation (residues 18-862) was similar to that of full-length Pah1p indicating that the extreme N-terminus did not contain any PKC target sites. On the other hand, the extent of phosphorylations in the truncations containing residues

FIGURE 18. Characterization of Pah1p phosphorylation by PKC. Phosphorylation of Pah1p by PKC was measured under standard reaction conditions by varying the reaction time (*A*), the amount of PKC (*B*), the ATP concentration (*C*), and the Pah1p concentration (*D*). Following the phosphorylation reactions, the samples were subjected to SDS-PAGE; the polyacrylamide gels were dried and then subjected to phosphorimaging analysis. The relative amounts of phosphate incorporated into Pah1p were quantified using ImageQuant software. A portion of a representative image is shown above the plot. The data shown are the averages of three experiments \pm S.D. (*error bars*).

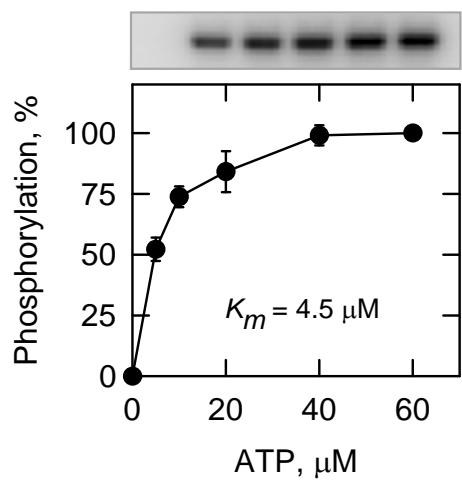
A



B



C



D

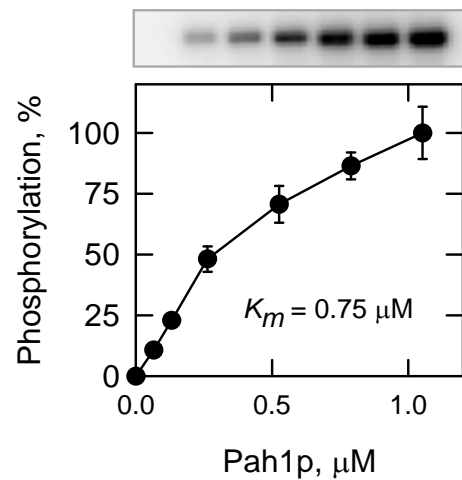


FIGURE 19. PKC phosphorylates Pah1p on a serine residue. Purified recombinant Pah1p (1 μ g) was phosphorylated with PKC (2 unit) and [γ - 32 P]ATP (1 nmol) for 20 min. After the kinase reaction, Pah1p was subjected to SDS-PAGE and was transferred to PVDF membrane. The portion of PVDF membrane containing 32 P-labeled Pah1p was hydrolyzed with 6 N HCl for 90 min at 110 $^{\circ}$ C, and the hydrolysates were separated by 2-dimensional electrophoresis. The positions of the standard phosphoamino acids phosphoserine (*P-Ser*), phosphothreonine (*P-Thr*), and phosphotyrosine (*P-Tyr*) are indicated.

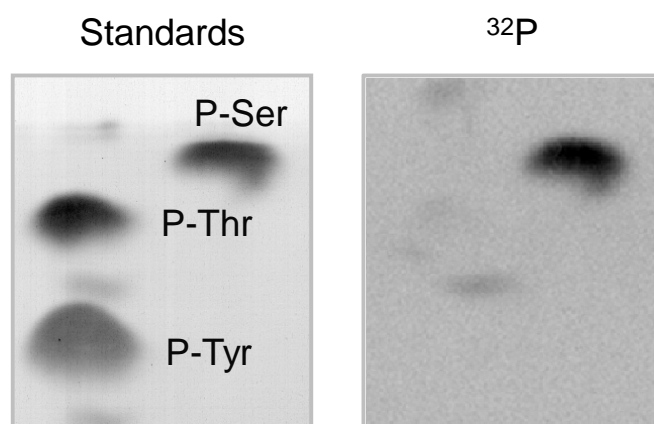
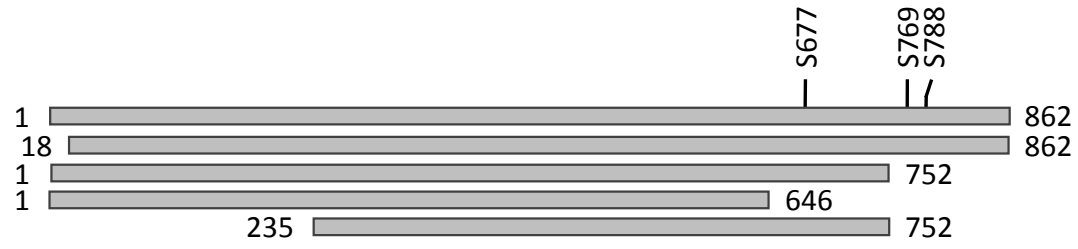
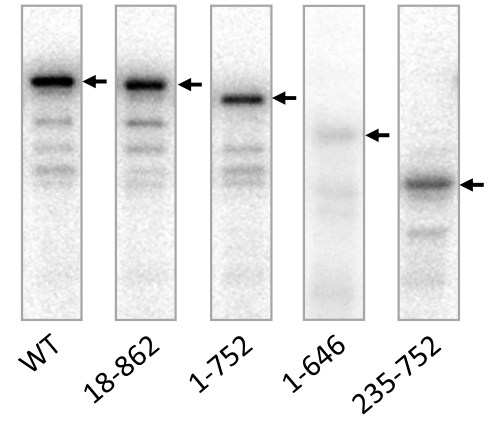
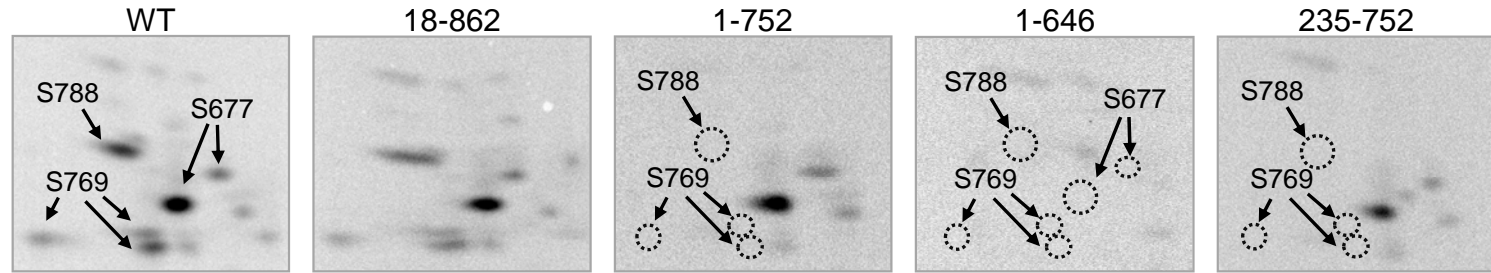
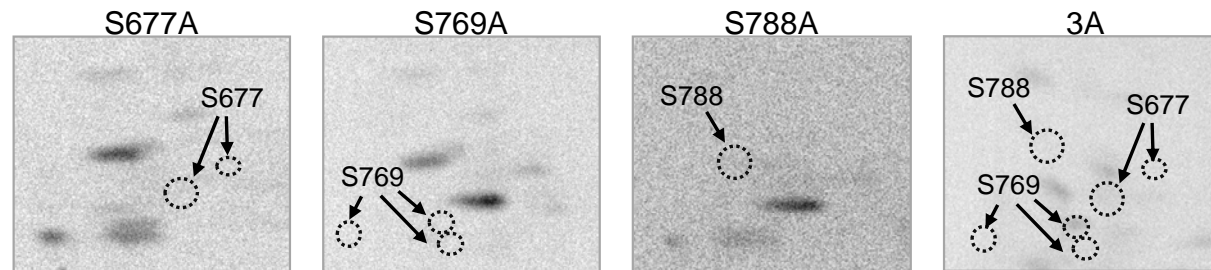


FIGURE 20. Phosphopeptide mapping analysis of Pah1p mutations phosphorylated by PKC. *A*, the schematic diagram shows the full length and truncated versions of *E. coli*-expressed recombinant Pah1p. The positions of the Pah1p phosphorylation sites are indicated in the full length protein. *B*, 1 μ g of purified recombinant Pah1p (wild type and truncations) was incubated with 2 units of PKC and 1 nmol [γ - 32 P]ATP for 20 min. The phosphorylated samples were resolved by SDS-PAGE, transferred to PVDF membrane and subjected to phosphorimaging analysis. The positions of the wild type and truncated Pah1p forms are indicated by the arrows. *C* and *D*, phosphopeptide mapping analyses of samples shown in panel *B* and 32 P-labeled Pah1p with mutations in the phosphorylation sites shown in panel *A*. Samples were digested with L-1-tosylamido-2-phenylethyl chloromethyl ketone-trypsin, and the resulting peptides were separated on cellulose thin layer plates by electrophoresis (from *left* to *right*) followed by chromatography (from *bottom* to *top*). The identity of the phosphorylation sites in the radioactive phosphopeptides of the wild type enzyme was determined by comparison with the maps of the Pah1p mutant enzymes. The positions of the phosphopeptides that were absent in the maps of the mutant enzymes (*dotted line ellipse*) are indicated in the figure.

A**B****C****D**

1-752, 1-646, and 235-752 were reduced by 65 %, 92 %, and 70 %, respectively (Fig. 20B). Analyses of the phosphopeptide maps derived from the ³²P-labeled truncations revealed that the major PKC target sites were located at the C-terminal region of Pah1p between residues 646 and 862 (Fig. 20C). In addition, mass spectrometry analysis of the Pah1p phosphorylated by PKC identified Ser-773 and Ser-788 as phosphorylation sites. Thus, alanine mutations of these sites as well as three additional putative PKC target sites (Ser-677, Ser-694, and Ser-769) located between residues 646 and 862 were constructed and expressed in *E. coli*. Each of the mutant enzymes was purified and tested as a substrate for PKC. The S677A, S769A, and S788A mutations affected the phosphopeptide map pattern of Pah1p (Fig. 20D). By comparing the map patterns of wild type and mutant Pah1p, we assigned which sites were contained in the phosphopeptides derived from wild type Pah1p after phosphorylation (Fig. 20C, *WT*). Multiple phosphopeptide signals of Ser-769 (Fig. 20D, *S769A*) may be due to incomplete proteolytic digestion because there are multiple trypsin sites in close proximity to Ser-769 (NRTKS⁷⁶⁹RR). The major signals present in the map from wild type Pah1p were absent from the phosphopeptide map of the 3A mutation (S677A/S769A/S788A) (Fig. 20D, *3A*) indicating that Ser-677, Ser-769 and Ser-788 were the major target sites for PKC. As indicated above, Ser-677 and Ser-788 were also target sites of PKA (Fig. 10).

PKC Phosphorylation-deficient 3A Mutations Affect the Pah1p

Phosphorylation *in vivo* and *in vitro*

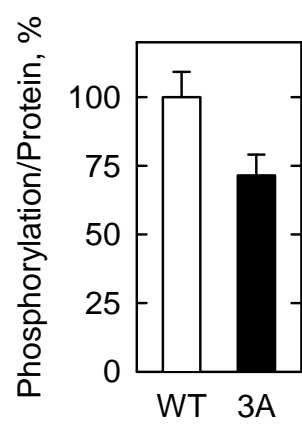
To examine the effect of PKC phosphorylation of Pah1p *in vivo*, we constructed a *PAHI* allele that contained the combination of the S677A, S769A, and S788A mutations

(3A) and expressed it on a single copy plasmid in *pah1Δ dpp1Δ lpp1Δ* mutant cells. The triple mutant lacks nearly all PAP activity and allowed us to eliminate interference from the PAP activity encoded by the *DPP1* and *LPP1* genes (see below). Cells expressing wild type or phosphorylation-deficient 3A mutant were grown to the exponential phase in medium containing radioactive orthophosphate to label the phosphorylated enzyme. Inositol, a growth medium constituent that attenuates yeast Pkc1p PKC activity (189), was not included in the growth medium so the phosphorylation of Pah1p would be favored. Following growth, Pah1p was immunoprecipitated with anti-Pah1p antibodies, and subjected to SDS-PAGE. The ³²P-label Pah1p on the SDS-acrylamide gel was transferred to a PVDF membrane for immunoblot and phosphorimaging analyses. This experiment showed that the 3A mutations caused a 30% reduction in the phosphorylation state of Pah1p (Fig. 21A). The immunoblot analysis indicated that the 3A mutation did not affect the abundance of Pah1p. These data supported the conclusion that Pah1p was phosphorylated by PKC *in vivo*. The phosphorylation remaining in Pah1p with the 3A mutations can be attributed to phosphorylations mediated by PKA (see above), Pho85p-Pho80p (65), and Cdc28p-cyclin B (64).

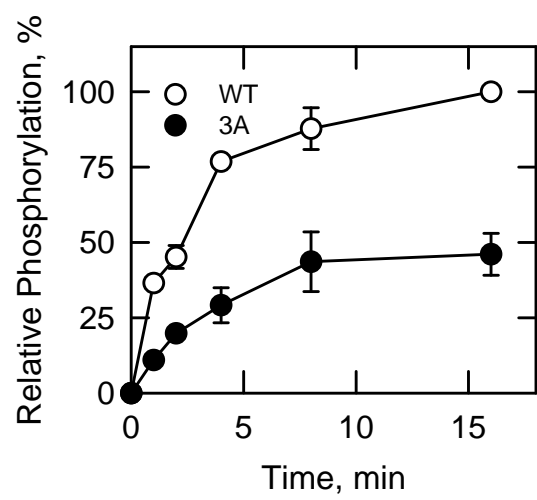
The effect of the 3A mutations on the phosphorylation of Pah1p by PKC was also examined *in vitro*. Purified recombinant wild type and 3A mutant Pah1p were phosphorylated with PKC and [γ -³²P]ATP (Fig. 21B). 3A mutations caused a 54% decrease in phosphorylation (Fig. 21A). The remaining phosphorylations in the 3A mutant can be attributed to multiple minor phosphorylation sites in the enzyme that were shown in the phosphopeptide map (Fig. 20) and not identified.

FIGURE 21. Effects of the 3A mutations on *in vivo* phosphorylation and the time-dependent phosphorylation of Pah1p. *A*, *pah1Δ dpp1Δ lpp1Δ* yeast cells expressing wild type or the 3A mutant Pah1p were grown in the medium containing ^{32}P i (15 $\mu\text{Ci/ml}$) to the exponential phase. The cell extracts were prepared and immunoprecipitated with 5 μg anti-Pah1p antibody. The immunoprecipitated samples were subjected to immunoblot analysis and phosphorimaging. The protein and phosphorylation extents of samples were determined by ImageQuant software. The relative phosphorylation/Pah1p of the 3A mutations was compared with the wild type enzyme that was set at 100%. *B*, wild type and 3A mutant Pah1p were expressed and purified from *E. coli*. The recombinant Pah1p (1 μg) was phosphorylated with PKC (2 unit) and [γ - ^{32}P]ATP (2 nmol) for the indicated time. After the phosphorylation reactions, the samples were separated by SDS-PAGE; the polyacrylamide gel was dried, and then subjected to phosphorimaging analysis. The relative amounts of phosphate incorporated into Pah1p were quantified using ImageQuant software. The maximum amount of phosphorylation for wild type Pah1p was set a 100%. The data shown are the averages of three experiments \pm S.D. (*error bars*).

A



B



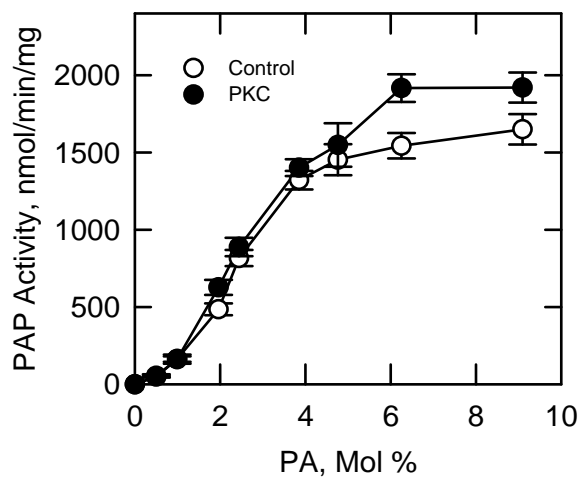
Effect of Pah1p Phosphorylation by PKC on PAP Activity

The effect of Pah1p phosphorylation by PKC on PAP activity was examined. The purified recombinant Pah1p was fully phosphorylated with PKC using unlabeled ATP. The control reaction lacked PKC. Following the phosphorylation reaction, a portion (8 μ l) of the reaction mixture was diluted into the PAP assay mixture, and activity was measured by following the formation of $^{32}\text{P}_i$ from ^{32}P -labeled PA. As described previously (47), the unphosphorylated enzyme showed positive cooperative (Hill number of 2.8) kinetics with respect to the PA surface concentration (Fig. 22A). The PKC-phosphorylated form of Pah1p exhibited the cooperative behavior to PA (Hill number of 2.3) as well. The PKC phosphorylation of Pah1p caused a small increase in V_{\max} (from $1,685 \pm 50$ to $2,098 \pm 100$ nmol/min/mg), and a small increase in the K_m value for PA (from 2.5 ± 0.1 to 2.8 ± 0.2 mol %). Thus, the phosphorylation of Pah1p by PKC caused only slight increase (1.1-fold) in its catalytic efficiency. In addition, the individual, double and triple phosphorylation site mutations also had little effect on PAP activity (Fig. 22B).

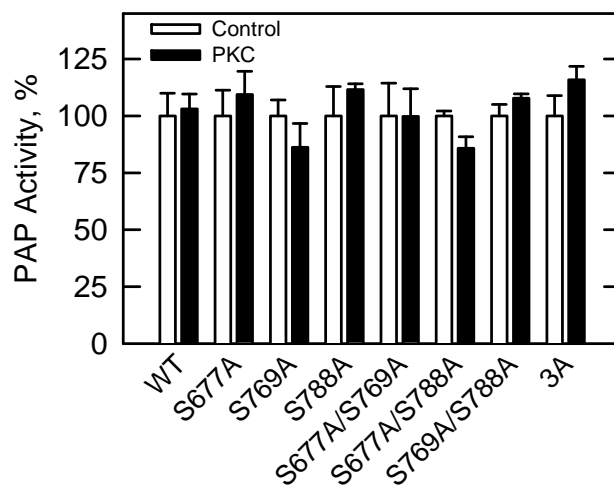
We examined the PAP activity in cell extracts derived from the *pah1 Δ dpp1 Δ lpp1 Δ* triple mutant expressing the wild type, phosphorylation-deficient (3A) and the phosphorylation-mimic (3D, S677D/S769D/S788D) mutant Pah1p. The PAP activity in cells expressing Pah1p 3A was not significantly different when compared with that from cells expressing the wild type Pah1p (Fig. 22C). However, the PAP activity from cells expressing Pah1p 3D was 30% greater when compared with the control activity (Fig. 22C).

FIGURE 22. Effect of PKC phosphorylation site mutations on PAP activity. The purified recombinant wild type and phosphorylation site mutant forms of Pah1p were incubated with and without PKC (10 unit) and ATP (2 nmol) for 4 min. The PAP activities of the unphosphorylated (*control*) and phosphorylated wild type and phosphorylation mutant forms of Pah1p were measured as a function of the PA surface concentration (mol %) of PA (*A*), or at fixed PA surface concentrations (*B*). *C*, *pah1Δ dpp1Δ lpp1Δ* yeast cells expressing wild type, 3A or 3D mutant Pah1p were grown to the exponential phase. Cell extracts were prepared and assayed for PAP activity. The values indicated are the average of three experiments \pm S.D. (*error bars*). ★, $p < 0.05$ versus WT and 3A.

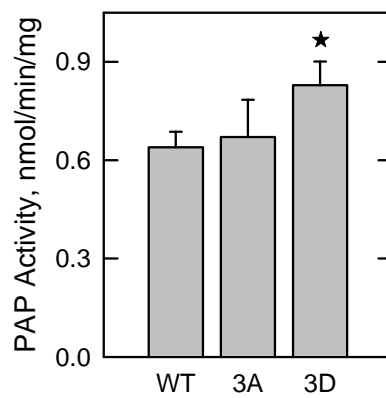
A



B



C

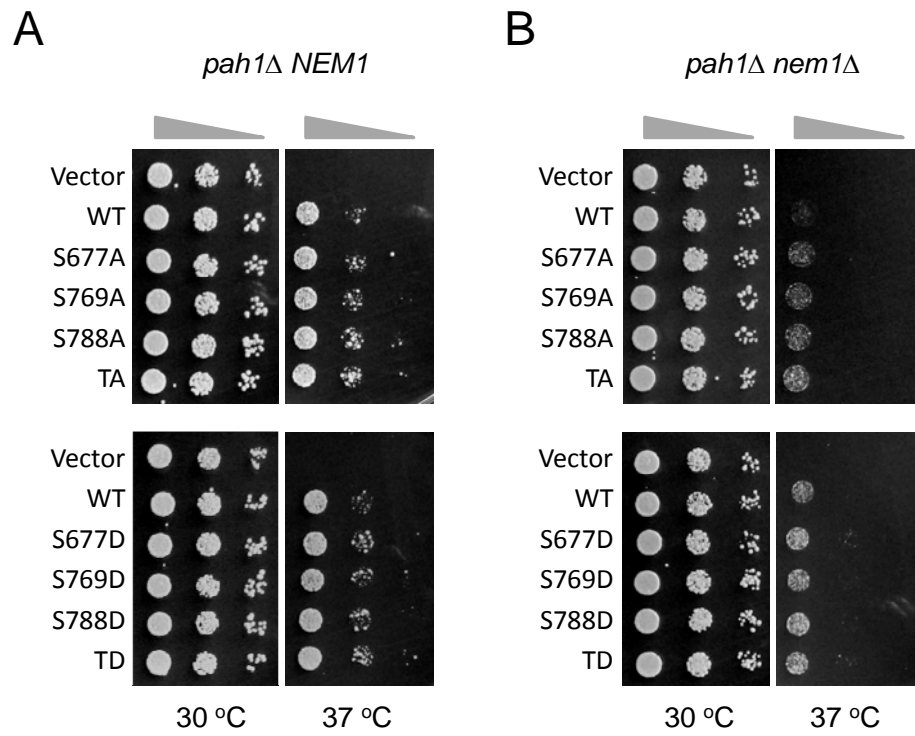


Effects of the PKC Phosphorylation Site Mutations on Temperature Sensitivity, Pah1p Abundance and Localization, and Lipid Composition

To investigate the physiological effects of PKC phosphorylation, the phosphorylation-deficient and phosphorylation-mimic forms of Pah1p were expressed from a single copy plasmid in *pah1Δ NEM1* and *pah1Δ nem1Δ* mutant cells. As discussed above, the Pah1p enzymes were expressed in the *nem1Δ* mutant background to assess the contribution of the Nem1p-Spo7p protein phosphatase complex on Pah1p function and to facilitate examination of the PKC mutations in a background that favors phosphorylation of the non-mutated sites in the enzyme. As discussed above, the effect of mutations on Pah1p function can be assessed by complementation of the temperature sensitive phenotype caused by the *pah1Δ* mutation. As shown above, the wild type enzyme complements this phenotype (e.g., permits growth at 37 °C) in *NEM1*-containing cells, but not in cells with the *nem1Δ* mutation (Fig. 23). Thus, the dephosphorylation by Nem1p-Spo7p is required for proper Pah1p function. The growth of cells expressing the PKC phosphorylation site mutations was not different from the growth of cells expressing wild type Pah1p (Fig. 23). Thus, the phosphorylation by PKC did not affect the function of Pah1p that regulates growth at 37 °C.

The effect of the PKC phosphorylation site mutations on the amount of Pah1p and its cellular location were examined. The Pah1p in the cell extract, cytosol and membrane fractions was detected by immunoblot analysis using anti-Pah1p antibodies. This analysis indicated that neither the individual (S677A/D, S769A/D, and S788A/D) nor the combined (3A/D) PKC phosphorylation site mutations caused a significant effect on the

FIGURE 23. Effect of PKC phosphorylation site mutations on the complementation of temperature sensitivity of *pah1Δ NEM1* and *pah1Δ nem1Δ* mutant cells. Ten-fold serial dilution of *pah1Δ NEM1* (A) and *pah1Δ nem1Δ* (B) cells carrying the wild type and indicated phosphorylation mutations Pah1p were spotted onto agar plate and were incubated at 30 and 37 °C for 3-4 days.



level of Pah1p (Fig. 24) and its distribution between cytosol and membrane fractions (data not shown).

To examine the effects of PKC phosphorylation on lipid composition, *pah1Δ NEM1* and *pah1Δ nem1Δ* cells expressing the wild type, phosphorylation-deficient 3A, and phosphorylation-mimic 3D forms of Pah1p were grown with [2-¹⁴C]acetate to label lipids. As discussed above, the lipid composition was analyzed from stationary phase cells, the growth condition where Pah1p PAP function is most pronounced (46, 47). Lipids were extracted and analyzed by TLC. The amounts of TAG and phospholipids of *pah1Δ NEM1* cells expressing wild type and the PKC phosphorylation site mutations were comparable (Fig. 25). As described above and previously (64, 65), the TAG level of *pah1Δ nem1Δ* cells expressing wild type Pah1p decreased from 22% to 3.6%, indicating the importance of the Nem1p-Spo7p-mediated dephosphorylation for the function of Pah1p. None of the PKC phosphorylation site mutations could bypass the requirement of Nem1p-Spo7p dephosphorylation and exhibited a similar low level of TAG (Fig. 25).

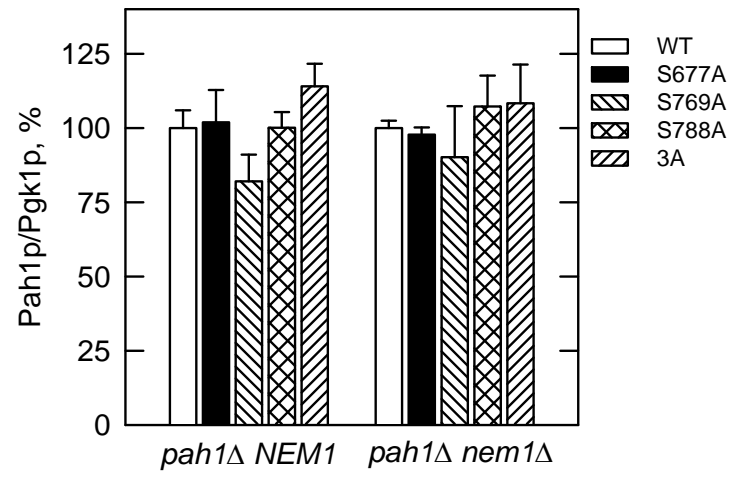
The Interrelations of Pah1p Phosphorylation by PKA, PKC and Pho85p-Pho80p

Pah1p is heavily phosphorylated *in vivo* (79) and has been found to be a substrate for multiple protein kinases including Cdc28p-cyclin B (64), Pho85p-Pho80p (65) and PKA (shown here). We questioned whether the phosphorylation of Pah1p by one protein kinase would affect the phosphorylation by another protein kinase. In these experiments Pah1p was fully phosphorylated by one protein kinase using unlabeled ATP.

FIGURE 24. Effect of PKC phosphorylation site mutations on protein abundance.

Wild type and indicated phosphorylation mutations of Pah1p were expressed in *pah1Δ NEM1* (A) and *pah1Δ nem1Δ* (B) cells. Cell extracts were prepared from exponential phase cells and subjected to the immunoblot analysis using anti-Pah1p and anti-phosphoglycerate kinase. The relative amounts of Pah1p/phosphoglycerate kinase were determined by ImageQuant analysis

A



B

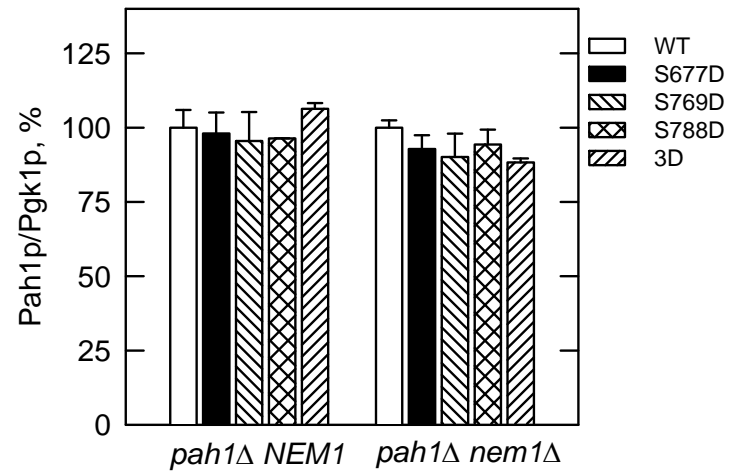
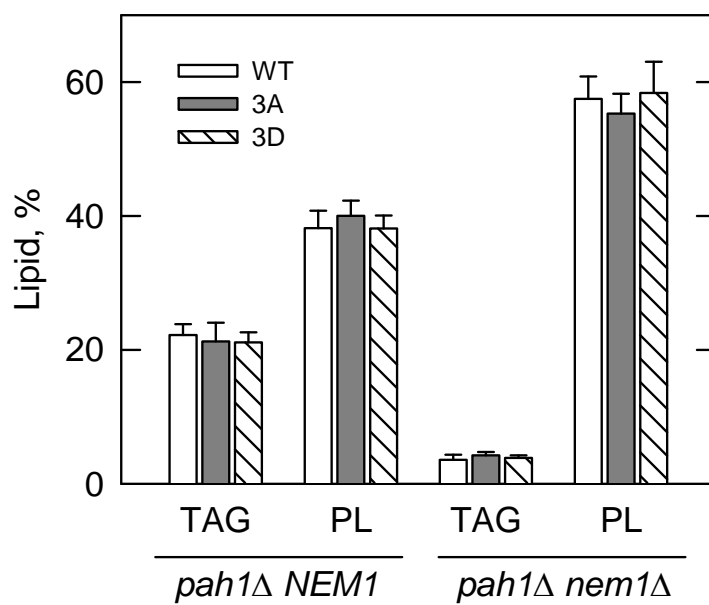
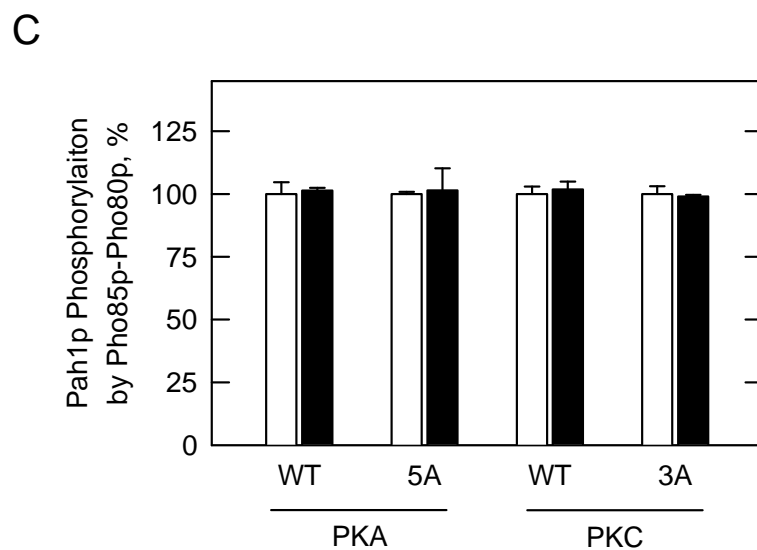
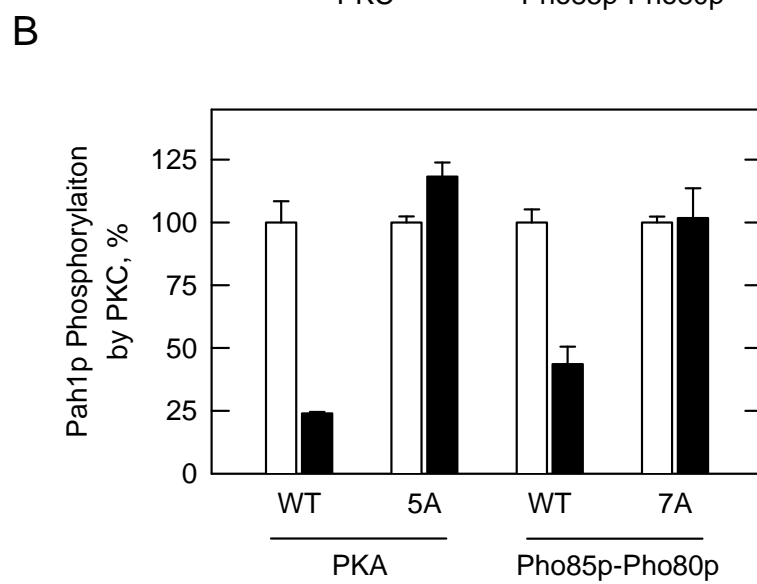
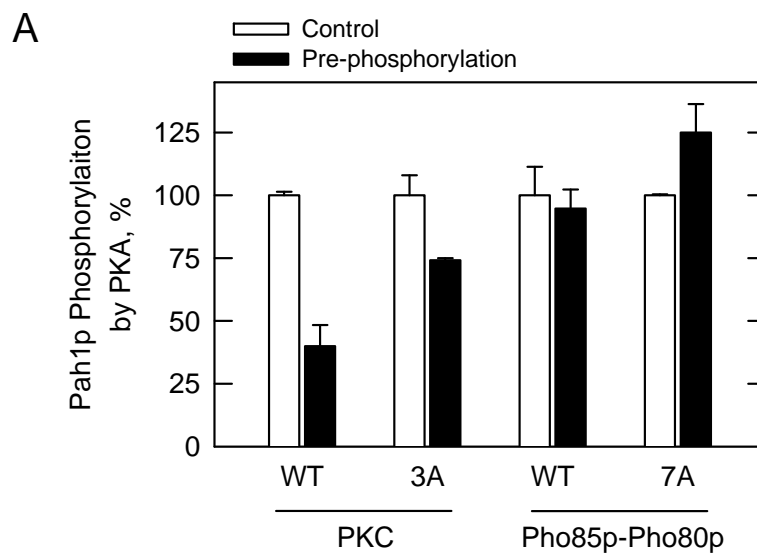


FIGURE 25. Effect of PKC phosphorylation sites mutations on the content of TAG and phospholipids. Wild type and indicated phosphorylation mutations Pah1p were expressed in *pah1Δ NEM1 (A)* and *pah1Δ nem1Δ (B)* cells. Cells were grown to stationary phase in the presence of [2-¹⁴C]acetate (1 μCi/ml). Lipids were extracted, separated by one dimensional TLC and the images were subjected to ImageQuant analysis. The percentage shown for TAG and phospholipids are normalized to the total ¹⁴C-label chloroform-soluble fraction. The values indicated are the average of three experiments ± S.D. (*error bars*).



After the reaction, the phosphorylated Pah1p was subjected to phosphorylation by a second protein kinase using [γ - 32 P]ATP. The control reaction mixture did not contain the first protein kinase. The extent of phosphorylation by the second protein kinase was determined by phosphorimaging and ImageQuant analysis after SDS-PAGE. The pre-phosphorylation of wild type Pah1p with PKC caused a 60% reduction in the phosphorylation by PKA (Fig. 26A). This inhibitory effect was reduced by 57% in the 3A mutations (Fig. 26A), which attenuated PKC phosphorylation (Fig. 21). The Pho85p-Pho80p pre-phosphorylation of Pah1p (wild type and 7A mutant) did not affect the phosphorylation by PKA (Fig. 26A). PKA pre-phosphorylation of Pah1p caused a 76% decrease in the phosphorylation by PKC, and this effect was obviated by the PKA phosphorylation-deficient 5A mutations (Fig. 26B). Pre-phosphorylation with Pho85p-Pho80p caused a 56% reduction in the phosphorylation by PKC, and the 7A mutations prevented this effect (Fig. 26B). Neither the pre-phosphorylation by PKA (wild type and 5A mutations) nor the pre-phosphorylation by PKC (wild type and 3A mutations) affected the phosphorylation of Pah1p by Pho85p-Pho80p (Fig. 26C).

FIGURE 26. The interrelations of Pah1p phosphorylation by PKA, PKC, and Pho85p-Pho80p. The purified recombinant wild type and phosphorylation site mutant Pah1p proteins were pre-phosphorylated with the indicated protein kinases (shown in the X axis) by incubating with ATP in the presence (*pre-phosphorylation*) or absence of kinase (*control*). Samples were then subjected to phosphorylation by the second protein kinase (shown in the Y axis) with [γ - 32 P]ATP. The 32 P-labeled Pah1p was resolved by SDS-PAGE and analyzed by phosphorimaging. The relative amounts of phosphate incorporated into Pah1p were quantified using ImageQuant software. The values indicated are the average of three experiments \pm S.D. (*error bars*).



DISCUSSION

Pah1p PAP in yeast plays a crucial role in lipid homeostasis by controlling the relative proportions of its substrate PA and its product DAG (46, 47). The imbalance of these lipid intermediates due to a defect in PAP activity results in a variety of cellular dysfunctions that include the misregulation of lipid synthesis, an abnormal expansion of the nuclear/ER membrane, defects in lipid droplet formation and vacuole fragmentation, and acute sensitivity to fatty acid induced toxicity (46-48, 68, 80, 82). Phosphorylation/dephosphorylation of Pah1p has emerged as a major mechanism by which its PAP activity is regulated in yeast. Phosphorylation is associated with the inhibition of PAP, whereas dephosphorylation is associated with its stimulation (64, 65, 79). The stimulatory effect of dephosphorylation can be attributed to an increase in Pah1p PAP catalytic activity and to the translocation of the enzyme from the cytosol to the membrane where its substrate PA resides (47, 64, 65, 79). Whereas the dephosphorylation of Pah1p is mediated by a single protein phosphatase (i.e., Nem1p-Spo7p complex), its phosphorylation is mediated by multiple protein kinases (64, 65, 79, 133, 170).

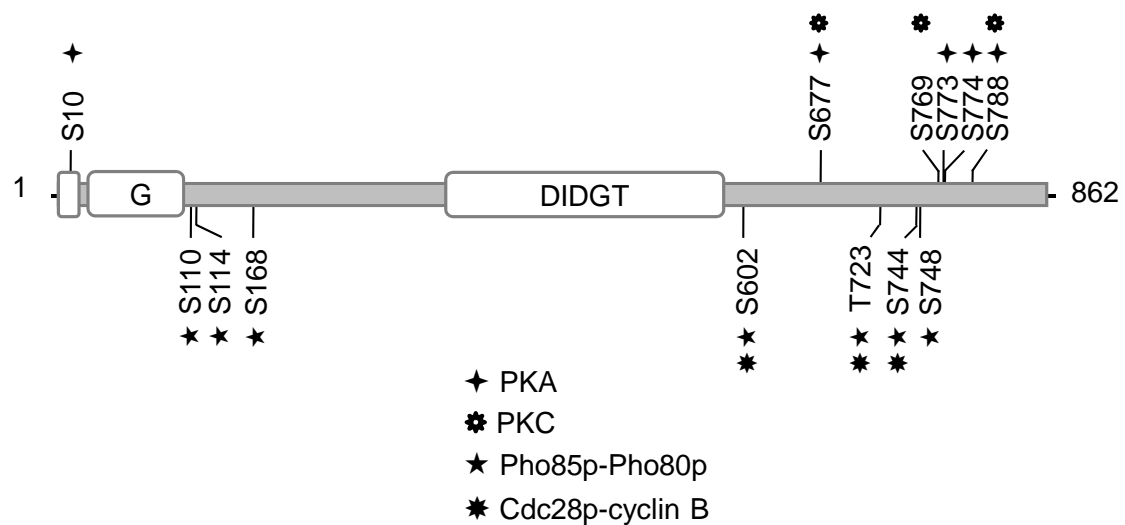
Pah1p is a target for Pho85p-Pho80p, Cdc28p-cyclin B, Dbf2p-Mob1p, PKA, PKC, and CKII (65, 68, 138-140, 148, 170, 190). In this work, we advanced the understanding of this complex regulation by characterizing the phosphorylation of Pah1p by PKA and PKC, identifying the major sites of phosphorylation by these protein kinases, and determining their biochemical and physiological relevance. Moreover, this work established that the phosphorylations by PKA, PKC, Pho85p-Pho80p, and Cdc28p-cyclin B were interrelated.

PKA and PKC utilized Pah1p as a substrate with high specificity having K_m values for Pah1p and ATP within the micromolar range previously found for the phosphorylations by Pho85p-Pho80p and Cdc28p-cyclin B (64, 65) (Fig. 27B). The phosphorylation by PKA caused a decrease in PAP catalytic efficiency as reflected in a decrease in V_{max} and an increase in K_m for PA. In contrast, the phosphorylation of Pah1p by PKC had a small stimulatory effect on the catalytic efficiency of PAP. This small stimulatory effect was corroborated by the small increase in PAP activity exhibited by the PKC phosphorylation-mimic 3D mutant. The phosphorylations by PKA and PKC also caused a decrease in Pah1p interaction with PC-PA liposome membranes (170), supporting a negative regulatory role for these phosphorylations in membrane association.

Using site-specific mutagenesis, we identified five PKA phosphorylation sites (Ser-10, Ser-677, Ser-773, Ser-774 and Ser-788) and three PKC sites (Ser-677, Ser-769, and Ser-788) (Fig. 27A). Of these sites, Ser-773, Ser-774 and Ser-769 have also been identified as phosphorylation sites by mass spectrometry analyses (79, 136). With the exception of Ser-10 (PKA site), which is located within the amphipathic helix at the N-terminus of Pah1p, the remaining phosphorylation sites were located at the C-terminus of the protein (Fig. 27A). PKA and PKC had overlapping sites of phosphorylation, namely Ser-677 and Ser-788. Overlapping sites for PKA and PKC is not uncommon because the recognition motifs for both protein kinases are similar (138, 149, 151). For example, PKA and PKC phosphorylate the phospholipid synthesis enzymes CTP synthetase (Ser-424) (191, 192) and choline kinase (Ser-30) (183, 193) at the same sites. Considering that five sites were targets of PKA and three sites were targets for PKC, the stoichiometry values of these phosphorylations were only 1 and 0.8 mol phosphate/mol Pah1p,

FIGURE 27. Summary of Pah1p phosphorylation by PKA, PKC, Pho85p-Pho80p, and Cdc28p-cyclin B. *A.* the diagram shows the domain structure and identified phosphorylation sites of Pah1p. *B.* the table shows the constants for phosphorylation of Pah1p by the indicated protein kinases.

A



B

Protein kinases	Constants			
	K_{mATP} μM	K_{mPah1p} μM	Hill _{Pah1p} n	Stoichiometry mol Pi/mol
PKA	4.4	0.44	1.9	1.0
PKC	4.5	0.75	-	0.8
Pho85p-Pho80p	3.7	0.25	1.8	4.0
Cdc28p-cyclin B	5.8	0.21	2.0	0.8

respectively. One explanation for this is that not all sites were phosphorylated to the same extent. For example, the phosphopeptide mapping experiments indicated that Ser-677 and Ser-773 were the most heavily phosphorylated sites for PKA and Ser-677 was the most strongly phosphorylated site for PKC when compared with the other sites. Another explanation might be that phosphorylation of one site inhibited the phosphorylation of another site (194). The simultaneous mutations of the five PKA sites to alanine (e.g., 5A mutations) eliminated the PKA-mediated phosphorylation of Pah1p and the inhibition of PAP activity. On the other hand, the simultaneous mutations of the three PKC sites to alanine (e.g., 3A mutations) eliminated most, but not all of the PKC-mediated phosphorylation of Pah1p. Thus, additional PKC sites must be present in Pah1p, but their identity is still unknown.

The effects of the PKA and PKC phosphorylations on Pah1p function (e.g., TAG synthesis) were examined using the phosphorylation-deficient and phosphorylation-mimic mutants. Although Ser-10 was not the most heavily phosphorylated PKA site, its phosphorylation inhibited membrane association (cell fractionation studies) and TAG synthesis. Ironically, the phosphorylation of Ser-10 stabilized Pah1p abundance. None of the other single PKA site mutations found at the C-terminal end of Pah1p affected these properties, but their phosphorylations might be a mechanism by which the phosphorylation and function of Ser-10 or other sites might be controlled. Whether the phosphorylation of Ser-10 specifically affected the function of the amphipathic helix will require additional studies. As indicated above, S677A/D and S788A/D, the mutations of the two PKA/PKC overlapping sites, did not affect Pah1p function with respect to TAG synthesis.

Of the protein kinases known to phosphorylate Pah1p, Pho85p-Pho80p has the greatest effect on PAP function (65, 148). The phosphorylation by this complex inhibits PAP activity, location, and function in lipid synthesis, as well as stabilizing enzyme abundance (65). Cdc28p-cyclin B phosphorylates three of the sites phosphorylated by Pho85p-Pho80p (Fig. 27), but the phosphorylation of the three individual sites does not impart much regulation (148). The phosphorylation of Pah1p by PKA at Ser-10 had similar effects on PAP regulation as that of Pho85p-Pho80p, but the extent the PKA-mediated regulation was not as great. However, in combination with the 7A mutations, the S10A and S10D mutations had greater effects. On the one hand, the S10A mutation enhanced the regulatory effects that the 7A mutations have on enzyme abundance, localization, and role in TAG synthesis. In fact, the enhanced effects of S10A on PAP function resulted in a slow growth phenotype during the exponential phase. This phenotype could be complemented by supplementations of inositol and choline indicating that increased PAP function with respect to TAG synthesis was detrimental to membrane phospholipid synthesis. A similar phenomenon has been described for cells that massively overexpress (*GALI10*-directed expression of a high copy number plasmid) the 7A mutations (79, 148). However, in the present work, increased PAP function was governed by low copy expression of S10A + 7A, emphasizing the importance of the PKA-mediated phosphorylation at Ser-10. On the other hand, the S10D mutation attenuated the positive effects 7A have on Pah1p association with membranes and on the synthesis of TAG. S10D also reversed the destabilizing effect that the 7A mutations have on Pah1p abundance. It was also noteworthy that S10D mutation alone caused a loss of growth at 37 °C when the mutant enzyme was expressed in the *nem1Δ* mutant

background. Collectively, these data indicated that the PKA-mediated phosphorylation of Ser-10 functions in conjunction with the phosphorylations mediated by Pho85p-Pho80p and Cdc28p-cyclin B, and that phosphoSer-10 should be dephosphorylated for proper PAP function. The paradoxical effects of phosphorylation/dephosphorylation on Pah1p abundance/function appear to be an additional mechanism by which cells control the levels of PA and DAG to maintain lipid homeostasis.

“Cross-talk” between phosphorylations has been shown for several proteins that are multiply phosphorylated (194, 195). In this work, we showed that a specific phosphorylation of recombinant Pah1p by Cdc28p-cyclin B, Pho85p-Pho80p, PKA and PKC does not require a prior phosphorylation by another protein kinase (64, 65). We also showed, however, that the phosphorylation of Pah1p by one protein kinase affected the phosphorylation by other protein kinase. Pho85p-Pho80p and PKC have distinct phosphorylation target sites in Pah1p. The pre-phosphorylation of Pah1p with Pho85p-Pho80p caused a 66% decrease in the phosphorylation by PKC, and as expected, this effect was obviated by the 7A mutation. The effect of Pho85p-Pho80p phosphorylation on the subsequent phosphorylation by PKC may be due to a structure change in Pah1p as a consequence of the Pho85p-Pho80p-mediated phosphorylation. For example, Pho85p-Pho80p phosphorylation at Thr-752 is thought to change Pah1p structure that is reflected in a shift in electrophoretic mobility upon SDS-PAGE (64, 65). That the phosphorylation of Pah1p by Pho85p-Pho80p did not affect the phosphorylation by PKA indicated that the affected sites in the PKC phosphorylation were not at the PKA/PKC overlapping sites. Moreover, these data indicate that the phosphorylation by PKC at the non-overlapping site(s) must occur prior to the phosphorylation by Pho85p-Pho80p. In the reverse

experiment, the phosphorylation of Pah1p by PKC had essentially no effect on the phosphorylation by Pho85p-Pho80p.

The PKA phosphorylation of Pah1p prevented the phosphorylation by PKC and *vice versa*. The simplest explanation for these effects was that Ser-677 and Ser-788 were found to be target sites for both protein kinases. Whereas the 5A mutations abolished the effect of PKA on PKC phosphorylation, the 3A mutations partially reversed the effects of PKC on the phosphorylation by PKA. These data supported the conclusion that additional PKC sites yet to be identified were present in Pah1p. Whether this site(s) is simply another PKA target site or a site that is unique and its phosphorylation affects PKC phosphorylation by another mechanism is unknown. Additional work is needed to address this question. An interrelationship between PKA and PKC phosphorylations have also been shown for the phospholipid synthesis repressor Opi1p (184). However, in this case the phosphorylation of Opi1p by PKA or PKC stimulated the subsequent phosphorylation by the other protein kinase (184). In fact, the sites phosphorylated in Opi1p by PKA and PKC are not overlapping (196, 197).

PKA activity is associated with rapid cell growth, enhanced metabolic activity, and an increase in membrane phospholipid synthesis (29, 149, 150). The PKC-mediated cell wall integrity pathway is essential for lipid homeostasis and cell viability in the absence of inositol supplementation (189). With respect to phospholipid synthesis, PKA phosphorylates and has positive effects on the activities/functions of Cho1p PS synthase (169, 198), Ura7p CTP synthetase (181, 191, 192), and Cki1p choline kinase (193, 199). The phosphorylations of Ura7p CTP synthetase (182, 192, 200, 201) and Cki1p choline kinase (183) by PKC also result in a stimulation of these enzyme activities and phospholipid

synthesis. PS synthase and choline kinase catalyze the committed steps in the synthesis of PC (most abundant phospholipid) via the CDP-DAG and Kennedy pathways, respectively (6, 29). The essential CTP synthetase enzyme (202) provides the CTP required for PC synthesis via both biosynthetic pathways (6, 29). In the exponential phase of growth, the synthesis of phospholipids occurs at the expense of TAG (203). Thus, the PKA-mediated stimulation of these phospholipid biosynthetic activities coupled to the PKA-mediated inhibition of Pah1p PAP coordinates lipid synthesis during growth. An increased TAG level is associated with the absence of inositol in the medium, a condition where yeast PKC is activated (43); however, as indicated above, the PKC-mediated phosphorylations of the C-terminal sites in Pah1p did not have major effects on lipid synthesis, suggesting the elevated TAG level in response to the lack of inositol may be due to other regulated enzymes functions.

There are checks and balances in lipid metabolism whereby a biochemical form of regulation is counterbalanced by a transcriptional form of regulation (6, 29). The PKA-mediated phosphorylation of Pah1p and that of the transcriptional repressor Opi1p (196) appear to be components of this form of regulation. Opi1p is tethered to the nuclear/ER membrane through interactions with Scs2p and PA (77, 78). These interactions are destabilized when PA levels are reduced, a consequence that causes the translocation of Opi1p from the nuclear/ER membrane into the nucleus where it binds to Ino2p and attenuates the transcriptional activation of UAS_{INO}-containing genes by the Ino2p-Ino4p complex (6, 29, 78, 131). Pah1p PAP activity regulates PA levels and the transcriptional regulation of phospholipid synthesis gene expression. For example, loss of PAP activity and the elevation of PA content result in the derepression of UAS_{INO}-containing genes

(48, 68, 79). *CHO1* (encoding PS synthase) and *CKII* (encoding choline kinase) are UAS_{INO} -containing genes (6). While the PKA-mediated phosphorylation of Pah1p inhibits PAP activity for elevated PA content, the phosphorylation of Opi1p at Ser-31 and Ser-251 by PKA stimulates its repressor activity (196). How PKA stimulates Opi1p function is unknown, but the introduction of negative charges to Opi1p might destabilize its interaction with PA and/or Scs2p at the nuclear/ER membrane. Nonetheless, the PKA-mediated phosphorylations of Pah1p and Opi1p could work together in balancing lipid synthesis from the PA node in the pathways.

CONCLUSIONS AND FUTURE DIRECTIONS

It has become apparent that phosphorylation/dephosphorylation is a key regulatory mechanism controlling Pah1p PAP functions in *S. cerevisiae*. Pah1p is a heavily phosphorylated protein that contains multiple sites of phosphorylation (64, 65, 79, 135, 136, 204). This and previous studies have shown that Pho85p-Pho80p, Cdc28p-cyclin B, PKA, and PKC phosphorylate Pah1p at many of the sites and regulate PAP (64, 65, 204). The protein kinases involved in the phosphorylation of the remaining sites are still unclear and additional studies are needed to identify them. The complex regulation of phosphorylation governs the localization (e.g., cytosol *versus* membrane), activity, and stability of Pah1p. The current work also indicates that many of the phosphorylations are interconnected whereby phosphorylation by one protein kinase may or may not influence the phosphorylation and regulation by another protein kinase. Clearly, the unraveling of this complex regulation is a daunting task.

Studies with the phosphorylation-deficient and phosphorylation-mimic Pah1p mutants, as well as those with mutants defective in the Nem1p-Spo7p protein phosphatase complex, point to the importance of dephosphorylation in the overall regulation of PAP localization and function (64, 65, 68, 79, 133, 204). The Nem1p-Spo7p complex, which is associated with the nuclear/ER membrane, was identified (133) prior to the identification of Pah1p as a PAP enzyme (47). At the time of its discovery, however, the complex required to form a spherical nucleus was not known to be a protein phosphatase that regulates PAP activity. In subsequent studies, it was shown that Nem1p is the catalytic subunit, and Spo7p is the regulatory subunit (68). The protein phosphatase activity of the Nem1p-Spo7p complex is dependent on the catalytic motif

DXDXT in Nem1p, and the binding of Spo7p to Nem1p is required for the phosphatase activity of the holoenzyme (68). Both subunits of the analogous complex (CTDNEP1 (formally known as dullard) and NEP1-R1) in mammalian cells are also required for phosphatase function *in vivo* (147, 205).

Genetic analyses have shown that Pah1p for its function requires both Nem1p and Spo7p. Thus, the *nem1Δ* and *spo7Δ* mutants exhibit the same phenotypes shown by the *pah1Δ* mutant (48, 68) such as temperature sensitivity, the induced expression of UAS_{INO}-containing genes, the aberrant expansion of the nuclear/ER membrane, an increase in phospholipid content, and a decrease in TAG content (64, 133). The loss of Pah1p function in the *nem1Δ* and *spo7Δ* mutants is due to a lack of its association with the membrane where its substrate PA resides. These data indicate that no other protein phosphatase acts on Pah1p. Interestingly, overexpression of *PAH1* complements the *nem1Δ* and *spo7Δ* mutants (68). We postulate that the complementation occurs by unphosphorylated or hypophosphorylated Pah1p molecules that are produced by limited protein kinase activity, and can directly interact with the membrane. Clearly, under normal physiological conditions, the membrane localization of Pah1p is governed by the Nem1p-Spo7p complex that catalyzes its dephosphorylation. Therefore, knowledge of the enzymological properties and substrate specificity of the Nem1p-Spo7p complex will lead to a better understanding of the mechanism by which Pah1p translocates to the membrane for its function *in vivo*.

The phosphatase activities of Nem1p-Spo7p and the mammalian counterpart have been measured with *p*-nitrophenylphosphate and with phosphopeptide substrates (68, 205, 206). These substrates, however, are not physiologically relevant. Our laboratory is now

in a unique position to enzymatically synthesize a physiological substrate, phosphorylated Pah1p, for characterizing the enzymological properties of Nem1p-Spo7p and its substrate specificity. As shown in this work, recombinant Pah1p can be phosphorylated with specific protein kinases at specific sites (e.g., sites phosphorylated by PKA, PKC, etc.). Then each of these phosphorylated forms can then be tested as substrates for Nem1p-Spo7p phosphatase activity. Thus, substrate specificity or order of dephosphorylation of Pah1p sites phosphorylated by any one protein kinase can be determined. Finally, the interdependencies of the various dephosphorylation reactions can also be examined. Clearly, there is much more work needed to fully understand the complex regulation of Pah1p by phosphorylation/dephosphorylation.

REFERENCES

1. Lehninger, A. L., Nelson, D. L., and Cox, M. M. (1993) *Principles of Biochemistry*, Second Ed., Worth Publishers, New York
2. Reue, K. and Brindley, D. N. (2008) Multiple roles for lipins/phosphatidate phosphatase enzymes in lipid metabolism. *J. Lipid Res.* **49**, 2493-2503
3. Gaspar, M. L., Aregullin, M. A., Jesch, S. A., Nunez, L. R., Villa-Garcia, M., and Henry, S. A. (2007) The emergence of yeast lipidomics. *Biochim. Biophys. Acta* **1771**, 241-254
4. Paltauf, F., Kohlwein, S. D., and Henry, S. A. (1992) in *The Molecular and Cellular Biology of the Yeast Saccharomyces: Gene Expression* (Jones, E. W., Pringle, J. R., and Broach, J. R., eds) pp. 415-500, Cold Spring Harbor Laboratory, Cold Spring Harbor, NY
5. Carman, G. M. and Henry, S. A. (1999) Phospholipid biosynthesis in the yeast *Saccharomyces cerevisiae* and interrelationship with other metabolic processes. *Prog. Lipid Res.* **38**, 361-399
6. Henry, S. A., Kohlwein, S., and Carman, G. M. (2012) Metabolism and regulation of glycerolipids in the yeast *Saccharomyces cerevisiae*. *Genetics* **190**, 317-349
7. Carman, G. M. and Henry, S. A. (1989) Phospholipid biosynthesis in yeast. *Annu. Rev. Biochem.* **58**, 635-669
8. Ichimura, Y., Kirisako, T., Takao, T., Satomi, Y., Shimonishi, Y., Ishihara, N., Mizushima, N., Tanida, I., Kominami, E., Ohsumi, M., Noda, T., and Ohsumi, Y. (2000) A ubiquitin-like system mediates protein lipidation. *Nature* **408**, 488-492
9. Athenstaedt, K. and Daum, G. (1997) Biosynthesis of phosphatidic acid in lipid particles and endoplasmic reticulum of *Saccharomyces cerevisiae*. *J. Bacteriol.* **179**, 7611-7616
10. Athenstaedt, K., Weys, S., Paltauf, F., and Daum, G. (1999) Redundant systems of phosphatidic acid biosynthesis via acylation of glycerol-3-phosphate or dihydroxyacetone phosphate in the yeast *Saccharomyces cerevisiae*. *J. Bacteriol.* **181**, 1458-1463
11. Zheng, Z. and Zou, J. (2001) The initial step of the glycerolipid pathway: identification of glycerol 3-phosphate/dihydroxyacetone phosphate dual substrate acyltransferases in *Saccharomyces cerevisiae*. *J. Biol. Chem.* **276**, 41710-41716
12. Jain, S., Stanford, N., Bhagwat, N., Seiler, B., Costanzo, M., Boone, C., and Oelkers, P. (2007) Identification of a Novel Lysophospholipid Acyltransferase in *Saccharomyces cerevisiae*. *J. Biol. Chem.* **282**, 30562-30569

13. Benghezal, M., Roubaty, C., Veepuri, V., Knudsen, J., and Conzelmann, A. (2007) *SLC1* and *SLC4* Encode Partially Redundant Acyl-Coenzyme A 1-Acylglycerol-3-phosphate O-Acyltransferases of Budding Yeast. *J. Biol. Chem.* **282**, 30845-30855
14. Chen, Q., Kazachkov, M., Zheng, Z., and Zou, J. (2007) The yeast acylglycerol acyltransferase LCA1 is a key component of Lands cycle for phosphatidylcholine turnover. *FEBS Lett.* **581**, 5511-5516
15. Carter, J. R. and Kennedy, E. P. (1966) Enzymatic synthesis of cytidine diphosphate diglyceride. *J. Lipid Res.* **7**, 678-683
16. Shen, H., Heacock, P. N., Clancey, C. J., and Dowhan, W. (1996) The *CDS1* gene encoding CDP-diacylglycerol synthase in *Saccharomyces cerevisiae* is essential for cell growth. *J. Biol. Chem.* **271**, 789-795
17. Nikawa, J. and Yamashita, S. (1984) Molecular cloning of the gene encoding CDP-diacylglycerol- inositol 3-phosphatidyl transferase in *Saccharomyces cerevisiae*. *Eur. J. Biochem.* **143**, 251-256
18. Nikawa, J., Kodaki, T., and Yamashita, S. (1987) Primary structure and disruption of the phosphatidylinositol synthase gene of *Saccharomyces cerevisiae*. *J. Biol. Chem.* **262**, 4876-4881
19. Klig, L. S. and Henry, S. A. (1984) Isolation of the yeast *INO1* gene: located on an autonomously replicating plasmid, the gene is fully regulated. *Proc. Natl. Acad. Sci. USA* **81**, 3816-3820
20. Dean-Johnson, M. and Henry, S. A. (1989) Biosynthesis of inositol in yeast. Primary structure of *myo*- inositol-1-phosphate synthase (EC 5.5.1.4) and functional analysis of its structural gene, the *INO1* locus. *J. Biol. Chem.* **264**, 1274-1283
21. Murray, M. and Greenberg, M. L. (2000) Expression of yeast *INMI* encoding inositol monophosphatase is regulated by inositol, carbon source and growth stage and is decreased by lithium and valproate. *Mol. Microbiol.* **36**, 651-661
22. Letts, V. A., Klig, L. S., Bae-Lee, M., Carman, G. M., and Henry, S. A. (1983) Isolation of the yeast structural gene for the membrane-associated enzyme phosphatidylserine synthase. *Proc. Natl. Acad. Sci. USA* **80**, 7279-7283
23. Nikawa, J., Tsukagoshi, Y., Kodaki, T., and Yamashita, S. (1987) Nucleotide sequence and characterization of the yeast *PSS* gene encoding phosphatidylserine synthase. *Eur. J. Biochem.* **167**, 7-12
24. Kiyono, K., Miura, K., Kushima, Y., Hikiji, T., Fukushima, M., Shibuya, I., and Ohta, A. (1987) Primary structure and product characterization of the

- Saccharomyces cerevisiae CHO1* gene that encodes phosphatidylserine synthase. *J. Biochem.* **102**, 1089-1100
25. Clancey, C. J., Chang, S.-C., and Dowhan, W. (1993) Cloning of a gene (*PSDI*) encoding phosphatidylserine decarboxylase from *Saccharomyces cerevisiae* by complementation of an *Escherichia coli* mutant. *J. Biol. Chem.* **268**, 24580-24590
 26. Trotter, P. J., Pedretti, J., Yates, R., and Voelker, D. R. (1995) Phosphatidylserine decarboxylase 2 of *Saccharomyces cerevisiae*. Cloning and mapping of the gene, heterologous expression, and creation of the null allele. *J. Biol. Chem.* **270**, 6071-6080
 27. Trotter, P. J., Pedretti, J., and Voelker, D. R. (1993) Phosphatidylserine decarboxylase from *Saccharomyces cerevisiae*. Isolation of mutants, cloning of the gene, and creation of a null allele. *J. Biol. Chem.* **268**, 21416-21424
 28. Bremer, J. and Greenberg, D. M. (1961) Methyl transferring enzyme system of microsomes in the biosynthesis of lecithin (phosphatidylcholine). *Biochim. Biophys. Acta* **46**, 205-216
 29. Carman, G. M. and Han, G.-S. (2011) Regulation of phospholipid synthesis in the yeast *Saccharomyces cerevisiae*. *Ann. Rev. Biochem.* **80**, 859-883
 30. Kodaki, T. and Yamashita, S. (1987) Yeast phosphatidylethanolamine methylation pathway: Cloning and characterization of two distinct methyltransferase genes. *J. Biol. Chem.* **262**, 15428-15435
 31. Summers, E. F., Letts, V. A., McGraw, P., and Henry, S. A. (1988) *Saccharomyces cerevisiae cho2* mutants are deficient in phospholipid methylation and cross-pathway regulation of inositol synthesis. *Genetics* **120**, 909-922
 32. McGraw, P. and Henry, S. A. (1989) Mutations in the *Saccharomyces cerevisiae OPI3* gene: Effects on phospholipid methylation, growth, and cross pathway regulation of phospholipid synthesis. *Genetics* **122**, 317-330
 33. Kim, K., Kim, K.-H., Storey, M. K., Voelker, D. R., and Carman, G. M. (1999) Isolation and characterization of the *Saccharomyces cerevisiae EKII* gene encoding ethanolamine kinase. *J. Biol. Chem.* **274**, 14857-14866
 34. Hosaka, K., Kodaki, T., and Yamashita, S. (1989) Cloning and characterization of the yeast *CKI* gene encoding choline kinase and its expression in *Escherichia coli*. *J. Biol. Chem.* **264**, 2053-2059
 35. Min-Seok, R., Kawamata, Y., Nakamura, H., Ohta, A., and Takagi, M. (1996) Isolation and characterization of *ECT1* gene encoding CTP:phosphoethanolamine cytidyltransferase of *Saccharomyces cerevisiae*. *J. Biochem.* **120**, 1040-1047

36. Tsukagoshi, Y., Nikawa, J., and Yamashita, S. (1987) Molecular cloning and characterization of the gene encoding cholinephosphate cytidylyltransferase in *Saccharomyces cerevisiae*. *Eur. J. Biochem.* **169**, 477-486
37. Hjelmstad, R. H. and Bell, R. M. (1988) The sn-1,2-diacylglycerol ethanolaminephosphotransferase of *Saccharomyces cerevisiae*. Isolation of mutants and cloning of the *EPT1* gene. *J. Biol. Chem.* **263**, 19748-19757
38. Hjelmstad, R. H. and Bell, R. M. (1991) sn-1,2-diacylglycerol choline- and ethanolaminephosphotransferases in *Saccharomyces cerevisiae*. Nucleotide sequence of the *EPT1* gene and comparison of the *CPT1* and *EPT1* gene products. *J. Biol. Chem.* **266**, 5094-5103
39. Hjelmstad, R. H. and Bell, R. M. (1987) Mutants of *Saccharomyces cerevisiae* defective in sn-1,2- diacylglycerol cholinephosphotransferase: Isolation, characterization, and cloning of the *CPT1* gene. *J. Biol. Chem.* **262**, 3909-3917
40. Hjelmstad, R. H. and Bell, R. M. (1990) The sn-1,2-diacylglycerol cholinephosphotransferase of *Saccharomyces cerevisiae*. Nucleotide sequence, transcriptional mapping, and gene product analysis of the *CPT1* gene. *J. Biol. Chem.* **265**, 1755-1764
41. Rajakumari, S., Grillitsch, K., and Daum, G. (2008) Synthesis and turnover of non-polar lipids in yeast. *Prog. Lipid Res.* **47**, 157-171
42. Fakas, S., Konstantinou, C., and Carman, G. M. (2011) *DGKI*-encoded diacylglycerol kinase activity is required for phospholipid synthesis during growth resumption from stationary phase in *Saccharomyces cerevisiae*. *J. Biol. Chem.* **286**, 1464-1474
43. Gaspar, M. L., Hofbauer, H. F., Kohlwein, S. D., and Henry, S. A. (2011) Coordination of Storage Lipid Synthesis and Membrane Biogenesis: EVIDENCE FOR CROSS-TALK BETWEEN TRIACYLGLYCEROL METABOLISM AND PHOSPHATIDYLINOSITOL SYNTHESIS. *J. Biol. Chem.* **286**, 1696-1708
44. Listenberger, L. L., Han, X., Lewis, S. E., Cases, S., Farese, R. V., Jr., Ory, D. S., and Schaffer, J. E. (2003) Triglyceride accumulation protects against fatty acid-induced lipotoxicity. *Proc. Natl. Acad. Sci. U. S. A* **100**, 3077-3082
45. Petschnigg, J., Wolinski, H., Kolb, D., Zellnig, G., Kurat, C. F., Natter, K., and Kohlwein, S. D. (2009) Good fat - essential cellular requirements for triacylglycerol synthesis to maintain membrane homeostasis in yeast. *J. Biol. Chem.* **284**, 30981-30993
46. Fakas, S., Qiu, Y., Dixon, J. L., Han, G.-S., Ruggles, K. V., Garbarino, J., Sturley, S. L., and Carman, G. M. (2011) Phosphatidate phosphatase activity plays a key role in protection against fatty acid-induced toxicity in yeast. *J. Biol. Chem.* **286**, 29074-29085

47. Han, G.-S., Wu, W.-I., and Carman, G. M. (2006) The *Saccharomyces cerevisiae* lipin homolog is a Mg²⁺-dependent phosphatidate phosphatase enzyme. *J Biol. Chem.* **281**, 9210-9218
48. Han, G.-S., Siniossoglou, S., and Carman, G. M. (2007) The cellular functions of the yeast lipin homolog Pah1p are dependent on its phosphatidate phosphatase activity. *J. Biol. Chem.* **282**, 37026-37035
49. Oelkers, P., Cromley, D., Padamsee, M., Billheimer, J. T., and Sturley, S. L. (2002) The *DGA1* gene determines a second triglyceride synthetic pathway in yeast. *J Biol. Chem.* **277**, 8877-8881
50. Oelkers, P., Tinkelenberg, A., Erdeniz, N., Cromley, D., Billheimer, J. T., and Sturley, S. L. (2000) A lecithin cholesterol acyltransferase-like gene mediates diacylglycerol esterification in yeast. *J Biol. Chem.* **275**, 15609-15612
51. Sorger, D. and Daum, G. (2002) Synthesis of triacylglycerols by the acyl-coenzyme A:diacyl-glycerol acyltransferase Dga1p in lipid particles of the yeast *Saccharomyces cerevisiae*. *J. Bacteriol.* **184**, 519-524
52. Kohlwein, S. D. (2010) Triacylglycerol homeostasis: insights from yeast. *J. Biol. Chem.* **285**, 15663-15667
53. Athenstaedt, K. and Daum, G. (2003) YMR313c/TGL3 Encodes a Novel Triacylglycerol Lipase Located in Lipid Particles of *Saccharomyces cerevisiae*. *J. Biol. Chem.* **278**, 23317-23323
54. Athenstaedt, K. and Daum, G. (2005) Tgl4p and Tgl5p, two triacylglycerol lipases of the yeast *Saccharomyces cerevisiae* are localized to lipid particles. *J. Biol. Chem.* **280**, 37301-37309
55. Rajakumari, S. and Daum, G. (2010) Multiple functions as lipase, steryl ester hydrolase, phospholipase, and acyltransferase of Tgl4p from the yeast *Saccharomyces cerevisiae*. *J. Biol. Chem.* **285**, 15769-15776
56. Han, G.-S., O'Hara, L., Siniossoglou, S., and Carman, G. M. (2008) Characterization of the yeast *DGKI*-encoded CTP-dependent diacylglycerol kinase. *J. Biol. Chem.* **283**, 20443-20453
57. Smith, S. W., Weiss, S. B., and Kennedy, E. P. (1957) The enzymatic dephosphorylation of phosphatidic acids. *J. Biol. Chem.* **228**, 915-922
58. Brindley, D. N. (1984) Intracellular translocation of phosphatidate phosphohydrolase and its possible role in the control of glycerolipid synthesis. *Prog. Lipid Res.* **23**, 115-133
59. Carman, G. M. and Han, G.-S. (2006) Roles of phosphatidate phosphatase enzymes in lipid metabolism. *Trends Biochem Sci* **31**, 694-699

60. Brindley, D. N., Pilquil, C., Sariahmetoglu, M., and Reue, K. (2009) Phosphatidate degradation: phosphatidate phosphatases (lipins) and lipid phosphate phosphatases. *Biochim. Biophys. Acta* **1791**, 956-961
61. Hubscher, G., Brindley, D. N., Smith, M. E., and Sedgwick, B. (1967) Stimulation of biosynthesis of glyceride. *Nature* **216**, 449-453
62. Martin-Sanz, P., Hopewell, R., and Brindley, D. N. (1984) Long-chain fatty acids and their acyl-CoA esters cause the translocation of phosphatidate phosphatase from the cytosolic to the microsomal fraction of rat liver. *FEBS LETTERS* **175**, 284-288
63. Lin, Y.-P. and Carman, G. M. (1989) Purification and characterization of phosphatidate phosphatase from *Saccharomyces cerevisiae*. *J. Biol. Chem.* **264**, 8641-8645
64. Choi, H.-S., Su, W.-M., Morgan, J. M., Han, G.-S., Xu, Z., Karanasios, E., Siniossoglou, S., and Carman, G. M. (2011) Phosphorylation of phosphatidate phosphatase regulates its membrane association and physiological functions in *Saccharomyces cerevisiae*. Identification of Ser⁶⁰², Thr⁷²³, and Ser⁷⁴⁴ as the sites phosphorylated by *CDC28* (*CDK1*)-encoded cyclin-dependent kinase. *J. Biol. Chem.* **286**, 1486-1498
65. Choi, H.-S., Su, W. M., Han, G.-S., Plote, D., Xu, Z., and Carman, G. M. (2012) Pho85p-Pho80p phosphorylation of yeast Pah1p phosphatidate phosphatase regulates its activity, location, abundance, and function in lipid metabolism. *J. Biol. Chem.* **287**, 11290-11301
66. Karanasios, E., Han, G.-S., Xu, Z., Carman, G. M., and Siniossoglou, S. (2010) A phosphorylation-regulated amphipathic helix controls the membrane translocation and function of the yeast phosphatidate phosphatase. *Proc. Natl. Acad. Sci. U. S. A.* **107**, 17539-17544
67. Hosaka, K. and Yamashita, S. (1984) Regulatory role of phosphatidate phosphatase in triacylglycerol synthesis of *Saccharomyces cerevisiae*. *Biochim. Biophys. Acta* **796**, 110-117
68. Santos-Rosa, H., Leung, J., Grimsey, N., Peak-Chew, S., and Siniossoglou, S. (2005) The yeast lipin Smp2 couples phospholipid biosynthesis to nuclear membrane growth. *EMBO J* **24**, 1931-1941
69. Schuller, H. J., Hahn, A., Troster, F., Schutz, A., and Schweizer, E. (1992) Coordinate genetic control of yeast fatty acid synthase genes *FAS1* and *FAS2* by an upstream activation site common to genes involved in membrane lipid biosynthesis. *EMBO J.* **11**, 107-114

70. Chirala, S. S. (1992) Coordinated regulation and inositol-mediated and fatty acid-mediated repression of fatty acid synthase genes in *Saccharomyces cerevisiae*. *Proc. Natl. Acad. Sci. U. S. A* **89**, 10232-10236
71. Hasslacher, M., Ivessa, A. S., Paltauf, F., and Kohlwein, S. D. (1993) Acetyl-CoA carboxylase from yeast is an essential enzyme and is regulated by factors that control phospholipid metabolism. *J. Biol. Chem.* **268**, 10946-10952
72. Chirala, S. S., Zhong, Q., Huang, W., and Al-Feel, W. (1994) Analysis of *FAS3/ACC* regulatory region of *Saccharomyces cerevisiae*: identification of a functional UAS_{INO} and sequences responsible for fatty acid mediated repression. *Nucleic Acids Res.* **22**, 412-418
73. Lopes, J. M., Hirsch, J. P., Chorgo, P. A., Schulze, K. L., and Henry, S. A. (1991) Analyses of sequences in the *INO1* promoter that are involved in its regulation by phospholipid precursors. *Nucl. Acids Res.* **19**, 1687-1693
74. Nikoloff, D. M., McGraw, P., and Henry, S. A. (1992) The *INO2* gene of *Saccharomyces cerevisiae* encodes a helix-loop-helix protein that is required for activation of phospholipid synthesis. *Nucleic Acids Res.* **20**, 3253
75. Ambroziak, J. and Henry, S. A. (1994) *INO2* and *INO4* gene products, positive regulators of phospholipid biosynthesis in *Saccharomyces cerevisiae*, form a complex that binds to the *INO1* promoter. *J. Biol. Chem.* **269**, 15344-15349
76. White, M. J., Hirsch, J. P., and Henry, S. A. (1991) The *OPI1* gene of *Saccharomyces cerevisiae*, a negative regulator of phospholipid biosynthesis, encodes a protein containing polyglutamine tracts and a leucine zipper. *J. Biol. Chem.* **266**, 863-872
77. Loewen, C. J. R., Roy, A., and Levine, T. P. (2003) A conserved ER targeting motif in three families of lipid binding proteins and in Opi1p binds VAP. *EMBO J.* **22**, 2025-2035
78. Loewen, C. J. R., Gaspar, M. L., Jesch, S. A., Delon, C., Ktistakis, N. T., Henry, S. A., and Levine, T. P. (2004) Phospholipid metabolism regulated by a transcription factor sensing phosphatidic acid. *Science* **304**, 1644-1647
79. O'Hara, L., Han, G.-S., Peak-Chew, S., Grimsey, N., Carman, G. M., and Siniossoglou, S. (2006) Control of phospholipid synthesis by phosphorylation of the yeast lipin Pah1p/Smp2p Mg²⁺-dependent phosphatidate phosphatase. *J Biol. Chem.* **281**, 34537-34548
80. Adeyo, O., Horn, P. J., Lee, S., Binns, D. D., Chandrabhas, A., Chapman, K. D., and Goodman, J. M. (2011) The yeast lipin orthologue Pah1p is important for biogenesis of lipid droplets. *J. Cell Biol.* **192**, 1043-1055

81. Fei, W., Shui, G., Zhang, Y., Krahmer, N., Ferguson, C., Kapterian, T. S., Lin, R. C., Dawes, I. W., Brown, A. J., Li, P., Huang, X., Parton, R. G., Wenk, M. R., Walther, T. C., and Yang, H. (2011) A role for phosphatidic acid in the formation of "supersized" lipid droplets. *PLoS. Genet.* **7**, e1002201
82. Sasser, T., Qiu, Q. S., Karunakaran, S., Padolina, M., Reyes, A., Flood, B., Smith, S., Gonzales, C., and Fratti, R. A. (2011) The yeast lipin 1 orthologue Pah1p regulates vacuole homeostasis and membrane fusion. *J. Biol. Chem.* **287**, 2221-2236
83. Han, G.-S., O'Hara, L., Carman, G. M., and Siniosoglou, S. (2008) An unconventional diacylglycerol kinase that regulates phospholipid synthesis and nuclear membrane growth. *J. Biol. Chem.* **283**, 20433-20442
84. Chae, M., Han, G.-S., and Carman, G. M. (2012) The *Saccharomyces cerevisiae* actin patch protein App1p is a phosphatidate phosphatase enzyme. *J. Biol. Chem.* **287**, 40186-40196
85. Chae, M. and Carman, G. M. (2013) Characterization of the yeast actin patch protein App1p phosphatidate phosphatase. *J. Biol. Chem.* **288**, 6427-6437
86. Toke, D. A., Bennett, W. L., Dillon, D. A., Wu, W.-I., Chen, X., Ostrander, D. B., Oshiro, J., Cremesti, A., Voelker, D. R., Fischl, A. S., and Carman, G. M. (1998) Isolation and characterization of the *Saccharomyces cerevisiae* *DPP1* gene encoding for diacylglycerol pyrophosphate phosphatase. *J. Biol. Chem.* **273**, 3278-3284
87. Toke, D. A., Bennett, W. L., Oshiro, J., Wu, W. I., Voelker, D. R., and Carman, G. M. (1999) Isolation and characterization of the *Saccharomyces cerevisiae* *LPP1* gene encoding a Mg²⁺-independent phosphatidate phosphatase. *J. Biol. Chem.* **273**, 14331-14338
88. Stuke, J. and Carman, G. M. (1997) Identification of a novel phosphatase sequence motif. *Protein Science* **6**, 469-472
89. Toke, D. A., McClintick, M. L., and Carman, G. M. (1999) Mutagenesis of the phosphatase sequence motif in diacylglycerol pyrophosphate phosphatase from *Saccharomyces cerevisiae*. *Biochemistry* **38**, 14606-14613
90. Faulkner, A. J., Chen, X., Rush, J., Horazdovsky, B., Waechter, C. J., Carman, G. M., and Sternweis, P. C. (1999) The *LPP1* and *DPP1* gene products account for most of the isoprenoid phosphatase activities in *Saccharomyces cerevisiae*. *J. Biol. Chem.* **274**, 14831-14837
91. Brindley, D. N., English, D., Pilquil, C., Buri, K., and Ling, Z. C. (2002) Lipid phosphate phosphatases regulate signal transduction through glycerolipids and sphingolipids. *Biochim. Biophys. Acta* **1582**, 33-44

92. Brindley, D. N. (2004) Lipid phosphate phosphatases and related proteins: signaling functions in development, cell division, and cancer. *J Cell Biochem* **92**, 900-912
93. Grimsey, N., Han, G.-S., O'Hara, L., Rochford, J. J., Carman, G. M., and Siniossoglou, S. (2008) Temporal and spatial regulation of the phosphatidate phosphatases lipin 1 and 2. *J. Biol. Chem.* 29166-29174
94. P 環 erfy, M., Phan, J., Xu, P., and Reue, K. (2001) Lipodystrophy in the *fld* mouse results from mutation of a new gene encoding a nuclear protein, lipin. *Nat. Genet.* **27**, 121-124
95. Phan, J. and Reue, K. (2005) Lipin, a lipodystrophy and obesity gene. *Cell Metab* **1**, 73-83
96. Donkor, J., Sariahmetoglu, M., Dewald, J., Brindley, D. N., and Reue, K. (2007) Three Mammalian Lipins Act as Phosphatidate Phosphatases with Distinct Tissue Expression Patterns. *J Biol. Chem.* **282**, 3450-3457
97. Han, G.-S. and Carman, G. M. (2010) Characterization of the human *LPIN1*-encoded phosphatidate phosphatase isoforms. *J. Biol. Chem.* **285**, 14628-14638
98. Nadra, K., De Preux Charles, A.-S., Medard, J.-J., Hendriks, W. T., Han, G.-S., Gres, S., Carman, G. M., Saulnier-Blache, J.-S., Verheijen, M. H. G., and Chrast, R. (2008) Phosphatidic acid mediates demyelination in *Lpin1* mutant mice. *Genes Dev.* **22**, 1647-1661
99. Finck, B. N., Gropler, M. C., Chen, Z., Leone, T. C., Croce, M. A., Harris, T. E., Lawrence, J. C., Jr., and Kelly, D. P. (2006) Lipin 1 is an inducible amplifier of the hepatic PGC-1alpha/PPARalpha regulatory pathway. *Cell Metab* **4**, 199-210
100. Koh, Y. K., Lee, M. Y., Kim, J. W., Kim, M., Moon, J. S., Lee, Y. J., Ahn, Y. H., and Kim, K. S. (2008) Lipin1 Is a key factor for the maturation and maintenance of adipocytes in the regulatory network with CCAAT/enhancer-binding protein {alpha} and peroxisome proliferator-activated receptor {gamma}2. *J. Biol. Chem.* **283**, 34896-34906
101. Kim, H. B., Kumar, A., Wang, L., Liu, G. H., Keller, S. R., Lawrence, J. C., Jr., Finck, B. N., and Harris, T. E. (2010) Lipin 1 represses NFATc4 transcriptional activity in adipocytes to inhibit secretion of inflammatory factors. *Mol. Cell Biol.* **30**, 3126-3139
102. Zeharia, A., Shaag, A., Houtkooper, R. H., Hindi, T., de, L. P., Erez, G., Hubert, L., Saada, A., de, K. Y., Eshel, G., Vaz, F. M., Pines, O., and Elpeleg, O. (2008) Mutations in *LPIN1* Cause Recurrent Acute Myoglobinuria in Childhood. *Am. J. Hum. Genet.* **83**, 489-494

103. Wiedmann, S., Fischer, M., Koehler, M., Neureuther, K., Riegger, G., Doering, A., Schunkert, H., Hengstenberg, C., and Baessler, A. (2008) Genetic Variants Within the *LPIN1* Gene, Encoding Lipin, Are Influencing Phenotypes of the Metabolic Syndrome in Humans. *Diabetes* **57**, 209-217
104. Suviolahti, E., Reue, K., Cantor, R. M., Phan, J., Gentile, M., Naukkarinen, J., Soro-Paavonen, A., Oksanen, L., Kaprio, J., Rissanen, A., Salomaa, V., Kontula, K., Taskinen, M. R., Pajukanta, P., and Peltonen, L. (2006) Cross-species analyses implicate Lipin 1 involvement in human glucose metabolism. *Hum. Mol. Genet.* **15**, 377-386
105. Al-Mosawi, Z. S., Al-Saad, K. K., Ijadi-Maghsoodi, R., El-Shanti, H. I., and Ferguson, P. J. (2007) A splice site mutation confirms the role of LPIN2 in Majeed syndrome. *Arthritis Rheum.* **56**, 960-964
106. Donkor, J., Zhang, P., Wong, S., O'Loughlin, L., Dewald, J., Kok, B. P., Brindley, D. N., and Reue, K. (2009) A conserved serine residue is required for the phosphatidate phosphatase activity but not transcriptional coactivator functions of lipin-1 and lipin-2. *J. Biol. Chem.* **284**, 29968-29978
107. Stace, C. L. and Ktistakis, N. T. (2006) Phosphatidic acid- and phosphatidylserine-binding proteins. *Biochim. Biophys. Acta* **1761**, 913-926
108. Ryu, D., Oh, K. J., Jo, H. Y., Hedrick, S., Kim, Y. N., Hwang, Y. J., Park, T. S., Han, J. S., Choi, C. S., Montminy, M., and Koo, S. H. (2009) TORC2 regulates hepatic insulin signaling via a mammalian phosphatidic acid phosphatase, LIPIN1. *Cell Metab* **9**, 240-251
109. Gropler, M. C., Harris, T. E., Hall, A. M., Wolins, N. E., Gross, R. W., Han, X., Chen, Z., and Finck, B. N. (2009) Lipin 2 Is a Liver-enriched Phosphatidate Phosphohydrolase Enzyme That Is Dynamically Regulated by Fasting and Obesity in Mice. *J. Biol. Chem.* **284**, 6763-6772
110. Soto-Cardalda, A., Fakas, S., Pascual, F., Choi, H. S., and Carman, G. M. (2011) Phosphatidate phosphatase plays role in zinc-mediated regulation of phospholipid synthesis in yeast. *J. Biol. Chem.* **287**, 968-977
111. Mylonis, I., Sembongi, H., Befani, C., Liakos, P., Siniosoglou, S., and Simos, G. (2012) Hypoxia causes triglyceride accumulation by HIF-1-mediated stimulation of lipin 1 expression. *J. Cell Sci.* **125**, 3485-3493
112. Wu, W.-I. and Carman, G. M. (1994) Regulation of phosphatidate phosphatase activity from the yeast *Saccharomyces cerevisiae* by nucleotides. *J. Biol. Chem.* **269**, 29495-29501
113. Wu, W.-I., Lin, Y.-P., Wang, E., Merrill, A. H., Jr., and Carman, G. M. (1993) Regulation of phosphatidate phosphatase activity from the yeast *Saccharomyces cerevisiae* by sphingoid bases. *J. Biol. Chem.* **268**, 13830-13837

114. Wu, W.-I. and Carman, G. M. (1996) Regulation of phosphatidate phosphatase activity from the yeast *Saccharomyces cerevisiae* by phospholipids. *Biochemistry* **35**, 3790-3796
115. Vallee, B. L. and Falchuk, K. H. (1993) The biochemical basis of zinc physiology. *Physiol Rev.* **73**, 79-118
116. Zhao, H. and Eide, D. (1996) The yeast *ZRT1* gene encodes the zinc transporter protein of a high-affinity uptake system induced by zinc limitation. *Proc. Natl. Acad. Sci. U. S. A* **93**, 2454-2458
117. Waters, B. M. and Eide, D. J. (2002) Combinatorial control of yeast FET4 gene expression by iron, zinc, and oxygen. *J. Biol. Chem.* **277**, 33749-33757
118. MacDiarmid, C. W., Milanick, M. A., and Eide, D. J. (2003) Induction of the ZRC1 Metal Tolerance Gene in Zinc-limited Yeast Confers Resistance to Zinc Shock. *J. Biol. Chem.* **278**, 15065-15072
119. Han, G.-S., Johnston, C. N., Chen, X., Athenstaedt, K., Daum, G., and Carman, G. M. (2001) Regulation of the *Saccharomyces cerevisiae* *DPPI*-encoded diacylglycerol pyrophosphate phosphatase by zinc. *J. Biol. Chem.* **276**, 10126-10133
120. Han, S.-H., Han, G.-S., Iwanyshyn, W. M., and Carman, G. M. (2005) Regulation of the *PIS1*-encoded phosphatidylinositol synthase in *Saccharomyces cerevisiae* by zinc. *J Biol. Chem.* **280**, 29017-29024
121. Kersting, M. C. and Carman, G. M. (2006) Regulation of the *Saccharomyces cerevisiae* *EKII*-encoded ethanolamine kinase by zinc depletion. *J Biol. Chem.* **281**, 13110-13116
122. Soto, A. and Carman, G. M. (2008) Regulation of the *Saccharomyces cerevisiae* *CKII*-encoded choline kinase by zinc depletion. *J. Biol. Chem.* **283**, 10079-10088
123. Roberts, G. G. and Hudson, A. P. (2006) Transcriptome profiling of *Saccharomyces cerevisiae* during a transition from fermentative to glycerol-based respiratory growth reveals extensive metabolic and structural remodeling. *Mol. Genet. Genomics* **276**, 170-186
124. DeRisi, J. L., Iyer, V. R., and Brown, P. O. (1997) Exploring the metabolic and genetic control of gene expression on a genomic scale. *Science* **278**, 680-686
125. Joseph-Strauss, D., Zenvirth, D., Simchen, G., and Barkai, N. (2007) Spore germination in *Saccharomyces cerevisiae*: global gene expression patterns and cell cycle landmarks. *Genome Biol.* **8**, R241
126. Csaki, L. S. and Reue, K. (2010) Lipins: multifunctional lipid metabolism proteins. *Annu. Rev. Nutr.* **30**, 257-272

127. Harris, T. E. and Finck, B. N. (2011) Dual function lipin proteins and glycerolipid metabolism. *Trends Endocrinol. Metab*
128. Zhang, P., O'Loughlin, L., Brindley, D. N., and Reue, K. (2008) Regulation of lipin-1 gene expression by glucocorticoids during adipogenesis. *J. Lipid Res.* **49**, 1519-1528
129. Manmontri, B., Sariahmetoglu, M., Donkor, J., Bou, K. M., Sundaram, M., Yao, Z., Reue, K., Lehner, R., and Brindley, D. N. (2008) Glucocorticoids and cAMP selectively increase hepatic lipin-1 expression and insulin acts antagonistically. *J. Lipid Res.* **49**, 1056-1067
130. P 環 erfy, M., Phan, J., and Reue, K. (2005) Alternatively spliced lipin isoforms exhibit distinct expression pattern, subcellular localization, and role in adipogenesis. *J Biol. Chem.* **280**, 32883-32889
131. Carman, G. M. and Henry, S. A. (2007) Phosphatidic acid plays a central role in the transcriptional regulation of glycerophospholipid synthesis in *Saccharomyces cerevisiae*. *J. Biol. Chem.* **282**, 37293-37297
132. Ostrander, D. B., O'Brien, D. J., Gorman, J. A., and Carman, G. M. (1998) Effect of CTP synthetase regulation by CTP on phospholipid synthesis in *Saccharomyces cerevisiae*. *J. Biol. Chem.* **273**, 18992-19001
133. Siniossoglou, S., Santos-Rosa, H., Rappsilber, J., Mann, M., and Hurt, E. (1998) A novel complex of membrane proteins required for formation of a spherical nucleus. *EMBO J.* **17**, 6449-6464
134. Stuible, H. P., Meier, S., Wagner, C., Hannappel, E., and Schweizer, E. (1998) A novel phosphopantetheine:protein transferase activating yeast mitochondrial acyl carrier protein. *J. Biol. Chem.* **273**, 22334-22339
135. Saleem, R. A., Rogers, R. S., Ratushny, A. V., Dilworth, D. J., Shannon, P. T., Shteynberg, D., Wan, Y., Moritz, R. L., Nesvizhskii, A. I., Rachubinski, R. A., and Aitchison, J. D. (2010) Integrated phosphoproteomics analysis of a signaling network governing nutrient response and peroxisome induction. *Mol. Cell Proteomics.* **9**, 2076-2088
136. Soufi, B., Kelstrup, C. D., Stoehr, G., Frohlich, F., Walther, T. C., and Olsen, J. V. (2009) Global analysis of the yeast osmotic stress response by quantitative proteomics. *Mol. Biosyst.* **5**, 1337-1346
137. Taunton, J., Rowning, B. A., Coughlin, M. L., Wu, M., Moon, R. T., Mitchison, T. J., and Larabell, C. A. (2000) Actin-dependent propulsion of endosomes and lysosomes by recruitment of N-WASP. *J Cell Biol.* **148**, 519-530
138. Ptacek, J., Devgan, G., Michaud, G., Zhu, H., Zhu, X., Fasolo, J., Guo, H., Jona, G., Breitkreutz, A., Sopko, R., McCartney, R. R., Schmidt, M. C., Rachidi, N.,

- Lee, S. J., Mah, A. S., Meng, L., Stark, M. J., Stern, D. F., De Virgilio C., Tyers, M., Andrews, B., Gerstein, M., Schweitzer, B., Predki, P. F., and Snyder, M. (2005) Global analysis of protein phosphorylation in yeast. *Nature* **438**, 679-684
139. Dephoure, N., Howson, R. W., Blethrow, J. D., Shokat, K. M., and O'Shea, E. K. (2005) Combining chemical genetics and proteomics to identify protein kinase substrates. *Proc. Natl. Acad. Sci. U. S. A* **102**, 17940-17945
140. Ubersax, J. A., Woodbury, E. L., Quang, P. N., Paraz, M., Blethrow, J. D., Shah, K., Shokat, K. M., and Morgan, D. O. (2003) Targets of the cyclin-dependent kinase Cdk1. *Nature* **425**, 859-864
141. Enserink, J. M. and Kolodner, R. D. (2010) An overview of Cdk1-controlled targets and processes. *Cell Div.* **5**, 11
142. Moffat, J., Huang, D., and Andrews, B. (2000) Functions of Pho85 cyclin-dependent kinases in budding yeast. *Prog. Cell Cycle Res.* **4**, 97-106
143. Carroll, A. S. and O'Shea, E. K. (2002) Pho85 and signaling environmental conditions. *Trends Biochem. Sci.* **27**, 87-93
144. Huang, D., Friesen, H., and Andrews, B. (2007) Pho85, a multifunctional cyclin-dependent protein kinase in budding yeast. *Mol. Microbiol.* **66**, 303-314
145. Huffman, T. A., Mothe-Satney, I., and Lawrence, J. C., Jr. (2002) Insulin-stimulated phosphorylation of lipin mediated by the mammalian target of rapamycin. *Proc. Natl. Acad. Sci U. S. A* **99**, 1047-1052
146. Harris, T. E., Huffman, T. A., Chi, A., Shabanowitz, J., Hunt, D. F., Kumar, A., and Lawrence, J. C., Jr. (2007) Insulin Controls Subcellular Localization and Multisite Phosphorylation of the Phosphatidic Acid Phosphatase, Lipin 1. *J Biol. Chem.* **282**, 277-286
147. Han, S., Bahmanyar, S., Zhang, P., Grishin, N., Oegema, K., Crooke, R., Graham, M., Reue, K., Dixon, J. E., and Goodman, J. M. (2012) Nuclear Envelope Phosphatase 1-Regulatory Subunit 1 (Formerly TMEM188) Is the Metazoan Spo7p Ortholog and Functions in the Lipin Activation Pathway. *J. Biol. Chem.* **287**, 3123-3137
148. Kastaniotis, A. J., Autio, K. J., Sormunen, R. T., and Hiltunen, J. K. (2004) Htd2p/Yhr067p is a yeast 3-hydroxyacyl-ACP dehydratase essential for mitochondrial function and morphology. *Mol. Microbiol.* **53**, 1407-1421
149. Broach, J. R. and Deschenes, R. J. (1990) The function of RAS genes in *Saccharomyces cerevisiae*. *Adv. Cancer Res.* **54**, 79-139
150. Thevelein, J. M. (1994) Signal Transduction in Yeast. *Yeast* **10**, 1753-1790

151. Levin, D. E., Fields, F. O., Kunisawa, R., Bishop, J. M., and Thorner, J. (1990) A candidate protein kinase C gene, *PKC1*, is required for the *S. cerevisiae* cell cycle. *Cell* 62, 213-224
152. Levin, D. E. and Bartlett-Heubusch, E. (1992) Mutants in the *S. cerevisiae* *PKC1* gene display a cell cycle- specific osmotic stability defect. *J. Cell Biol.* 116, 1221-1229
153. Rose, M. D., Winston, F., and Heiter, P. (1990) *Methods in Yeast Genetics: A Laboratory Course Manual*, Cold Spring Harbor Laboratory Press, Cold Spring Harbor, N.Y.
154. Culbertson, M. R. and Henry, S. A. (1975) Inositol requiring mutants of *Saccharomyces cerevisiae*. *Genetics* 80, 23-40
155. Zwietering, M. H., Jongenburger, I., Rombouts, F. M., and van 't, R. K. (1990) Modeling of the bacterial growth curve. *Appl. Environ. Microbiol.* 56, 1875-1881
156. Sambrook, J., Fritsch, E. F., and Maniatis, T. (1989) *Molecular Cloning, A Laboratory Manual*, 2nd Ed., Cold Spring Harbor Laboratory, Cold Spring Harbor, N.Y.
157. Wimmer, C., Doye, V., Grandi, P., Nehrbass, U., and Hurt, E. C. (1992) A new subclass of nucleoporins that functionally interact with nuclear pore protein NSP1. *EMBO J.* 11, 5051-5061
158. Thomas, B. and Rothstein, R. (1989) Elevated recombination rates in transcriptionally active DNA. *Cell* 56, 619-630
159. Innis, M. A. and Gelfand, D. H. (1990) in *PCR Protocols. A Guide to Methods and Applications* (Innis, M. A., Gelfand, D. H., Sninsky, J. J., and White, T. J., eds) pp. 3-12, Academic Press, Inc., San Diego
160. Ito, H., Fukuda, Y., Murata, K., and Kimura, A. (1983) Transformation of intact yeast cells treated with alkali cations. *J. Bacteriol.* 153, 163-168
161. Sikorski, R. S. and Hieter, P. (1989) A system of shuttle vectors and yeast host strains designed for efficient manipulation of DNA in *Saccharomyces cerevisiae*. *Genetics* 122, 19-27
162. Jeffery, D. A., Springer, M., King, D. S., and O'Shea, E. K. (2001) Multi-site phosphorylation of Pho4 by the cyclin-CDK Pho80-Pho85 is semi-processive with site preference. *J. Mol. Biol.* 306, 997-1010
163. Han, G.-S., Sreenivas, A., Choi, M. G., Chang, Y. F., Martin, S. S., Baldwin, E. P., and Carman, G. M. (2005) Expression of human CTP synthetase in *Saccharomyces cerevisiae* reveals phosphorylation by protein kinase A. *J Biol. Chem.* 280, 38328-38336

164. Bradford, M. M. (1976) A rapid and sensitive method for the quantitation of microgram quantities of protein utilizing the principle of protein-dye binding. *Anal. Biochem.* **72**, 248-254
165. Carman, G. M. and Lin, Y.-P. (1991) Phosphatidate phosphatase from yeast. *Methods Enzymol.* **197**, 548-553
166. Laemmli, U. K. (1970) Cleavage of structural proteins during the assembly of the head of bacteriophage T4. *Nature (London)* **227**, 680-685
167. Burnette, W. (1981) Western blotting: Electrophoretic transfer of proteins from sodium dodecyl sulfate-polyacrylamide gels to unmodified nitrocellulose and radiographic detection with antibody and radioiodinated protein A. *Anal. Biochem.* **112**, 195-203
168. Haid, A. and Suissa, M. (1983) Immunochemical identification of membrane proteins after sodium dodecyl sulfate-polyacrylamide gel electrophoresis. *Methods Enzymol.* **96**, 192-205
169. Choi, H.-S., Han, G.-S., and Carman, G. M. (2010) Phosphorylation of yeast phosphatidylserine synthase by protein kinase A. Identification of Ser46^a and Ser47^a's major sites of phosphorylation. *J. Biol. Chem.* **285**, 11526-11536
170. Xu, Z., Su, W. M., and Carman, G. M. (2011) Fluorescence spectroscopy measures yeast *PAH1*-encoded phosphatidate phosphatase interaction with liposome membranes. *J. Lipid Res.* **53**, 522-528
171. MacDonald, R. C., MacDonald, R. I., Menco, B. P., Takeshita, K., Subbarao, N. K., and Hu, L. R. (1991) Small-volume extrusion apparatus for preparation of large, unilamellar vesicles. *Biochim. Biophys. Acta* **1061**, 297-303
172. Boyle, W. J., Van der Geer, P., and Hunter, T. (1991) Phosphopeptide mapping and phosphoamino acid analysis by two-dimensional separation on thin-layer cellulose plates. *Methods Enzymol.* **201**, 110-149
173. Yang, W.-L. and Carman, G. M. (1995) Phosphorylation of CTP synthetase from *Saccharomyces cerevisiae* by protein kinase C. *J. Biol. Chem.* **270**, 14983-14988
174. MacDonald, J. I. S. and Kent, C. (1994) Identification of phosphorylation sites in rat liver CTP:phosphocholine cytidylyltransferase. *J. Biol. Chem.* **269**, 10529-10537
175. Morlock, K. R., Lin, Y.-P., and Carman, G. M. (1988) Regulation of phosphatidate phosphatase activity by inositol in *Saccharomyces cerevisiae*. *J. Bacteriol.* **170**, 3561-3566
176. Bligh, E. G. and Dyer, W. J. (1959) A rapid method of total lipid extraction and purification. *Can. J. Biochem. Physiol.* **37**, 911-917

177. Henderson, R. J. and Tocher, D. R. (1992) in *Lipid Analysis* (Hamilton, R. J. and Hamilton, S., eds) pp. 65-111, IRL Press, New York
178. Toda, T., Cameron, S., Sass, P., Zoller, M., and Wigler, M. (1987) Three different genes in *S. cerevisiae* encode the catalytic subunits of the cAMP-dependent protein kinase. *Cell* **50**, 277-287
179. Nishizuka, Y. (1988) The molecular heterogeneity of protein kinase C and its implications for cellular regulation. *Nature* **334**, 661-665
180. Padmanabha, R. and Glover, C. V. C. (1987) Casein kinase II of yeast contains two distinct α polypeptides and an unusually large β subunit. *J. Biol. Chem.* **262**, 1829-1835
181. Yang, W.-L. and Carman, G. M. (1996) Phosphorylation and regulation of CTP synthetase from *Saccharomyces cerevisiae* by protein kinase A. *J. Biol. Chem.* **271**, 28777-28783
182. Yang, W.-L., Bruno, M. E. C., and Carman, G. M. (1996) Regulation of yeast CTP synthetase activity by protein kinase C. *J. Biol. Chem.* **271**, 11113-11119
183. Choi, M.-G., Kurnov, V., Kersting, M. C., Sreenivas, A., and Carman, G. M. (2005) Phosphorylation of the yeast choline kinase by protein kinase C. Identification of Ser25^a and Ser30^a as major sites of phosphorylation. *J Biol. Chem.* **280**, 26105-26112
184. Chang, Y.-F. and Carman, G. M. (2006) Casein kinase II phosphorylation of the yeast phospholipid synthesis transcription factor Opi1p. *J Biol. Chem.* **281**, 4754-4761
185. Krebs, E. G. and Beavo, J. A. (1979) Phosphorylation-dephosphorylation of enzymes. *Ann. Rev. Biochem.* **48**, 923-959
186. Carman, G. M., Deems, R. A., and Dennis, E. A. (1995) Lipid signaling enzymes and surface dilution kinetics. *J. Biol. Chem.* **270**, 18711-18714
187. Lin, Y.-P. and Carman, G. M. (1990) Kinetic analysis of yeast phosphatidate phosphatase toward Triton X-100/phosphatidate mixed micelles. *J. Biol. Chem.* **265**, 166-170
188. Han, G.-S. and Carman, G. M. (2004) Assaying lipid phosphate phosphatase activities. *Methods Mol. Biol.* **284**, 209-216
189. Nunez, L. R., Jesch, S. A., Gaspar, M. L., Almaguer, C., Villa-Garcia, M., Ruiz-Noriega, M., Patton-Vogt, J., and Henry, S. A. (2008) Cell wall integrity MAPK pathway is essential for lipid homeostasis. *J. Biol. Chem.* **283**, 34204-34217

190. Mah, A. S., Elia, A. E., Devgan, G., Ptacek, J., Schutkowski, M., Snyder, M., Yaffe, M. B., and Deshaies, R. J. (2005) Substrate specificity analysis of protein kinase complex Dbf2-Mob1 by peptide library and proteome array screening. *BMC. Biochem.* **6**, 22
191. Park, T.-S., Ostrander, D. B., Pappas, A., and Carman, G. M. (1999) Identification of Ser42^a as the protein kinase A phosphorylation site in CTP synthetase from *Saccharomyces cerevisiae*. *Biochemistry* **38**, 8839-8848
192. Choi, M.-G., Park, T. S., and Carman, G. M. (2003) Phosphorylation of *Saccharomyces cerevisiae* CTP synthetase at Ser42^b by protein kinases A and C regulates phosphatidylcholine synthesis by the CDP-choline pathway. *J. Biol. Chem.* **278**, 23610-23616
193. Yu, Y., Sreenivas, A., Ostrander, D. B., and Carman, G. M. (2002) Phosphorylation of *Saccharomyces cerevisiae* choline kinase on Ser30^a and Ser85^b by protein kinase A regulates phosphatidylcholine synthesis by the CDP-choline pathway. *J. Biol. Chem.* **277**, 34978-34986
194. Roach, P. J. (1991) Multisite and hierarchal protein phosphorylation. *J. Biol. Chem.* **266**, 14139-14142
195. Lutterbach, B. and Hann, S. R. (1994) Hierarchical phosphorylation at N-terminal transformation-sensitive sites in c-Myc protein is regulated by mitogens and in mitosis. *Mol. Cell Biol.* **14**, 5510-5522
196. Sreenivas, A. and Carman, G. M. (2003) Phosphorylation of the yeast phospholipid synthesis regulatory protein opi1p by protein kinase a. *J. Biol. Chem.* **278**, 20673-20680
197. Sreenivas, A., Villa-Garcia, M. J., Henry, S. A., and Carman, G. M. (2001) Phosphorylation of the yeast phospholipid synthesis regulatory protein Opi1p by protein kinase C. *J. Biol. Chem.* **276**, 29915-29923
198. Kinney, A. J. and Carman, G. M. (1988) Phosphorylation of yeast phosphatidylserine synthase *in vivo* and *in vitro* by cyclic AMP-dependent protein kinase. *Proc. Nat. Acad. Sci. USA* **85**, 7962-7966
199. Kim, K.-H. and Carman, G. M. (1999) Phosphorylation and regulation of choline kinase from *Saccharomyces cerevisiae* by protein kinase A. *J. Biol. Chem.* **274**, 9531-9538
200. Pappas, A., Yang, W.-L., Park, T.-S., and Carman, G. M. (1998) Nucleotide-dependent Tetramerization of CTP Synthetase from *Saccharomyces cerevisiae*. *J. Biol. Chem.* **273**, 15954-15960
201. Park, T.-S., O'Brien, D. J., and Carman, G. M. (2003) Phosphorylation of CTP synthetase on Ser36^a, Ser33^b, Ser35^c, and Ser45^d regulates the levels of CTP and

- phosphatidylcholine synthesis in *Saccharomyces cerevisiae*. *J. Biol. Chem.* **278**, 20785-20794
202. Ozier-Kalogeropoulos, O., Adeline, M.-T., Yang, W.-L., Carman, G. M., and Lacroute, F. (1994) Use of synthetic lethal mutants to clone and characterize a novel CTP synthetase gene in *Saccharomyces cerevisiae*. *Mol. Gen. Genet.* **242**, 431-439
 203. Taylor, F. R. and Parks, L. W. (1979) Triacylglycerol metabolism in *Saccharomyces cerevisiae* relation to phospholipid synthesis. *Biochim. Biophys. Acta* **575**, 204-214
 204. Su, W.-M., Han, G.-S., Casciano, J., and Carman, G. M. (2012) Protein kinase A-mediated phosphorylation of Pah1p phosphatidate phosphatase functions in conjunction with the Pho85p-Pho80p and Cdc28p-cyclin B kinases to regulate lipid synthesis in yeast. *J. Biol. Chem.* **287**, 33364-33376
 205. Kim, Y., Gentry, M. S., Harris, T. E., Wiley, S. E., Lawrence, J. C., Jr., and Dixon, J. E. (2007) A conserved phosphatase cascade that regulates nuclear membrane biogenesis. *Proc. Natl. Acad. Sci. U. S. A* **104**, 6596-6601
 206. Wu, R., Garland, M., Dunaway-Mariano, D., and Allen, K. N. (2011) *Homo sapiens* Dullard protein phosphatase shows a preference for the insulin-dependent phosphorylation site of lipin1. *Biochemistry* **50**, 3045-3047

CURRICULUM VITAE

Wen-Min Su

Education

- 2007-2013 Ph.D., Food Science, Rutgers University
- 2001-2003 M.S., Agricultural Chemistry, National Taiwan University, Taiwan
- 1997-2001 B.S., Food Science, National Chung Hsing University, Taiwan

Academic Experience

- 2008-2013 Graduate Assistant, Department of Food Science, Rutgers University
- 2003-2006 Research Assistant, Institute of Molecular and Cellular Biology, National Taiwan University, Taiwan

Publications

- Su, W. M.** and G.M. Carman. Interrelationships of Pah1p phosphatidate phosphatase phosphorylations by protein kinase C, protein kinase A, and Pho85p-Pho80p kinases. Identification of Ser677, Ser769, and Ser788 as the sites phosphorylated by protein kinase C. In preparation.
- Su, W. M.**, G. S. Han, J Casciano, and G. M. Carman. 2012. Protein kinase A-mediated phosphorylation of Pah1p phosphatidate phosphatase functions in conjunction with the Pho85p-Pho80p and Cdc28p-Cyclin B kinases to regulate lipid synthesis in Yeast. *J. Biol. Chem.* 287: 33364-33376.
- Choi, H. S., **W. M. Su**, G. S. Han, D. Plote, Z. Xu, and G. M. Carman. 2012. Pho85p-Pho80p phosphorylation of yeast Pah1p phosphatidate phosphatase regulates its activity, location, abundance, and function in lipid metabolism. *J. Biol. Chem.* 287: 11290-11301.
- Xu, Z., **W. M. Su**, G. M. Carman. 2012. Fluorescence spectroscopy measures yeast *PAH1*-encoded phosphatidate phosphatase interaction with liposome membranes. *J. Lipid Res.* 53: 522-528.
- Choi, H. S., **W. M. Su**, J. M. Morgan, G. S. Han, Z. Xu, E. Karanasios, S. Siniosoglou, and G. M. Carman. 2011. Phosphorylation of phosphatidate phosphatase regulates its membrane association and physiological functions in *Saccharomyces cerevisiae*. Identification of Ser602, Thr723, and Ser744 as the sites phosphorylated by *CDC28* (*CDK1*)-encoded cyclin-dependent kinase. *J. Biol. Chem.* 286: 1486-1498.